Finite Elements for Differential Geometry

Michael Neunteufel

January 31, 2023

Contents

Introduction

This lecture on *Finite Elements for Differential Geometry* aims to derive and discuss finite elements and numerical methods for problems based and arising in (discrete) differential geometry.

The first part is devoted to problems involving extrinsic differential geometry, where the computational domain is embedded in the surrounding Euclidean space, e.g., a plate or surface in 3D. To solve nonlinear shell problems we first discuss the equations of elasticity (continuum mechanics). Then dimension reductions to (linear) beams and plates are presented revealing several typical discretization problems appearing for those problem classes. Non-standard finite elements like vector-valued tangential-continuous Nédélec, and normal-continuous Raviart–Thomas/Brezzi–Douglas–Marini elements as well as matrix valued normal-normal continuous Hellan–Herrmann–Johnson and tangential-tangential continuous Regge elements are motivated, constructed, and analyzed. Further, tools from so-called extrinsic differential geometry are repeated, where a $d-1$-dimensional sub-manifold is embedded in the surrounding $\mathbb{R}^d$. We use the concept of fundamental forms and related quantities (e.g. metric and Weingarten tensor), (covariant) derivatives and finite elements on surfaces. The discrete (distributional) curvature approximation is discussed. Combining the knowledge of differential geometry and finite elements we derive, discuss, and simulate nonlinear shells, which get deformed under external forces.

In the second part of this lecture we concentrate on the theory of Riemannian manifolds and the computation and approximation of their intrinsic quantities. Therefore, we do not assume this manifolds to be embedded. In terms of curvature, although the outer normal vector is not available any more, the Gauss and geodesic curvature can still be computed. The approximation of the metric tensor by solely tangential-tangential continuous Regge finite elements and the question of computing geodesics and distributional Gauss curvature will be fundamental. Again, we repeat and use tools of (discrete) differential geometry, like the Gauss–Bonnet theorem, to define, analyze, and implement the resulting methods.

Chapter 1

Continuum mechanics

This section is devoted to the introduction of the equations of continuum mechanics (elasticity) to describe how an elastic body gets deformed in the presence of forces like gravity. Literature to (nonlinear) elasticity and continuum mechanics are e.g. [14, 35, 50, 10, 32].

1.1 Strain tensors

Let $\Omega \subset \mathbb{R}^d$ be an open and bounded domain in $d = 2, 3$ dimensions and let the boundary $\partial\Omega$ be sufficiently smooth. Then $\overline{\Omega}$ describes the reference configuration of a body, also called undeformed configuration. The boundary is split into a Dirichlet and Neumann part Γ_D and Γ_N, respectively, with $\Gamma_D \cap \Gamma_N = \emptyset$ and $\overline{\Gamma_D} \cup \overline{\Gamma_N} = \partial\Omega$. Further, we assume that the measure of Γ_D is not zero, i.e., $|\Gamma_D| \neq 0$.

Applying external forces to the body leads to *deformation* represented by the function

$$\begin{aligned} \Phi : \overline{\Omega} &\to \mathbb{R}^d \\ x &\mapsto \Phi(x), \end{aligned} \tag{1.1.1}$$

which can be split additively into the identity function and the *displacement* u

$$\Phi = \mathrm{id} + u. \tag{1.1.2}$$

Next, we introduce the *deformation gradient*

$$\boldsymbol{F} := \boldsymbol{I} + \nabla u = \nabla\Phi, \tag{1.1.3}$$

where $\boldsymbol{I}$ denotes the identity matrix. A deformation is called *permissible* if the *deformation determinant* $J := \det(\boldsymbol{F})$ is greater than zero, $J > 0$, which entails that the material is non-interpenetrable, i.e., the orientation is preserved and volume elements with positive measure have also positive measure after the deformation.

To measure the quadratic change of lengths of the deformation the (right) *Cauchy–Green strain tensor* is introduced as

$$\boldsymbol{C} := \boldsymbol{F}^\top \boldsymbol{F}. \tag{1.1.4}$$

It is also called *metric tensor* in the context of differential geometry and shells (Chapter 4). There holds for $\Phi \in C^2(\Omega, \mathbb{R}^d)$ with Taylor's theorem for $\|\Delta x\| \to 0$

$$\begin{aligned} \frac{\|\Phi(x+\Delta x) - \Phi(x)\|^2}{\|\Delta x\|^2} &= \frac{\|\Phi(x) + \nabla\Phi\Delta x + \mathcal{O}(\|\Delta x\|^2) - \Phi(x)\|^2}{\|\Delta x\|^2} = \frac{\Delta x^\top \boldsymbol{F}^\top \boldsymbol{F}\Delta x + \mathcal{O}(\|\Delta x\|^3)}{\|\Delta x\|^2} \\ &= \frac{\Delta x^\top \boldsymbol{C}\Delta x}{\|\Delta x\|^2} + \mathcal{O}(\|\Delta x\|), \end{aligned} \tag{1.1.5}$$

i.e., it measures the change of lengths.

If $\boldsymbol{C} = \boldsymbol{I}$, then the body does not get deformed, however, it could be rotated or translated. The following theorem states that these motions are exactly the kernel of $\boldsymbol{C} - \boldsymbol{I}$, so-called *rigid body motions* (or *Euclidean motion*).

Theorem 1.1.1 *Let Ω be a connected domain and $\Phi \in C^1(\Omega, \mathbb{R}^d)$. Then a deformation is a rigid body motion if and only if*

$$\Phi \in RB := \{\Psi(x) = a + \boldsymbol{Q}x \,|\, a \in \mathbb{R}^d \wedge \boldsymbol{Q} \in \mathrm{SO}(d)\}, \tag{1.1.6}$$

where $\mathrm{SO}(d) := \{\boldsymbol{A} \in \mathbb{R}^{d\times d} \,|\, \det \boldsymbol{A} = 1$ and $\boldsymbol{A}^{-1} = \boldsymbol{A}^\top\}$ denotes the special orthogonal group.

Proof: See e.g., [14, Theorem 1.8-1]. □

This motivates the definition of the *Green strain tensor*

$$\boldsymbol{E} := \frac{1}{2}(\boldsymbol{C} - \boldsymbol{I}) \tag{1.1.7}$$

measuring the real strains induced by the deformation Φ. Its kernel is exactly the rigid body motions, $\ker \boldsymbol{E} = RB$. Inserting (1.1.3)–(1.1.4) yields the representation

$$\boldsymbol{E} = \frac{1}{2}\left(\nabla u^\top \nabla u + \nabla u^\top + \nabla u\right). \tag{1.1.8}$$

Assuming $\nabla u = \mathcal{O}(\varepsilon)$ with $1 \gg \varepsilon > 0$ small and neglecting all higher order terms gives the *linearized strain tensor*

$$\boldsymbol{\varepsilon}(u) := \frac{1}{2}\left(\nabla u^\top + \nabla u\right) = \operatorname{sym}(\nabla u) \tag{1.1.9}$$

used in linear elasticity.

1.2 Hyperelastic materials

We consider *hyperelastic constitutive relations*, i.e., the deformation energy is given by a potential $\Psi : \Omega \times \mathbb{R}^{d\times d} \to \mathbb{R}$

$$E_{\text{def}} = \int_\Omega \Psi(x, \boldsymbol{F}(u(x)))\, dx. \tag{1.2.1}$$

More general elastic materials and a derivation based on conservation laws can be found in the literature. Further, for ease of presentation we assume that the potential is *homogeneous*, i.e.,

$$\Psi(x, \cdot) = \Psi(\cdot). \tag{1.2.2}$$

Given Dirichlet data u_D on Γ_D, a static body load f, and traction forces g on Γ_N we can define the following minimization problem

$$\mathcal{W}(u) := \int_\Omega \Psi(\boldsymbol{F}(u)) - f \cdot u\, dx - \int_{\Gamma_N} g \cdot u\, ds \to \min!. \tag{1.2.3}$$

Gravity is a classical body force, whereas a car driving over a bridge is an example of a traction force.

We seek for a function u in the set of admissible displacements given by

$$U := \{u : \Omega \to \mathbb{R}^d \,|\, u = u_D \text{ on } \Gamma_D,\ \det(\boldsymbol{F}(u)) > 0\}. \tag{1.2.4}$$

Note, that the constraint $\det(\boldsymbol{F}(u)) > 0$ is often given implicitly in the material law or is neglected in the small deformation case.

To compute the weak formulation of (1.2.3) we take the first variation in direction δu, well-known as the *principle of virtual works*, yielding

$$D_u\mathcal{W}(u)[\delta u] = \int_\Omega \frac{\partial \Psi}{\partial \boldsymbol{F}} : \nabla \delta u - f \cdot \delta u\, dx - \int_{\Gamma_N} g \cdot \delta u\, ds \stackrel{!}{=} 0 \tag{1.2.5}$$

for all admissible test functions δu, i.e., $\delta u \in U_{\Gamma_D}$, where

$$U_{\Gamma_D} := \{\delta u : \Omega \to \mathbb{R}^d \,|\, \delta u = 0 \text{ on } \Gamma_D\}. \tag{1.2.6}$$

In (1.2.5) we used the Frobenius scalar product of two matrices $\boldsymbol{A} : \boldsymbol{B} = \sum_{i,j=1}^d \boldsymbol{A}_{ij}\boldsymbol{B}_{ij}$ and the chain rule $D_u\Psi(\boldsymbol{F}(u))[\delta v] = \frac{\partial \Psi}{\partial \boldsymbol{F}}(\boldsymbol{F}(u)) : D_u(\boldsymbol{F}(u))[\delta u]$.

By defining the *first Piola–Kirchhoff stress tensor*

$$\boldsymbol{P} := \frac{\partial \Psi}{\partial \boldsymbol{F}} \tag{1.2.7}$$

and integration by parts in (1.2.5), we obtain the Euler–Lagrange equation of (1.2.3)

$$\begin{cases} -\operatorname{div}(\boldsymbol{P}) = f & \text{in } \Omega, \\ u = u_D & \text{on } \Gamma_D, \\ \boldsymbol{P}n = g & \text{on } \Gamma_N, \end{cases} \tag{1.2.8}$$

where n denotes the outer normal vector of Ω, cf. Figure 1.1.

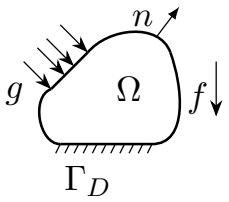

Figure 1.1: Initial configuration of a body Ω with Dirichlet boundary Γ_D, external forces f and g, and outer normal vector n.

Definition 1.2.1 *We call a hyperelastic potential*

- objective *(*frame-indifferent*), if for all positive definite* $\boldsymbol{F} \in \mathbb{M}_+(d) := \{\boldsymbol{A} \in \mathbb{R}^{d\times d} \,|\, x^\top \boldsymbol{A} x > 0 \text{ for all } 0 \neq x \in \mathbb{R}^d\}$ *and* $\boldsymbol{Q} \in \mathrm{SO}(d)$

$$\Psi(\boldsymbol{Q}\boldsymbol{F}) = \Psi(\boldsymbol{F}). \tag{1.2.9}$$

- isotropic*, if for all* $\boldsymbol{F} \in \mathbb{M}_+(d)$ *and* $\boldsymbol{Q} \in \mathrm{SO}(d)$

$$\Psi(\boldsymbol{F}\boldsymbol{Q}) = \Psi(\boldsymbol{F}). \tag{1.2.10}$$

For an isotropic material as e.g., steel there are no preferred directions. Wood is a classical example of a strongly anisotropic material.

Example 1.2.2 *The potential* $\Psi(\boldsymbol{F}) := \frac{\mu}{4}\left(\boldsymbol{F}^\top\boldsymbol{F} - \boldsymbol{I}\right) : \left(\boldsymbol{F}^\top\boldsymbol{F} - \boldsymbol{I}\right) + \frac{\lambda}{8}\operatorname{tr}(\boldsymbol{F}^\top\boldsymbol{F} - \boldsymbol{I})^2$*, with* $\mu > 0$*,* $\lambda \geq 0$ *is objective and isotropic (Exercise!).*

A crucial consequence of objectivity is that the energy potential only depends on the Cauchy–Green strain tensor.

Theorem 1.2.3 *A potential* $\Psi : \mathbb{R}^{d\times d} \to \mathbb{R}$ *is frame-indifferent if and only if it is a function of the Cauchy–Green strain tensor* $\boldsymbol{C} = \boldsymbol{F}^\top\boldsymbol{F}$*, i.e.,*

$$\Psi(\boldsymbol{F}) = \hat{\Psi}(\boldsymbol{C}). \tag{1.2.11}$$

Proof: See e.g., [10, Chapter VI, Theorem 1.6]. □

Assuming a frame-indifferent and isotropic potential yields that it is a function of the invariants of the Cauchy–Green strain tensor.

Theorem 1.2.4 (Rivlin–Ericksen) *Let* $\mathbb{S}_>(d) := \{\boldsymbol{A} \in \mathbb{R}^{d\times d} \,|\, \boldsymbol{A}^\top = \boldsymbol{A} \text{ and } \det \boldsymbol{A} > 0\}$ *denote the set of symmetric matrices with positive determinant. An energy potential* $\Psi : \mathbb{R}^{d\times d} \to \mathbb{R}$ *is frame-indifferent and isotropic if and only if there exists a function* $\overline{\Psi} : \mathbb{S}_>(d) \to \mathbb{R}$ *depending only on the invariants of the characteristic polynomial* $\det(\lambda\boldsymbol{I} - \boldsymbol{C}) = \lambda^3 - I_1(\boldsymbol{C})\lambda^2 - I_2(\boldsymbol{C})\lambda - I_3(\boldsymbol{C})$ *such that*

$$\Psi(\boldsymbol{F}) = \overline{\Psi}(I_1(\boldsymbol{C}), I_2(\boldsymbol{C}), I_3(\boldsymbol{C})) = \gamma_0(I_1, I_2, I_3)\boldsymbol{I} + \gamma_1(I_1, I_2, I_3)\boldsymbol{C} + \gamma_2(I_1, I_2, I_3)\boldsymbol{C}^2, \tag{1.2.12}$$

where, with $\operatorname{tr}(\boldsymbol{C})$ *and* $\det(\boldsymbol{C})$ *denoting the trace and determinant of* $\boldsymbol{C}$*,*

$$I_1(\boldsymbol{C}) = \operatorname{tr}(\boldsymbol{C}), \qquad I_2(\boldsymbol{C}) = \frac{1}{2}\left(\operatorname{tr}(\boldsymbol{C})^2 - \operatorname{tr}(\boldsymbol{C}^2)\right), \qquad I_3(\boldsymbol{C}) = \det(\boldsymbol{C}). \tag{1.2.13}$$

Proof: See e.g., [45]. □

We will consider frame-indifferent potentials and write Ψ independently of arguments $\boldsymbol{F}$, $\boldsymbol{C}$, and $\boldsymbol{E}$.

Using Theorem 1.2.3, the weak form (1.2.5) can be rewritten as: Find $u \in U$ such that for all $v \in U_{\Gamma_D}$

$$\int_\Omega 2\frac{\partial\Psi}{\partial\boldsymbol{C}}(\boldsymbol{C}(u)) : \operatorname{sym}(\boldsymbol{F}^\top(u)\nabla v)\,dx = \int_\Omega f\cdot v\,dx + \int_{\Gamma_N} g\cdot v\,ds, \tag{1.2.14}$$

where we utilized that $D_u\boldsymbol{C}(u)[v] = D_u\big(\boldsymbol{F}(u)^\top\big)[v]\boldsymbol{F}(u) + \boldsymbol{F}(u)^\top D_u\big(\boldsymbol{F}(u)\big)[v] = 2\,\mathrm{sym}(\boldsymbol{F}^\top(u)\nabla v)$.

Defining the *second Piola–Kirchhoff stress tensor*

$$\boldsymbol{\Sigma} := 2\frac{\partial \Psi}{\partial \boldsymbol{C}} \tag{1.2.15}$$

and exploiting the symmetry of $\boldsymbol{\Sigma}$ gives

$$\int_\Omega \boldsymbol{F}\boldsymbol{\Sigma} : \nabla v\, dx = \int_\Omega f \cdot v\, dx + \int_{\Gamma_N} g \cdot v\, ds. \tag{1.2.16}$$

Consequently, we obtain the relation

$$\boldsymbol{P} = \boldsymbol{F}\boldsymbol{\Sigma}. \tag{1.2.17}$$

Note that in contrast to $\boldsymbol{\Sigma}$, $\boldsymbol{P}$ is not symmetric. For the sake of completeness, the symmetric *Cauchy stress tensor* $\boldsymbol{\sigma}$ acting on the deformed configuration of the body is introduced by

$$\boldsymbol{\sigma} = \frac{1}{J}\boldsymbol{F}\boldsymbol{\Sigma}\boldsymbol{F}^\top = \frac{1}{J}\boldsymbol{P}\boldsymbol{F}^\top = \frac{1}{J}\frac{\partial \Psi}{\partial \boldsymbol{F}}\boldsymbol{F}^\top. \tag{1.2.18}$$

Then by applying the transformation theorem and the chain rule ($v \circ \Phi^{-1} = \tilde{v}$, $(\nabla_x v) \circ \Phi^{-1} = \nabla_{\tilde{x}}\tilde{v}\boldsymbol{F}$)

$$\int_{\tilde{\Omega}} \frac{1}{J}\boldsymbol{F}\boldsymbol{\Sigma} : (\nabla_{\tilde{x}}\tilde{v}\boldsymbol{F})\, d\tilde{x} = \int_{\tilde{\Omega}} \boldsymbol{\sigma} : \nabla_{\tilde{x}}\tilde{v}\, d\tilde{x}.$$

The *St. Venant–Kirchhoff* material law

$$\Psi_{\mathrm{VK}}(\boldsymbol{E}) = \mu\|\boldsymbol{E}\|_F^2 + \frac{\lambda}{2}\,\mathrm{tr}(\boldsymbol{E})^2, \qquad \|\boldsymbol{A}\|_F^2 := \boldsymbol{A} : \boldsymbol{A}, \tag{1.2.19}$$

is widely used to model nonlinear behavior in a moderate deformation regime. It may happen for large deformations, however, that elements get compressed heavily and are even pressed through others.

Exercise 1.2.5 *From the Rivlin–Ericksen theorem the potential in the Green strain tensor is of the form* $\Psi(\boldsymbol{E}) = \Psi(\,\mathrm{tr}(\boldsymbol{E}),\, \mathrm{tr}(\boldsymbol{E}^2), \det \boldsymbol{E})$. *Assume that* Ψ *has at* $\boldsymbol{E} = 0$ *a local minimum with value 0 and is smooth. Then there holds with* $\mu := \Psi_{,2}(\,\mathrm{tr}(\boldsymbol{E}),\, \mathrm{tr}(\boldsymbol{E}^2), \det \boldsymbol{E})$ *and* $\mu := \Psi_{,11}(\,\mathrm{tr}(\boldsymbol{E}),\, \mathrm{tr}(\boldsymbol{E}^2), \det \boldsymbol{E})$, *where.* $\Psi_{,2}(\cdot,\cdot,\cdot)$ *denotes the partial derivative with respect to the second argument and* $\Psi_{,11}(\cdot,\cdot,\cdot)$ *two derivatives in the first one,*

$$\Psi(\boldsymbol{E}) = \frac{\lambda}{2}\,\mathrm{tr}(\boldsymbol{E})^2 + \mu\,\boldsymbol{E} : \boldsymbol{E} + \mathcal{O}(\|\boldsymbol{E}\|^3).$$

The material law of *Neo–Hooke*

$$\Psi_{\mathrm{NH}}(\boldsymbol{C}) = \frac{\mu}{2}\,(\,\mathrm{tr}(\boldsymbol{C} - \boldsymbol{I}) - \log(\det(\boldsymbol{C}))) + \frac{\lambda}{8}(\log(\det(\boldsymbol{C})))^2 \tag{1.2.20}$$

prevents the non-physical behavior of the St. Venant–Kirchhoff material law as there holds

$$\Psi_{\mathrm{NH}}(\boldsymbol{C}) \to \infty \quad \text{ for } \det(\boldsymbol{C}) = (\det(\boldsymbol{F}))^2 \to 0 \text{ or } \det(\boldsymbol{C}) \to \infty, \tag{1.2.21}$$

i.e., infinite energy is needed to completely compress or stretch the material. We remark that, especially in the (nearly) incompressible regime, a slightly different material law of Neo–Hooke is also used, namely

$$\tilde{\Psi}_{\mathrm{NH}}(\boldsymbol{C}) = \frac{\mu}{2}\,(\,\mathrm{tr}(\boldsymbol{C} - \boldsymbol{I}) - \log(\det(\boldsymbol{C}))) + \frac{\lambda}{2}(\underbrace{\sqrt{\det(\boldsymbol{C})}}_{=\det \boldsymbol{F}} - 1)^2. \tag{1.2.22}$$

The two material constants $\mu > 0$ and $\lambda > 0$ used above are the so-called Lamé parameters. Two more physically interpretable constants are the Young's modulus $E > 0$, representing the stiffness of a solid material, and the Poisson's ratio $0 \le \nu < 1/2$[1]. The latter describes the amount of expansion or

[1] For meta-materials the Poisson ratio can also take negative values.

Figure 1.2: Two solutions of rubber strip clamped on left and right boundary.

contraction in the perpendicular direction to the force compressing or stretching the material. Physical units are $[\mu] = [\lambda] = [E] = \frac{N}{m^2} = Pa$ Pascal, whereas the Poisson ratio is dimensionless. To convert these parameters the following formulae are used

$$\nu = \frac{\lambda}{2(\lambda+\mu)}, \qquad E = \frac{\mu(3\lambda+2\mu)}{\lambda+\mu}, \tag{1.2.23a}$$

$$\lambda = \frac{E\nu}{(1+\nu)(1-2\nu)}, \qquad \mu = \frac{E}{2(1+\nu)}. \tag{1.2.23b}$$

Note, that in the limit $\nu \to \frac{1}{2}$, or equivalently $\lambda \to \infty$, the material is called incompressible necessitating special (numerical) treatment.

1.3 Theoretical results of nonlinear elasticity

The question of existence and uniqueness of this (highly nonlinear) equations is delicate. From physical examples it is known that we cannot expect uniqueness. Considering e.g., a rubber strip where both ends are fixed and neglecting gravity the identity is a trivial solution for the displacement. When twisting one of the ends by 2π (360°) we obtain a different solution to the same boundary conditions, see Figure 1.2. In this manner we can even produce infinitely many solutions by twisting. Other examples are given e.g., by buckling (bifurcations) or snap through problems, where for one external force two different solutions exist (one before and one after the snap through).

For existence one approach exploits, if possible, the polyconvex structure of the energy potential Ψ in its invariants $I_i(\boldsymbol{C})$, compare (1.2.13), proving the existence of minimizers [7]. The material law of St. Venant–Kirchhoff is not polyconvex, but the Neo–Hooke material law falls in this category. A large class of Ogden-type materials fulfills this assumption. Another ansatz uses the implicit function theorem obtaining a unique solution for small data. Therefore, however, rather strong regularity assumptions have to be made [14].

Only little rigorous mathematical numerical analysis for finite elasticity has been accomplished so far. E.g., in [12] a priori error estimates for finite element discretizations in nonlinear elasticity are discussed for polyconvex materials under the assumption of sufficiently small right-hand sides.

1.4 Linearized elasticity

Under the assumption of small deformations all three stress tensors (1.2.7), (1.2.15), and (1.2.18) reduce to one, which we denote by $\boldsymbol{\sigma}$ (e.g., $\boldsymbol{P} = \boldsymbol{F}\boldsymbol{\Sigma} = (\boldsymbol{I} + \nabla u)\boldsymbol{\Sigma} = \boldsymbol{\Sigma} + \mathcal{O}(\varepsilon^2)$ as $\nabla u = \mathcal{O}(\varepsilon)$ by assumption). Assuming a quadratic potential $\Psi(\cdot)$ we deduce a linear stress-strain relation by $\boldsymbol{\sigma} = \mathcal{C}\boldsymbol{\varepsilon}$, where $\mathcal{C}$ denotes the fourth order elasticity tensor. For an isotropic and frame-indifferent material the stress-strain relation is of the form

$$\begin{pmatrix} \boldsymbol{\sigma}_{11} \\ \boldsymbol{\sigma}_{22} \\ \boldsymbol{\sigma}_{33} \\ \boldsymbol{\sigma}_{12} \\ \boldsymbol{\sigma}_{13} \\ \boldsymbol{\sigma}_{23} \end{pmatrix} = \frac{E}{(1+\nu)(1-2\nu)} \begin{pmatrix} 1-\nu & \nu & \nu & & & \\ \nu & 1-\nu & \nu & & & \\ \nu & \nu & 1-\nu & & & \\ & & & 1-2\nu & & \\ & & & & 1-2\nu & \\ & & & & & 1-2\nu \end{pmatrix} \begin{pmatrix} \boldsymbol{\varepsilon}_{11} \\ \boldsymbol{\varepsilon}_{22} \\ \boldsymbol{\varepsilon}_{33} \\ \boldsymbol{\varepsilon}_{12} \\ \boldsymbol{\varepsilon}_{13} \\ \boldsymbol{\varepsilon}_{23} \end{pmatrix}, \tag{1.4.1}$$

or in matrix notation $\boldsymbol{\sigma} = \frac{E}{(1+\nu)(1-2\nu)}((1-2\nu)\boldsymbol{\varepsilon} + \nu\,\mathrm{tr}(\boldsymbol{\varepsilon})\boldsymbol{I}) = 2\mu\boldsymbol{\varepsilon} + \lambda\,\mathrm{tr}(\boldsymbol{\varepsilon})\boldsymbol{I}$. For $\nu \neq \frac{1}{2}$ relation (1.4.1) can be inverted, $\boldsymbol{\varepsilon} = \mathcal{C}^{-1}\boldsymbol{\sigma}$,

$$\begin{pmatrix} \boldsymbol{\varepsilon}_{11} \\ \boldsymbol{\varepsilon}_{22} \\ \boldsymbol{\varepsilon}_{33} \\ \boldsymbol{\varepsilon}_{12} \\ \boldsymbol{\varepsilon}_{13} \\ \boldsymbol{\varepsilon}_{23} \end{pmatrix} = \frac{1}{E} \begin{pmatrix} 1 & -\nu & -\nu & & & \\ -\nu & 1 & -\nu & & & \\ -\nu & -\nu & 1 & & & \\ & & & 1+\nu & & \\ & & & & 1+\nu & \\ & & & & & 1+\nu \end{pmatrix} \begin{pmatrix} \boldsymbol{\sigma}_{11} \\ \boldsymbol{\sigma}_{22} \\ \boldsymbol{\sigma}_{33} \\ \boldsymbol{\sigma}_{12} \\ \boldsymbol{\sigma}_{13} \\ \boldsymbol{\sigma}_{23} \end{pmatrix}, \tag{1.4.2}$$

and $\mathcal{C}^{-1}$ is called the *compliance tensor*. Relation (1.4.2) can be written compactly as

$$\boldsymbol{\varepsilon} = \frac{1}{E}\left((1+\nu)\boldsymbol{\sigma} - \nu\ \mathrm{tr}(\boldsymbol{\sigma})\boldsymbol{I}\right) = \frac{1}{E}\left((1+\nu)\,\mathrm{dev}(\boldsymbol{\sigma}) + \frac{1-2\nu}{2}\,\mathrm{tr}(\boldsymbol{\sigma})\boldsymbol{I}\right), \tag{1.4.3}$$

where $\mathrm{dev}(\boldsymbol{A}) = \boldsymbol{A} - \frac{1}{d}\,\mathrm{tr}(\boldsymbol{A})\boldsymbol{I}$ denotes the deviatoric (trace-free) part of a matrix. Here, the case $\nu = \frac{1}{2}$ is well-defined leading to the identity $\boldsymbol{\varepsilon} = \frac{1+\nu}{E}\,\mathrm{dev}(\boldsymbol{\sigma})$, which is unique up to the trace of $\boldsymbol{\sigma}$.

The strong form of (1.2.8) becomes in the linearized case

$$\begin{cases} -\mathrm{div}(\boldsymbol{\sigma}) = f & \text{in } \Omega, \\ u = u_D & \text{on } \Gamma_D, \\ \boldsymbol{\sigma} n = g & \text{on } \Gamma_N, \end{cases} \tag{1.4.4}$$

and the variational problem (inserting the stress-strain relation) reads: Find $u \in U$ such that for all $v \in U_{\Gamma_D}$

$$\int_\Omega \mathcal{C}\boldsymbol{\varepsilon}(u) : \boldsymbol{\varepsilon}(v)\,dx = \int_\Omega f \cdot v\,dx + \int_{\Gamma_N} g \cdot v\,ds. \tag{1.4.5}$$

The material laws of St. Venant–Kirchhoff and Neo–Hooke reduce to the linear material law of Hooke

$$\Psi_{\mathrm{H}}(\boldsymbol{\varepsilon}) := \mu\|\boldsymbol{\varepsilon}\|_F^2 + \frac{\lambda}{2}(\,\mathrm{tr}(\boldsymbol{\varepsilon}))^2 \tag{1.4.6}$$

and we obtain the problem: Find $u \in U$ such that for all test functions $v \in U_{\Gamma_D}$

$$\int_\Omega 2\mu\,\boldsymbol{\varepsilon}(u) : \boldsymbol{\varepsilon}(v) + \lambda\,\mathrm{div}(u)\mathrm{div}(v)\,dx = \int_\Omega f \cdot v\,dx + \int_{\Gamma_N} g \cdot v\,ds. \tag{1.4.7}$$

The unique solvability of (1.4.5) is proven in the next section. Note that (1.4.5) and (1.4.7) coincide for $\mathcal{C}$ defined as in (1.4.1).

1.5 Analysis of linear elasticity

We use the classical Lax–Milgram Lemma for elliptic problems to prove existence and uniqueness for the linear elasticity problem (1.4.7).

Lemma 1.5.1 (Lax–Milgram) *Let $a(\cdot,\cdot) : V \times V \to \mathbb{R}$ be a continuous and elliptic bilinear form with constants α and β, respectively. Then, for all $f \in V^*$ there exists a unique solution $u \in V$ of the problem*

$$a(u,v) = f(v), \qquad \text{for all } v \in V \tag{1.5.1}$$

and there holds the stability estimate

$$\|u\|_V \leq \frac{1}{\beta}\|f\|_{V^*}. \tag{1.5.2}$$

Surprisingly, the full gradient of a vector valued function can be bounded by its symmetric part, cf. [20], at the cost of possibly large constants for anisotropic domains.

Lemma 1.5.2 (Korn's inequality) *Let Ω be a connected and bounded Lipschitz domain (i.e., the boundary can locally be parameterized by a Lipschitz function). Then there exists a constant $\hat{c}_K > 0$ such that*

$$\hat{c}_K^2 \|u\|_{H^1}^2 \leq \|u\|_{L^2}^2 + \|\boldsymbol{\varepsilon}(u)\|_{L^2}^2 \tag{1.5.3}$$

for all $u \in H^1(\Omega, \mathbb{R}^d)$ and $\hat{c}_K$ depends only on Ω. Assume further that $\Gamma_D \subset \partial\Omega$ has positive measure. Then there exists a constant $c_K > 0$ such that

$$c_K^2 \|u\|_{H^1}^2 \leq \|\boldsymbol{\varepsilon}(u)\|_{L^2}^2 \tag{1.5.4}$$

for all $u \in H^1_{\Gamma_D}(\Omega, \mathbb{R}^d)$. The constants $\hat{c}_K$ and c_K tend to zero for deteriorating aspect ratio.

Korn's inequality relies on the fact that by setting Dirichlet boundary conditions at parts of the boundary the kernel of the symmetric gradient operator consisting of linearized rigid body motions

$$\ker \boldsymbol{\varepsilon}(\cdot) = RB^{\text{lin}} := \{\Phi(x) = \boldsymbol{A}\, x + b \,|\, b \in \mathbb{R}^d,\, \boldsymbol{A} \in \mathbb{R}^{d\times d} \text{ with } \boldsymbol{A}^\top = -\boldsymbol{A}\} \tag{1.5.5}$$

is locked.

Corollary 1.5.3 *The bilinear form*

$$a(u, v) := \int_\Omega 2\mu\, \boldsymbol{\varepsilon}(u) : \boldsymbol{\varepsilon}(v) + \lambda \operatorname{div} u \operatorname{div} v \, dx \tag{1.5.6}$$

is continuous and coercive (elliptic) with

$$\begin{aligned} |a(u, v)| &\leq (2\mu + \lambda) \|u\|_{H^1} \|v\|_{H^1}, \\ a(u, u) &\geq 2\mu\, c_K^2 \|u\|_{H^1}^2. \end{aligned}$$

Céa's lemma yields the following a-prior finite element error estimate for Lagrange elements $u_h \in U_h \subset U$

$$\|u - u_h\|_{H^1}^2 \leq \frac{2\mu + \lambda}{2\mu\, c_K^2} \inf_{v_h \in U_h} \|u - v_h\|_{H^1}^2, \tag{1.5.7}$$

from which we deduce that the problem is ill conditioned if the material is nearly incompressible, $\lambda \gg \mu$, or the geometry is anisotropic leading a small Korn constant, $c_K \ll 1$.

Exercise 1.5.4

1. *Proof Corollary 1.5.3 and that the right-hand sides* (1.4.7) *are continuous functionals in $H^1(\Omega, \mathbb{R}^d)$.*
2. *Show that Korn's inequality is sharp by constructing a specific displacement on $\Omega = (0, 1) \times (-t/2, t/2)$ and $U = \{u \in H^1(\Omega, \mathbb{R}^2) \,|\, u(0, \cdot) = 0\}$ and showing that $c_K \leq ct$. Hint: Find u such that $\|\boldsymbol{\varepsilon}(u)\|^2 / \|\nabla u\| \leq ct^2$.*

Chapter 2

Beams and Plates

2.1 Timoschenko and Bernoulli beam

We saw in the previous chapter that for strong anisotropic structures the elasticity problem is ill-posed (due to Korn's inequality) and numerical simulations showed so-called locking behavior. Discretizing thin-walled structures with isotropic (small) elements is rather inefficient due to the huge amount of elements needed. Using elements reflecting the structure and aspect ratio would be more economic, but lead to (shear) locking behavior. For structures, where one dimension is of magnitudes smaller than the other directions it is expected that the behavior of the material in this direction can be described with a less amount of parameters such that a dimension reduction to the mid-surface is an attractive strategy. One has to mesh and discretize objects of one dimension less leading to smaller matrices. Additionally to the computational speed-up it was hoped that the locking behavior of full elasticity is cured. However, as we will see, the shear locking problem is shifted but not circumvented. Nevertheless, the resulting beam and plate equations yield more insight into the problem, which will be useful when going to general (nonlinear) shells

2.1.1 Dimension reduction to beams

If we have a structure $\Omega \subset \mathbb{R}^2$ where one dimension is significantly thinner than the other a dimension reduction to a one-dimensional problem can be done. If the two-dimensional structure is of the form $\Omega = (0,1) \times (-t/2, t/2)$ we can perform a reduction to the mid-surface $\mathcal{S} = (0,1) \times \{0\}$. We assume for simplicity that Dirichlet boundary conditions are prescribed on the left and right boundary $\{0,1\} \times (-t/2, t/2)$ and Neumann boundaries at the top and bottom.

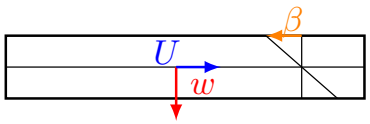

Figure 2.1: Horizontal deflection U, vertical deflection w, and rotation of normal β of a beam.

To derive the beam equation in the setting of linear elasticity we start with a Galerkin-semidiscretization by approximating an infinite sum in the thickness direction

$$u = (u^x, u^y) \approx \left(\sum_{i=0}^{N_x} u_i^x(x) y^i, \sum_{i=0}^{N_y} u_i^y(x) y^i \right). \tag{2.1.1}$$

We consider the lowest possible order, where the (linearized) rigid body motions are included, $N_x = 1$ and $N_y = 0$, leading to

$$u = (U(x) - y\,\beta(x), w(x)). \tag{2.1.2}$$

Here, $U(x)$ and $w(x)$ correspond to the horizontal and vertical deflection, respectively, and $\beta(x)$ is the rotation of the normal vector on the initial configuration, cf. Figure 2.1. Analogously, the test function is given by $v = (V(x) - y\delta(x), v(x))$. Inserting into the equation of linear elasticity (1.4.7) we obtain

$$\varepsilon(u) = \begin{pmatrix} U' - y\beta' & \frac{1}{2}(w' - \beta) \\ \frac{1}{2}(w' - \beta) & 0 \end{pmatrix}, \qquad \varepsilon(v) = \begin{pmatrix} V' - y\delta' & \frac{1}{2}(v' - \delta) \\ \frac{1}{2}(v' - \delta) & 0 \end{pmatrix},$$

$$\varepsilon(u) : \varepsilon(v) = (U' - y\beta')(V' - y\delta') + \frac{1}{2}(w' - \beta)(v' - \delta), \qquad \operatorname{div}(u)\operatorname{div}(v) = (U' - y\beta')(V' - y\delta')$$

and further

$$\begin{aligned} a(u,v) &= \int_0^1 \int_{-t/2}^{t/2} 2\mu\, \varepsilon(u) : \varepsilon(v) + \lambda \operatorname{div}(u) \operatorname{div}(v)\, dy\, dx \\ &= \int_0^1 \int_{-t/2}^{t/2} (2\mu + \lambda)(U' - y\beta')(V' - y\delta') + \frac{\mu}{2}(w' - \beta)(v' - \delta)\, dy\, dx \\ &= \int_0^1 (2\mu + \lambda) t\, U'V' + (2\mu + \lambda)\frac{t^3}{12}\beta'\delta' + \frac{t\,\mu}{2}(w' - \beta)(v' - \delta)\, dx. \end{aligned}$$

Assuming that the force is independent of the thickness direction $f = (f^x(x), f^y(x))$ the elasticity problem decouples into a Poisson-like *membrane problem*: Find $U \in H^1_0((0,1))$ such that for all $V \in H^1_0((0,1))$

$$(2\mu + \lambda)t \int_0^1 U'V' \, dx = t \int_0^1 f^x V \, dx \tag{2.1.3}$$

and the *bending problem*: Find $(w, \beta) \in H^1_0((0,1)) \times H^1_0((0,1))$ such that for all $(v, \delta) \in H^1_0((0,1)) \times H^1_0((0,1))$

$$(2\mu + \lambda)\frac{t^3}{12} \int_0^1 \beta'\delta' \, dx + \frac{t\,\mu}{2} \int_0^1 (w' - \beta)(v' - \delta) \, dx = t \int_0^1 f^y v \, dx. \tag{2.1.4}$$

Neglecting the Lamé parameters and constants and rescaling the right-hand side $f := \frac{1}{t^2} f^y$ we obtain the *Timoshenko beam* (also called Timoshenko–Ehrenfest beam): Find $(w, \beta) \in H^1_0((0,1)) \times H^1_0((0,1))$ such that for all $(v, \delta) \in H^1_0((0,1)) \times H^1_0((0,1))$

$$\int_0^1 \beta'\delta' \, dx + \frac{1}{t^2} \int_0^1 (w' - \beta)(v' - \delta) \, dx = \int_0^1 f\, v \, dx, \tag{2.1.5}$$

which corresponds to the minimization problem

$$\mathcal{W}(w, \beta) := \frac{1}{2} \int_0^1 (\beta')^2 \, dx + \frac{1}{2t^2} \int_0^1 (w' - \beta)^2 \, dx - \int_0^1 f\, w \, dx \to \min!. \tag{2.1.6}$$

The first term is the bending energy of the beam, measuring how strong the beam gets curved. The second term is called the shearing energy, which measures how much the deformed normal of the initial configuration deviates from the normal of the deformed configuration (given by w').

Obviously, the Timoshenko beam involves a parameter, the thickness t, such that the bending and shearing parts are scaled differently. Although the Timoshenko beam is $H^1_0 \times H^1_0$ elliptic, its constant depends on the thickness, which leads with Céa's Lemma a parameter dependent a-prior error estimate

$$\|(w_h, \beta_h) - (w, \beta)\|_X \le c(t) \inf_{(v_h, \delta_h) \in X_h} \|(v_h, \delta_h) - (w, \beta)\|_X. \tag{2.1.7}$$

In the limit of vanishing thickness, $t \to 0$, it acts as a penalty enforcing the constraint $\beta = w'$. Therefore, in the limit we can eliminate the rotation β leading to the fourth order minimization problem

$$\mathcal{W}(w) = \frac{1}{2} \int_0^1 (w'')^2 \, dx - \int_0^1 f\, w \, dx \to \min!, \tag{2.1.8}$$

which corresponds to the variational formulation: Find $w \in H^2_0((0,1))$ such that for all $v \in H^2_0((0,1))$

$$\int_0^1 w''v'' \, dx = \int_0^1 f\, v \, dx. \tag{2.1.9}$$

This fourth order ODE problem is called the *Euler–Bernoulli beam*.

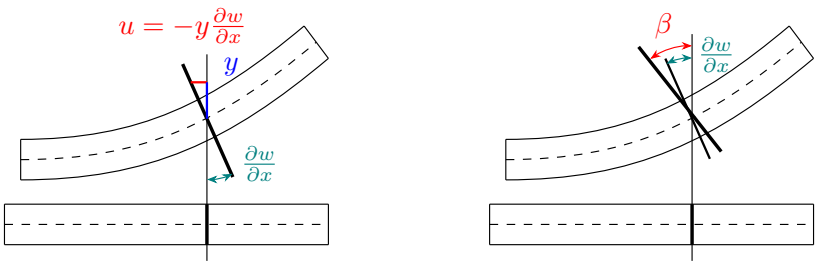

Figure 2.2: Rotation of Euler–Bernoulli beam and Timoshenko beam.

2.1.2 Discretization of Timoshenko beam

A straight forward discretization is to use Lagrangian finite elements of same order for the displacement and rotation $(w_h, \beta_h) \in U_h^k \times U_h^k$, which we will see may induce locking for small thickness parameter t. In the limit $t \to 0$ the shearing energy can be seen as penalty enforcing $w_h' = \beta_h$. In the lowest order case this identity forces the piece-wise constant w_h' to fit with the linear and continuous β_h leading to the trivial solution, $w_h = \beta_h = 0$. From the theory of mixed methods we will see that inserting an L^2-projection into the shearing term cures this problem be relaxing the constraint. In 1D this is equivalent to a numerical under-integration using only the mid-point rule for the shearing term. Using for w_h one polynomial order higher than β_h improves the locking behavior. This, however, leads to sub-optimal (linear) convergence rates for β. In Section 2.1.4 we analyze and present a shear locking free (discretized) method for the Timoshenko beam.

In the derivation we used clamped boundary conditions, $u, \beta \in H_0^1((0,1))$. Other boundary conditions like free, simply supported or constraint rotation are possible, define $Q := \frac{1}{t^2}(w' - \beta)$ and $M := \beta'$:

boundary condition	w	β	
clamped	D	D	$w = 0$, $\beta = 0$
simply supported	D	N	$w = 0$, $M = 0$
free	N	N	$Q = 0$, $M = 0$
constraint rotation	N	D	$Q = 0$, $\beta = 0$

Exercise 2.1.1 *Derive, implement, and test the different boundary conditions for the Timoshenko beam. Motivate the physical quantities Q and M.*

In the limit $t \to 0$ the equality $w' = \beta$ holds. Therefore, the rotation β has to coincide with the linearized normal vector of the deformed beam and can be eliminated from the equation leading to the Euler–Bernoulli beam.

2.1.3 Discretization of Euler–Bernoulli beam

Note that in contrast to the Timoshenko beam the thickness parameter t does not enter the Euler–Bernoulli beam equation anymore. Therefore it does not suffer from locking, but C^1-conforming finite elements are required as we are facing now a fourth order problem. In 1D the construction of C^1-elements is easy by e.g. Hermite polynomials. For higher dimensions this task is much more involved, especially if unstructured (triangular) grids are required. As pre-work for plates and shells we therefore focus on formulations enabling Lagrangian elements for the vertical deflection w.

Let us rewrite the Euler–Bernoulli beam as a mixed saddle-point problem by introducing the linearized moments $\sigma = w''$ as additional unknown

$$\int_0^1 \sigma\tau \, dx \qquad - \int_0^1 w''\tau \, dx = 0 \qquad \text{for all } \tau, \tag{2.1.10a}$$

$$- \int_0^1 \sigma \, v'' \, dx \qquad = - \int_0^1 f \, v \, dx \quad \text{for all } v, \tag{2.1.10b}$$

and use integration by parts such that all terms are well defined for $(w, \sigma) \in H_0^1((0,1)) \times H^1((0,1))$

$$\int_0^1 \sigma\tau \, dx \; + \int_0^1 w'\tau' \, dx = 0 \qquad \text{for all } \tau \in H^1((0,1)), \tag{2.1.11a}$$

$$\int_0^1 \sigma' v' \, dx \qquad = - \int_0^1 f \, v \, dx \quad \text{for all } v \in H_0^1((0,1)). \tag{2.1.11b}$$

We can use Lagrange finite elements for discretization. In the next section we show that this leads to a stable formulation and method.

Exercise 2.1.2 *Show that $\sigma \in H^1((0,1))$ together with $w \in H_0^1((0,1))$ leads to clamped boundary conditions, $w = w' = 0$. What changes if $\sigma \in H_0^1((0,1))$? How can we incorporate free boundary conditions at $x = 1$ and clamped boundary conditions at $x = 0$?*

2.1.4 Analysis of Timoshenko and Euler–Bernoulli beam

For analyzing mixed saddle-point problems the Lax–Milgram Lemma cannot be applied due to the missing coercivity on the whole product space. Brezzi's Theorem gives sufficient conditions proofing well-posedness for this kind of problems.

Brezzi's Theorem for saddle point problems

Indefinite saddle-point problems, arising e.g., for minimization problems under constrains, are of the following general form: Find $(u,p) \in V \times Q$ such that for all $(v,q) \in V \times Q$

$$a(u,v) + b(v,p) = f(v), \tag{2.1.12a}$$
$$b(u,q) \qquad\quad = g(q). \tag{2.1.12b}$$

Equation (2.1.12b) enforces a constraint on u, which can be incorporated as a penalty formulation yielding the structure ($t > 0$ small)

$$a(u,v) + b(v,p) \;= f(v), \tag{2.1.13a}$$
$$b(u,q) - t\,c(p,q) = g(q). \tag{2.1.13b}$$

Theorem 2.1.3 (Brezzi) *Assume that $a(\cdot,\cdot) : V \times V \to \mathbb{R}$ and $b(\cdot,\cdot) : V \times Q \to \mathbb{R}$ are continuous bilinear forms, i.e.,*

$$|a(u,v)| \le \alpha_2 \|u\|_V \|v\|_V \quad \text{for all } u,v \in V, \tag{2.1.14}$$
$$|b(u,q)| \le \beta_2 \|u\|_V \|q\|_Q \quad \text{for all } u \in V, \text{ for all } q \in Q. \tag{2.1.15}$$

Assume there holds coercivity of $a(\cdot,\cdot)$ on the kernel, i.e.,

$$a(u,u) \ge \alpha_1 \|u\|_V^2 \quad \text{for all } u \in V_0, \tag{2.1.16}$$
$$V_0 := \{u \in V \mid b(u,q) = 0 \quad \text{for all } q \in Q\} \tag{2.1.17}$$

and there holds the Ladyzhenskaya–Babuška–Brezzi (LBB) condition

$$\sup_{u \in V} \frac{b(u,q)}{\|u\|_V} \ge \beta_1 \|q\|_Q \quad \text{for all } q \in Q. \tag{2.1.18}$$

Then, the mixed problem (2.1.12) *is uniquely solvable. The solution fulfills the stability estimate*

$$\|u\|_V + \|p\|_Q \le c\,(\|f\|_{V^*} + \|g\|_{Q^*}) \tag{2.1.19}$$

with the constant c depending on $\alpha_1, \alpha_2, \beta_1$, and β_2.

Theorem 2.1.4 (extended Brezzi) *Assume all requirements of Theorem 2.1.3 are fulfilled. Further, let $c(\cdot,\cdot)$ be a continuous and non-negative bilinear form and $a(\cdot,\cdot)$ non-negative. Then, for $t \le 1$, the mixed problem* (2.1.13) *has a unique solution, fulfilling the following stability estimate independent of t*

$$\|u\|_V + \|p\|_Q \le c\,(\|f\|_{V^*} + \|g\|_{Q^*})\,, \qquad c \ne c(t). \tag{2.1.20}$$

Analysis of Timoshenko beam

We analyze the Timoshenko beam as mixed formulation by defining the shear $\gamma = \frac{1}{t^2}(w' - \beta)$ as additional unknown: Find $(w,\beta,\gamma) \in H_0^1((0,1)) \times H_0^1((0,1)) \times L^2((0,1))$ such that for all $(v,\delta,\xi) \in H_0^1((0,1)) \times H_0^1((0,1)) \times L^2((0,1))$

$$\int_0^1 \beta'\delta'\,dx \qquad + \int_0^1 (v' - \delta)\gamma\,dx = \int_0^1 f\,v\,dx, \tag{2.1.21a}$$
$$\int_0^1 (w' - \beta)\xi\,dx - t^2 \int_0^1 \gamma\,\xi\,dx \qquad = 0. \tag{2.1.21b}$$

Note, that we multiplied (2.1.21b) with t^2 such that the thickness appears in the numerator. The limit case $t = 0$ is therefore well-defined.

Proposition 2.1.5 *The mixed formulation of the Timoshenko beam* (2.1.21) *is uniquely solvable and stable.*

Proof: Continuity of the bilinear forms as well as non-negativity of $a(\cdot,\cdot)$ and $c(\cdot,\cdot)$ is obvious.

On the kernel

$$\begin{aligned} B_0 &= \Big\{(w,\beta) \in H_0^1((0,1)) \times H_0^1((0,1)) \,\Big|\, \int_0^1 (w'-\beta)\gamma \, dx = 0 \text{ for all } \gamma \in L^2((0,1))\Big\} \\ &= \{(w,\beta) \in H_0^1((0,1)) \times H_0^1((0,1)) \,|\, w' = \beta\} \end{aligned}$$

there holds with Friedrichs's inequality[1]

$$\|\beta'\|_{L^2}^2 = \frac{1}{2}|\beta|_{H^1}^2 + \frac{1}{2}|\beta|_{H^1}^2 \geq c\left(\|\beta\|_{H^1}^2 + \|\beta\|_{L^2}^2\right) \geq c\left(\|\beta\|_{H^1}^2 + \|w\|_{H^1}^2\right). \tag{2.1.22}$$

Further, following [10], for given $\gamma \in L^2((0,1))$ define $\rho(x) := x(1-x)$ and

$$A := \int_0^1 \gamma(s)\, ds \,/ \int_0^1 \rho(s)\, ds, \quad w(x) := \int_0^x \gamma(s)\, ds - A\int_0^x \rho(s)\, ds, \quad \beta(x) := -A\rho(x).$$

Then $\rho, w, \beta \in H_0^1((0,1))$ and there holds with a constant $c > 0$, $\|w'\|_{L^2} \leq c\|\gamma\|_{L^2}$, $\|\beta'\|_{L^2} \leq c\|\gamma\|_{L^2}$, and $w' - \beta = \gamma$. Thus, the LBB condition is fulfilled

$$\sup_{(w,\beta)\in H^1\times H^1} \frac{\int_0^1 (w'-\beta)\gamma \, dx}{\|w\|_{H^1} + \|\beta\|_{H^1}} \geq \frac{\|\gamma\|_{L^2}^2}{\|w'\|_{L^2} + \|\beta'\|_{L^2}} \geq \frac{1}{2c}\|\gamma\|_{L^2}. \tag{2.1.23}$$

Brezzi's Theorem 2.1.4 now finishes the proof giving the robust estimate

$$\|\beta\|_{H^1} + \|w\|_{H^1} + \frac{1}{t^2}\|w' - \beta\|_{L^2} \leq c\|f\|_{H^{-1}}, \quad c \neq c(t). \tag{2.1.24}$$

□

Using Lagrange elements for w and β and one polynomial order less L^2-conforming discontinuous (i.e. piece-wise polynomials) elements for γ gives a stable discretization for the Timoshenko beam, which can easily be shown (Exercise!). We obtain the optimal t-independent convergence rates:

Corollary 2.1.6 *Let (w,β,γ) be the solution of the continuous problem* (2.1.21) *and $(w_h,\beta_h,\gamma_h) \in U_{h,0}^k \times U_{h,0}^k \times Q_h^{k-1}$ (see Section 2.3 for the discrete spaces) the corresponding discrete one for a positive integer k. If the exact solution is smooth enough there holds*

$$\|w - w_h\|_{H^1} + \|\beta - \beta_h\|_{H^1} + \|\gamma - \gamma_h\|_{L^2} \leq ch^k(\|w\|_{H^{k+1}} + \|\beta\|_{H^{k+1}} + \|\gamma\|_{H^k}), \qquad c \neq c(t). \tag{2.1.25}$$

The second equality (2.1.21b) states in the discrete case that the shearing can be expressed as $\gamma_h = \frac{1}{t^2}\Pi^{L^2,k-1}(w_h' - \beta_h)$. Inserting this into the first equation (2.1.21a) yields the problem: Find $(w_h,\beta_h) \in U_{h,0}^k \times U_{h,0}^k$ such that for all $(v_h,\delta_h) \in U_{h,0}^k \times U_{h,0}^k$

$$\int_0^1 \beta_h'\delta_h' \, dx + \frac{1}{t^2}\int_0^1 \Pi^{L^2,k-1}(w_h' - \beta_h)\Pi^{L^2,k-1}(v_h' - \delta_h)\, dx = \int_0^1 f\, v_h \, dx, \tag{2.1.26}$$

which corresponds to a numerical under-integration of the shear term. E.g., in the lowest-order case the projection into piece-wise constants can be realized by using the mid-point rule for numerical integration.

As this (non-standard) primal method is equivalent to the mixed formulation we obtain the same stability and convergence results. Its advantage is that a positive definite stiffness matrix is obtained, whereas the mixed system leads to an indefinite matrix.

[1] Friedrich: $\|u\|_{H^1} \leq c_F|u|_{H^1}, \quad$ for all $u \in H_0^1(\Omega)$

Remark 2.1.7 *When using at least quadratic polynomials for the vertical deflection and rotation no shear locking occurs for the Timoshenko beam anymore, however, convergence rates with a sub-optimal rate are obtained for β in a pre-asymptotic regime depending on t. As we will see later for the Reissner–Mindlin plate (the 2D analog to the Timoshenko beam) its analysis and numerical treatment to avoid shear locking is more involved.*

Remark 2.1.8 *Setting $t = 0$ in* (2.1.21b) *leads a stable discretization for the Euler–Bernoulli beam.*

Exercise 2.1.9 *Show with Remark 2.1.8, that the solution of the Timoshenko beam $(w, \beta, \gamma)^{\mathrm{TB}}$ converges to the Euler–Bernoulli beam solution $(w, \beta, \gamma)^{\mathrm{EBB}}$*

$$\|(w, \beta, \gamma)^{\mathrm{TB}} - (w, \beta, \gamma)^{\mathrm{EBB}}\| \leq c\, t^2, \qquad c \neq c(t). \tag{2.1.27}$$

Hint: Take the difference of the solutions as new unknown for the difference of the corresponding equations and use Brezzi's Theorem.

2.1.5 Analysis of Bernoulli beam

From the Lax–Milgram Lemma we directly deduce that the Euler–Bernoulli beam is well-posed on $H_0^2((0,1))$ and Céa's Lemma yields a standard a-prior error estimate. The big drawback is that we need C^1 finite elements for a conforming discretization. In 1D Hermite polynomials are directly applicable, however, extensions to 2D Kirchhoff–Love plates are complicated. Therefore, we analyze the mixed method (2.1.11) with Brezzi enabling the usage of Lagrange finite elements.

Proposition 2.1.10 *The mixed formulation* (2.1.11) *of the Euler–Bernoulli beam yields a unique solution.*

Proof: By choosing $\sigma = w$ the LBB condition is obviously fulfilled. The kernel

$$V_0 = \left\{ \sigma \in H^1((0,1)) \,\middle|\, \int_0^1 \sigma' w' = 0, \quad \text{for all } w \in H_0^1((0,1)) \right\} = \{\sigma = ax + b \,|\, a, b \in \mathbb{R}\}$$

consists only of linear functions. As on finite dimensional spaces all norms are equivalent the kernel coercivity is also fulfilled. All bilinear forms are continuous with respect to the H^1-norm such that the conditions for Brezzi's theorem 2.1.3 are fulfilled. □

2.2 Reissner–Mindlin and Kirchhoff–Love plates

After the derivation of the beam equations we focus next on the 2D extension to plates, which can be derived from 3D elasticity.

2.2.1 Reissner–Mindlin plate equation

Assuming a thin three-dimensional plate $\Omega = (0,1)^2 \times (-t/2, t/2)$ we can perform analogously to beams a dimension reduction to the mid-surface $\mathcal{S} = (0,1)^2 \times \{0\}$ by a semi-discretization approach, which ansatz would read

$$u = (U_1(x,y) - z\beta_1(x,y), U_2(x,y) - z\beta_2(x,y), w(x,y)). \tag{2.2.1}$$

Note, that the horizontal displacement $U = (U_1, U_2)$ and the rotation $\beta = (\beta_1, \beta_2)$ are now two-dimensional quantities, whereas the vertical deflection w is again a scalar. Inserting into the three-dimensional elasticity problem and integrating over the thickness-direction would lead to a (less interesting) membrane problem and the Reissner–Mindlin plate-bending problem (Exercise!).

Again, we assume the structure to be clamped on all boundaries except the top and bottom one, where homogeneous Neumann boundary conditions are prescribed. We, however, consider a second different approach of derivation in this section, which leads to the same plate-bending equation. Therefore we postulate kinematic assumptions, which are named after Reissner and Mindlin:

H1. Lines normal to the mid-surface get deformed linearly, they remain lines.

H2. The displacements in z-direction are independent of the z-coordinate.

H3. Points on the mid-surface can only be deformed in z-direction.

H4. Stresses $\boldsymbol{\sigma}_{33}$ in normal direction vanish (called plane-stress assumption).

With H1–H3 the displacements are of the form

$$u_1(x,y,z) = -z\beta_1(x,y), \qquad u_2(x,y,z) = -z\beta_2(x,y), \qquad u_3(x,y,z) = w(x,y). \tag{2.2.2}$$

Hypothesis H3 directly enforces that the horizontal displacements of the membrane problem is eliminated and yields together with H1 the form of the shearing related horizontal displacements u_1 and u_2. H2 in combination with H1 gives the form of the vertical displacement. Assumption H4 is needed as from $u_3 = w(x,y)$ there follows $\boldsymbol{\varepsilon}_{33}(u) = 0$, i.e., no strains in thickness direction. Using (1.4.1) to compute $\boldsymbol{\sigma}_{33}$ yields $\boldsymbol{\sigma}_{33} = \frac{E}{(1+\nu)(1-2\nu)}\left((1-\nu)\boldsymbol{\varepsilon}_{33} + \nu(\boldsymbol{\varepsilon}_{11}+\boldsymbol{\varepsilon}_{22})\right) = \lambda(\boldsymbol{\varepsilon}_{11}+\boldsymbol{\varepsilon}_{22}) \neq 0$ in general. This is non-physical and leads to a not asymptotically correct model. It induces a too stiff behavior yielding artificial stiffness. Therefore $\boldsymbol{\sigma}_{33} = 0$ is postulated to re-obtain an asymptotically correct model, which converges to the 3D solution in the limit of vanishing thickness. Setting $\boldsymbol{\sigma}_{33} = 0$ induces that the material can stretch in thickness direction without inducing stresses.

Remark 2.2.1 *Increasing the ansatz that the vertical deflection is linear in z, $u_3(x,y,z) = w(x,y) + z\tilde{w}(x,y)$, where the linear term corresponds to the change of thickness, does not cure the problem and $\boldsymbol{\sigma}_{33} = 0$ has still to be forced. One needs to use a quadratic approach for u_3 to obtain an asymptotically correct model without the need of changing the 3D material law a prior.*

The 3D elasticity strain tensor now reads with (2.2.2)

$$\boldsymbol{\varepsilon}(u) = \begin{pmatrix} -z\partial_1\beta_1 & -z\frac{1}{2}(\partial_2\beta_1 + \partial_1\beta_2) & \frac{1}{2}(\partial_1 w - \beta_1) \\ & -z\partial_2\beta_2 & \frac{1}{2}(\partial_2 w - \beta_2) \\ \text{sym} & & 0 \end{pmatrix} \tag{2.2.3}$$

From H4, $\boldsymbol{\sigma}_{33} = 0$, we can express $\boldsymbol{\varepsilon}_{33} = -\frac{\nu}{1-\nu}(\boldsymbol{\varepsilon}_{11}+\boldsymbol{\varepsilon}_{22})$ by using (1.4.1) and reinserting yields

$$\begin{pmatrix} \boldsymbol{\sigma}_{11} \\ \boldsymbol{\sigma}_{22} \\ \boldsymbol{\sigma}_{12} \\ \boldsymbol{\sigma}_{13} \\ \boldsymbol{\sigma}_{23} \end{pmatrix} = \frac{E}{1-\nu^2} \begin{pmatrix} 1 & \nu & & 0 & \\ \nu & 1 & & & \\ & & 1-\nu & & \\ & & & 1-\nu & \\ & 0 & & & 1-\nu \end{pmatrix} \begin{pmatrix} \boldsymbol{\varepsilon}_{11} \\ \boldsymbol{\varepsilon}_{22} \\ \boldsymbol{\varepsilon}_{12} \\ \boldsymbol{\varepsilon}_{13} \\ \boldsymbol{\varepsilon}_{23} \end{pmatrix}. \tag{2.2.4}$$

E.g., there holds

$$\begin{aligned} \boldsymbol{\sigma}_{11} &= \frac{E}{(1+\nu)(1-2\nu)}\left((1-\nu)\boldsymbol{\varepsilon}_{11} + \nu\boldsymbol{\varepsilon}_{22} + \nu\boldsymbol{\varepsilon}_{33}\right) \\ &= \frac{E}{(1+\nu)(1-2\nu)}\left((1-\nu-\frac{\nu^2}{1-\nu})\boldsymbol{\varepsilon}_{11} + (\nu-\frac{\nu^2}{1-\nu})\boldsymbol{\varepsilon}_{22}\right) \\ &= \frac{E}{(1-\nu^2)(1-2\nu)}\left((1-2\nu+\nu^2-\nu^2)\boldsymbol{\varepsilon}_{11} + (\nu-2\nu^2)\boldsymbol{\varepsilon}_{22}\right) = \frac{E}{1-\nu^2}(\boldsymbol{\varepsilon}_{11}+\nu\boldsymbol{\varepsilon}_{22}). \end{aligned}$$

The energy $\|\boldsymbol{\varepsilon}\|_{\mathcal{C}}^2 = \mathcal{C}\boldsymbol{\varepsilon} : \boldsymbol{\varepsilon} = \boldsymbol{\sigma} : \boldsymbol{\varepsilon}$ reads

$$\boldsymbol{\sigma} : \boldsymbol{\varepsilon} = \sum_{i,j=1}^{2} \boldsymbol{\sigma}_{ij}\boldsymbol{\varepsilon}_{ij} + 2\sum_{j=1}^{2} \boldsymbol{\varepsilon}_{3j}\boldsymbol{\sigma}_{3j} = \frac{E}{1+\nu}\Big(\sum_{i,j=1}^{2} \boldsymbol{\varepsilon}_{ij}^2 + \frac{\nu}{1-\nu}(\boldsymbol{\varepsilon}_{11}+\boldsymbol{\varepsilon}_{22})^2 + 2\sum_{j=1}^{2}\boldsymbol{\varepsilon}_{3j}^2\Big).$$

Next, we integrate the arising terms over the thickness and insert the strain definition (2.2.3)

$$\int_{-t/2}^{t/2} \sum_{i,j=1}^{2} \varepsilon_{ij}^2 \, dz = \int_{-t/2}^{t/2} z^2 \underline{\varepsilon}(\beta) : \underline{\varepsilon}(\beta) \, dz = \frac{t^3}{12} \underline{\varepsilon}(\beta) : \underline{\varepsilon}(\beta),$$
$$\int_{-t/2}^{t/2} (\varepsilon_{11} + \varepsilon_{22})^2 \, dz = \frac{t^3}{12} \underline{\operatorname{div}}(\beta)^2,$$
$$\int_{-t/2}^{t/2} 2 \sum_{j=1}^{2} \varepsilon_{3j}^2 \, dz = \int_{-t/2}^{t/2} \frac{2}{4} (\underline{\nabla} w - \beta) \cdot (\underline{\nabla} w - \beta) \, dz = \frac{t}{2} \|\underline{\nabla} w - \beta\|^2,$$

where $\underline{\nabla}$, $\underline{\varepsilon}$, and $\underline{\operatorname{div}}$ denote the differential operators acting only on the first two indices $i, j = 1, 2$. Thus, the total energy $\mathcal{W}(w, \beta) = \frac{1}{2} \int_\Omega \boldsymbol{\sigma} : \boldsymbol{\varepsilon} \, d(x, y, z)$ becomes with the notation $ds = d(x, y)$

$$\mathcal{W}(w, \beta) = \frac{1}{2} \int_{\mathcal{S}} \boldsymbol{\sigma} : \boldsymbol{\varepsilon} \, d(s, z) = \frac{t^3 E}{24(1 - \nu^2)} \int_{\mathcal{S}} (1 - \nu) \|\underline{\varepsilon}(\beta)\|^2 + \nu \, \underline{\operatorname{div}}(\beta)^2 \, ds + \frac{Gt}{2} \int_{\mathcal{S}} \|\underline{\nabla} w - \beta\|^2 \, ds, \tag{2.2.5}$$

where $G = \frac{E}{2(1+\nu)}$ denotes the shearing modulus. Classically, the shear correction factor $\kappa = \frac{5}{6}$ is additionally inserted into the shearing energy term to compensate high-order effects of the shear stresses, which are not constant through the thickness (in some variational methods to derive plate equations the factor 5/6 directly appears).

The right-hand side f is assumed to act only vertically on the plate and is independent of the thickness $f = (0, 0, f^z(x, y))$. Integrating over the thickness and rescaling $f := t^{-2} f^z$ leads to the term $t^3 \int_{\mathcal{S}} f \, v \, ds$.

To simplify notation we set $\Omega = \mathcal{S}$, use dx for integration over the mid-surface, neglect the underline for the differential operators, and define the plate elasticity tensor

$$\mathcal{C}\boldsymbol{A} := \frac{E}{1 - \nu^2} ((1 - \nu)\boldsymbol{A} + \nu \operatorname{tr}(\boldsymbol{A})\boldsymbol{I}). \tag{2.2.6}$$

Note, that after the elimination of $\boldsymbol{\varepsilon}_{33}$ the Poisson ratio $\nu \in (0, 1)$ is allowed instead of $(0, \frac{1}{2})$.

All together, taking the variations of energy (2.2.5) (with the shear correction factor κ) and dividing by t^3 yields the clamped *Reissner–Mindlin plate equation*: Find $(w, \beta) \in H_0^1(\Omega) \times H_0^1(\Omega, \mathbb{R}^2)$ such that for all $(v, \delta) \in H_0^1(\Omega) \times H_0^1(\Omega, \mathbb{R}^2)$

$$\frac{1}{12} \int_\Omega \mathcal{C}\boldsymbol{\varepsilon}(\beta) : \boldsymbol{\varepsilon}(\delta) \, dx + \frac{\kappa G}{t^2} \int_\Omega (\nabla w - \beta) \cdot (\nabla v - \delta) \, dx = \int_\Omega f \, v \, dx. \tag{2.2.7}$$

Depending on the different combination of Dirichlet and Neumann boundary conditions for the vertical deflection w and the rotations β we distinguish between the following plate boundary conditions. Let $\boldsymbol{M} := \frac{1}{12} \mathcal{C}\boldsymbol{\varepsilon}(\beta)$ be the bending moment tensor and $Q := \frac{\kappa G}{t^2} (\nabla w - \beta)$ the shear force.

boundary condition	w	β_n	β_t	
clamped	D	D	D	$w = 0$, $\beta = 0$
free	N	N	N	$Q \cdot n = 0$, $\boldsymbol{M} n = 0$
hard simply supported	D	N	D	$w = 0$, $n^\top \boldsymbol{M} n = 0$, $\beta_t = 0$
soft simply supported	D	N	N	$w = 0$, $\boldsymbol{M} n = 0$

Table 2.1: Reissner–Mindlin plate boundary conditions spitted into the vertical deflection and normal/tangential components of the rotations. D denotes Dirichlet and N Neumann boundary.

By identifying e.g. two opposite edges also periodic boundary conditions can be prescribed.

Exercise 2.2.2 *Derive the boundary conditions for w, β, $\boldsymbol{M}$, and Q from the Reissner–Mindlin equations. What condition is obtained when using Dirichlet boundary conditions for w and β_n and Neumann for β_t?*

The Reissner–Mindlin plate equations entail additionally to shear locking possible boundary layers, where the (stress) solutions rapidly change. For generating accurate solutions these boundary layers need to be resolved. The scaling of the layer is of order $\mathcal{O}(t)$ and the strength differ on the prescribed boundary conditions. For clamped and hard simply supported plates the boundary layer is less intensive than for free and soft simply supported. An asymptotic boundary layer analysis can be found e.g. in [2]. An explanation of the appearance of boundary layers is that on the one hand we have prescribed the rotations at the boundary and on the other hand, for $t \to 0$, the equality $\nabla w = \beta$ is enforced by the shearing term. This might lead to discrepancies such that inside the boundary layer the rotations change from fitting the boundary conditions to minimizing the difference to ∇w. For Kirchhoff–Love plates, described in the next section these boundary layers do not occur, as the rotations β, which cause them, are eliminated from the equation.

The discretization and analysis of the Reissner–Mindlin plate is more involved than for the Timoshenko beam and postponed to Section 2.4.2.

Remark 2.2.3 *The analysis cannot be performed directly with Brezzi's Theorem 2.1.3 following the analysis of the Timoshenko beam. Instead a Helmholtz decomposition is performed such that the equation decompose into two Poisson problems and one Stokes problem, which can then be solved separately (Exercise!).*

2.2.2 Kirchhoff–Love plate equation

For thin plates like metal sheets the Kirchhoff–Love hypothesis is assumed additionally to H1–H4.

H5. Lines normal to the mid-surface are after deformation again normal to the deformed mid-surface.

It states that normal vectors of the original plate stay perpendicular to the mid-surface of the deformed plate. This means that no shearing occurs, i.e., the rotations β from the Reissner–Mindlin plate equation can be eliminated by the gradient of the vertical deflection w of the mid-surface. Note, that ∇w is the linearization of the rotated normal vector of the plate, cf. Figure 2.2 (and we will proof later in Lemma 4.2.5 that the linearization of the deformed normal vector is given by $\nu = \hat{\nu} - \nabla w + \mathcal{O}(\|\nabla w\|^2)$). Eliminating β from (2.2.7) leads to the Kirchhoff–Love plate equation, which is of the form of a biharmonic problem. Assuming clamped boundary conditions it reads: Find $w \in H_0^2(\Omega)$ such that for all $v \in H_0^2(\Omega)$

$$\int_\Omega \mathcal{C}\nabla^2 w : \nabla^2 v \, dx = \int_\Omega f\, v \, dx. \tag{2.2.8}$$

Like for the Euler–Bernoulli beam the thickness parameter t does not enter the equation. The problem is well-posed for $w \in H_0^2(\Omega)$ and reads in strong form

$$\begin{cases} \operatorname{div}(\operatorname{div}(\mathcal{C}\nabla^2 w)) = f & \text{in } \Omega, \\ w = \frac{\partial w}{\partial n} = 0 & \text{on } \partial\Omega. \end{cases} \tag{2.2.9}$$

Additionally to clamped boundary conditions also free and simply supported boundary conditions can be prescribed. The general case in strong form reads:

$$\operatorname{div}(\operatorname{div}(\boldsymbol{\sigma})) = f, \qquad \boldsymbol{\sigma} := \mathcal{C}\nabla^2 w \qquad \text{in } \Omega, \tag{2.2.10a}$$

$$w = 0, \quad \frac{\partial w}{\partial n} = 0 \qquad \text{on } \Gamma_c, \tag{2.2.10b}$$

$$w = 0, \quad \boldsymbol{\sigma}_{nn} = 0 \qquad \text{on } \Gamma_s, \tag{2.2.10c}$$

$$\boldsymbol{\sigma}_{nn} = 0, \ \frac{\partial \boldsymbol{\sigma}_{nt}}{\partial t} + \operatorname{div}(\boldsymbol{\sigma}) \cdot n = 0 \qquad \text{on } \Gamma_f, \tag{2.2.10d}$$

$$[\![\boldsymbol{\sigma}_{nt}]\!]_x = \boldsymbol{\sigma}_{n_1 t_1}(x) - \boldsymbol{\sigma}_{n_2 t_2}(x) = 0 \qquad \text{for all } x \in \mathcal{V}_{\Gamma_f}, \tag{2.2.10e}$$

where the boundary $\Gamma = \partial\Omega$ splits into clamped, simply supported, and free boundaries Γ_c, Γ_s, and Γ_f, respectively. $\mathcal{V}_{\Gamma_f}$ denotes the set of corner points where the two adjacent edges belong to Γ_f. Here, n and t denote the outer normal and tangential vector on the plate boundary. Physically, $\boldsymbol{\sigma}_{nn} := n^\top \boldsymbol{\sigma} n$ is

the normal bending moment, $\partial_t(t^\top \boldsymbol{\sigma} n) + n^\top \operatorname{div}(\boldsymbol{\sigma})$ the effective transverse shear force, and $\boldsymbol{\sigma}_{nt} := t^\top \boldsymbol{\sigma} n$ the torsion moment. Further, the shear force Q is given by $Q = -\operatorname{div}(\boldsymbol{\sigma})$.

Due to the increased regularity of w point forces f are well-defined for dimensions 2 and 3 (as then $H^2(\Omega) \hookrightarrow C^0(\Omega)$ by Sobolev inequalities. In 2D $H^1(\Omega) \not\hookrightarrow C^0(\Omega)$, the Dirac delta is a distribution in $H^{-1-\varepsilon}(\Omega)$, such that for Reissner–Mindlin plates we cannot prescribe a point force. In 1D this is valid as then $H^1(\Omega) \hookrightarrow C^0(\Omega)$. Another advantage is that the problem of shear locking is circumvented and no boundary layers occur.

To solve the Kirchhoff–Love plate equation with a conforming Galerkin method in the elliptic setting, however, would require H^2-conforming finite elements, where the derivatives have to be also continuous over elements, i.e. elements which are globally in $C^1(\Omega)$.

Remark 2.2.4 (Convergence to 3D elasticity) *Although it makes heuristically sense that the plate equations approximate the 3D elasticity problem for small thickness, the question of convergence arise. In [11] a rigorous proof was given that there holds under sufficient regularity assumptions on the domain Ω that*

$$\|u^{3\mathrm{d}} - u_{\mathrm{RM}}^{(1,1,2)}\| = \mathcal{O}(t^{\frac{1}{2}}), \qquad \|u^{3\mathrm{d}} - u_{\mathrm{KL}}^{(1,1,2)}\| = \mathcal{O}(t^{\frac{1}{2}}), \tag{2.2.11}$$

where $u^{3\mathrm{d}}$ denotes the full 3D computation and $u_{\mathrm{RM}}^{(1,1,2)}$, $u_{\mathrm{KL}}^{(1,1,2)}$ the Reissner–Mindlin and Kirchhoff–Love plate solutions where a quadratic instead of a constant ansatz for the vertical deflection has been made, $u_3 = w(x,y) + z^2 W(x,y)$, cf. (2.2.2). If the regularity assumptions are not fulfilled the exponent $\frac{1}{2}$ in the convergence rate gets reduced. The additional quadratic term is of higher-order and can be neglected.

2.3 Function spaces and finite elements for plates

After having the plate equations defined we turn to the definition of different finite element spaces used for discretization and analysis. Therefore, the classical Lagrange finite elements are needed as well as vector-valued spaces like Nédélec and Raviart–Thomas/Brezzi–Douglas–Marini and less common matrix-valued finite elements.

2.3.1 H^1 and Lagrange elements

The Sobolev space $H^1(\Omega) := \{u \in L^2(\Omega) \,|\, \nabla u \in L^2(\Omega, \mathbb{R}^d)\}$, with its norm $\|u\|_{H^1}^2 = \|u\|_{L^2}^2 + \|\nabla u\|_{L^2}^2$ and semi-norm $|u|_{H^1} = \|\nabla u\|_{L^2}$, is defined as the set of square-integrable functions, which have a weak derivative. Functions in $H^1(\Omega)$ have a well defined continuous trace operator $\operatorname{tr} : H^1(\Omega) \to H^{\frac{1}{2}}(\partial\Omega)$, which coincides with point evaluation for continuous fields, $\operatorname{tr} u = u|_{\partial\Omega}$ for $u \in C^0(\overline{\Omega})$. Therefore, we can prescribe Dirichlet boundary data. $H^{\frac{1}{2}}(\partial\Omega)$ denotes the trace space of $H^1(\Omega)$. It can be defined either as the set of traces of all $H^1(\Omega)$-functions or, equivalently, as Hilbert interpolation space between $L^2(\partial\Omega)$ and $H^1(\partial\Omega)$. Sobolev spaces $H^k(\Omega)$ can be defined e.g. by induction.

To define a conforming finite element subspace we consider a regular (shape regular or quasi uniform) triangulation[2] $\mathcal{T}$ of Ω. Further, the set of piece-wise polynomials up to order k on the triangulation is denoted by $\mathcal{P}^k(\mathcal{T})$. Further the set of edges and vertices of the triangulation are denoted by $\mathcal{E}$ and $\mathcal{V}$, respectively. The set of facets, which coincide with edges in 2D and faces in 3D, are given by $\mathcal{F}$. Analogously, we define e.g. $\mathcal{P}^k(\mathcal{F})$ as the set of polynomials living on the skeleton $\mathcal{F}$.

Now, the Lagrangian finite element space of order k defined by

$$U_h^k := \mathcal{P}^k(\mathcal{T}) \cap C^0(\Omega) \qquad U_{h,0}^k := \{u_h \in U_h^k \,|\, \operatorname{tr} u_h = 0 \text{ on } \partial\Omega\} \tag{2.3.1}$$

consists of piece-wise (smooth) polynomials and is globally continuous, such that $U_h^k \subset H^1(\Omega)$. If only parts of the boundary are used for defining zero boundary conditions we use the notation U_{h,Γ_D}^k.

Example 2.3.1 *Consider $\Omega \subset \mathbb{R}^2$ and linear elements U_h^1. A basis of U_h^1 is given by the set of hat-functions φ_i, fulfilling $\varphi_i(V_j) = \delta_{ij}$, where V_j denotes a vertex of $\mathcal{T}$. Thus $u_h = \sum_{i=1}^N \alpha_i \varphi_i \in U_h^1$. The α_i are the coefficients with respect to the basis $\{\varphi_i\}$. The corresponding functionals are given by*

[2] For simplicity we will solely consider non-curved elements in this section.

$\Psi_i : u \mapsto u(V_i)$ *such that* $\Psi_i(\varphi_j) = \delta_{ij}$. *The canonical interpolation operator* $\mathcal{I}_h^1 : C^0(\Omega) \to U_h^1$ *is given by* $u_h = \mathcal{I}_h^1 u = \sum_{i=0}^N \Psi_i(u)\varphi_i$ *(Note that point-evaluation is not well-defined for* $H^1(\Omega)$ *in dimensions 2 or higher).*

To extend the hat-function basis to higher-order several constructions exist as e.g. a hierarchical basis, where only new basis functions are added. We define the canonical interpolation operator $\mathcal{I}_h^k : C^0(\Omega) \to U_h^k$ by the following equations in two dimensions

$$\mathcal{I}_h^k u(V) = u(V) \qquad \text{for all } v \in \mathcal{V}, \tag{2.3.2a}$$

$$\int_E \mathcal{I}_h^k u q \, ds = \int_E u q \, ds \qquad \text{for all } q \in \mathcal{P}^{k-2}(E),\ E \in \mathcal{E}, \tag{2.3.2b}$$

$$\int_T \mathcal{I}_h^k u q \, dx = \int_T u q \, dx \qquad \text{for all } q \in \mathcal{P}^{k-3}(T),\ T \in \mathcal{T}, \tag{2.3.2c}$$

and analogously in 3D for tetrahedra.

Mostly, the shape functions are defined on a reference triangle/tetrahedron $\hat{T}$ and then mapped to the physical elements $T = \Phi(\hat{T})$. For Lagrange elements this is done by simple composition $u_h \circ \Phi = \hat{u}_h$. E.g., the barycentric coordinates $\hat{\lambda}$ on the reference triangle are directly mapped to the barycentric coordinates on the physical element by $\lambda \circ \phi = \hat{\lambda}$. Therefore, one can define the Lagrange elements by

$$U_h^k = \{u_h \in H^1(\Omega) \,|\, \text{ for all } T \in \mathcal{T}\ \exists \hat{u} \in \mathcal{P}^k(\hat{T}) : \ u|_T \circ \Phi = \hat{u}\}.$$

2.3.2 $H(\mathrm{curl})$ and Nédélec elements

The $H(\mathrm{curl})$ space in two and three dimensions is defined as the set of all L^2-functions, where the curl is also in L^2, $H(\mathrm{curl}, \Omega) := \{u \in L^2(\Omega, \mathbb{R}^d) \,|\, \mathrm{curl}\, u \in L^2(\Omega, \mathbb{R}^{2d-3})\}$, with the norm $\|u\|^2_{H(\mathrm{curl})} := \|u\|^2_{L^2} + \|\mathrm{curl}\, u\|^2_{L^2}$. In contrast to H^1 only the tangential trace is available $\mathrm{tr}_t : H(\mathrm{curl}, \Omega) \to H^{-\frac{1}{2}}(\partial\Omega, \mathbb{R}^{2d-3})$ such that $\mathrm{tr}_t u = u|_{\partial\Omega} \cdot t$ in 2D and $\mathrm{tr}_t u = u|_{\partial\Omega} \times n$ in 3D, respectively, for $u \in C^0(\overline{\Omega}, \mathbb{R}^d)$. $H^{-\frac{1}{2}}(\partial\Omega)$ denotes the dual space of $H^{\frac{1}{2}}(\partial\Omega)$ such that e.g. $\int_{\partial\Omega} \mathrm{tr}_t u \, \mathrm{tr}\, v \, ds$ is well defined for $u \in H(\mathrm{curl}, \Omega)$ and $v \in H^1(\Omega, \mathbb{R}^{2d-3})$. The trace theorem gives the hint that for a conforming discretization the finite element space should be tangential continuous, the normal component might jump over elements. The lowest-order Nédélec elements of first kind in three dimensions are element-wise of the form

$$\mathcal{N}_I^0(T) = \{a + x \times b \,|\, a, b \in \mathbb{R}^3\} \quad T \in \mathcal{T} \tag{2.3.3}$$

and the global finite element space is given by

$$\mathcal{N}_I^0 = \{v_h \in \Pi_{T\in\mathcal{T}} \mathcal{N}_I^0(T) \,|\, v_h \text{ is tangential continuous}\} \subset H(\mathrm{curl}, \Omega). \tag{2.3.4}$$

The functionals Ψ_i enforcing the tangential continuity are given by the edge moment of the tangential component, $\Psi_i(u) = \int_{E_i} u \cdot t_{E_i} \, ds$ enforcing the tangential continuity. The space has 6 degrees of freedom fitting to the 6 edges of a tetrahedron. The shape function corresponding to edge E_i is given by

$$\varphi_{E_i} = \lambda_{E_i^1} \nabla \lambda_{E_i^2} - \lambda_{E_i^2} \nabla \lambda_{E_i^1}, \tag{2.3.5}$$

where e.g., $\lambda_{E_i^1}$ denotes the barycentric coordinate of the first vertex of edge E_i.

By increasing to full polynomial space $\mathcal{P}^1(\mathcal{T}, \mathbb{R}^d)$ and adding the first tangential moments as functionals, $\Psi_i(u) = \int_{E_i} (\lambda_{E_i^2} - \lambda_{E_i^1}) \, u \cdot t_{E_i} \, ds$, the second type Nédélec elements are obtained. The arbitrary order k definitions are

$$\mathcal{N}_I^k := \{v_h \in \Pi_{T\in\mathcal{T}} \mathcal{N}_I^k(T) \,|\, v_h \text{ is t-continuous}\}, \qquad \mathcal{N}_I^k(T) := \{a + x \times b \,|\, a, b \in \mathcal{P}^k(T, \mathbb{R}^3)\}, \tag{2.3.6}$$

$$\mathcal{N}_{II}^k := \{v_h \in \mathcal{P}^k(\mathcal{T}, \mathbb{R}^3) \,|\, v_h \text{ is t-continuous}\} \qquad \mathcal{N}_{II,0}^k := \{v_h \in \mathcal{N}_{II}^k \,|\, \mathrm{tr}_t v_h = 0 \text{ on } \partial\Omega\}. \tag{2.3.7}$$

There holds the relation

$$\mathcal{N}_I^0 \subsetneq \mathcal{N}_{II}^1 = \mathcal{P}^1(\mathcal{T}, \mathbb{R}^d) \subsetneq \mathcal{N}_I^1 \subsetneq \mathcal{N}_{II}^2 = \mathcal{P}^2(\mathcal{T}, \mathbb{R}^d) \subsetneq \dots$$

and we will use the notation $\mathcal{N}$ if we do not specify the kind of Nédélec elements.

The canonical Nédélec interpolant will be denoted by $\mathcal{I}_h^{\mathcal{N}} : C^0(\Omega, \mathbb{R}^d) \to \mathcal{N}^k$ by the following equations for

- $\mathcal{N}_I$ elements by

$$\int_E \mathcal{I}_h^{\mathcal{N},k} u \cdot t_E \, q \, dl = \int_E u \cdot t_E \, q \, dl \qquad \text{for all } q \in \mathcal{P}^k(E), E \in \mathcal{E}, \tag{2.3.8a}$$

$$\int_F \mathcal{I}_h^{\mathcal{N},k} u_t \cdot q \, ds = \int_F u_t \cdot q \, ds \qquad \text{for all } q \in \mathcal{P}^{k-1}(F, \mathbb{R}^3) \cap n_F^\perp, F \in \mathcal{F}, \tag{2.3.8b}$$

$$\int_T \mathcal{I}_h^{\mathcal{N},k} u \cdot q \, dx = \int_T u \cdot q \, dx \qquad \text{for all } q \in \mathcal{P}^{k-2}(T, \mathbb{R}^3), T \in \mathcal{T}, \tag{2.3.8c}$$

  where $\mathcal{P}^{k-1}(F, \mathbb{R}^3) \cap n_F^\perp$ denote vector-valued polynomials living in the tangent plane of F.

- $\mathcal{N}_{II}$ elements by

$$\int_E \mathcal{I}_h^{\mathcal{N},k} u \cdot t_E \, q \, dl = \int_E u \cdot t_E \, q \, dl \qquad \text{for all } q \in \mathcal{P}^k(E), E \in \mathcal{E}, \tag{2.3.9a}$$

$$\int_F \mathcal{I}_h^{\mathcal{N},k} u_t \cdot q \, ds = \int_F u_t \cdot q \, ds \qquad \text{for all } q \in RT^{k-2}(F), F \in \mathcal{F}, \tag{2.3.9b}$$

$$\int_T \mathcal{I}_h^{\mathcal{N},k} u \cdot q \, dx = \int_T u \cdot q \, dx \qquad \text{for all } q \in RT^{k-3}(T), T \in \mathcal{T}, \tag{2.3.9c}$$

  where $RT^{k-2}(F)$ and $RT^{k-3}(T)$ are Raviart–Thomas spaces defined in (2.3.11).

When mapping Nédélec elements from the reference to the physical element we need to preserve the tangential continuity. Therefore the so-called covariant transformation is used, $u \circ \Phi = \boldsymbol{F}^{-\top} \hat{u}$ with $\boldsymbol{F} = \nabla\Phi$, as then with $E = \Phi(\hat{E})$

$$\int_E u \cdot t \, ds = \int_{\hat{E}} \hat{u} \cdot \hat{t} \, d\hat{s} \quad \text{and} \quad (\operatorname{curl} u) \circ \Phi = \begin{cases} \frac{1}{J} \operatorname{curl}_{\hat{x}} \hat{u} & \text{in 2D}, \\ \frac{1}{J} \boldsymbol{F} \operatorname{curl}_{\hat{x}} \hat{u} & \text{in 3D}. \end{cases} \tag{2.3.10}$$

2.3.3 $H(\mathrm{div})$ and Raviart–Thomas/Brezzi–Douglas–Marini elements

In a similar manner to the previous section we define $H(\mathrm{div}, \Omega) := \{u \in L^2(\Omega, \mathbb{R}^d) \,|\, \mathrm{div} u \in L^2(\Omega)\}$, $\|u\|^2_{H(\mathrm{div})} = \|u\|^2_{L^2} + \|\mathrm{div} u\|^2_{L^2}$. Now, the normal trace is well-defined, $\mathrm{tr}_n : H(\mathrm{div}, \Omega) \to H^{-\frac{1}{2}}(\partial\Omega)$, such that $\mathrm{tr}_n u = u|_{\partial\Omega} \cdot n$ for $u \in C^0(\overline{\Omega}, \mathbb{R}^d)$. The Raviart–Thomas (RT) elements consist of polynomials of order k where homogeneous polynomials $\mathcal{P}^{k,*}(T) := \{p \in \mathcal{P}^k(T) \,|\, p = \sum_{i=1}^m \alpha_i x_1^{k_{i1}} \cdots x_d^{k_{id}}, \sum_{l=1}^d k_{il} = k, \text{ for all } i \in \{1, \ldots, m\}\}$ are added and are normal continuous

$$RT^k(T) := \{a + cx \,|\, a \in \mathcal{P}^k(T, \mathbb{R}^d), c \in \mathcal{P}^{k,*}(T)\}, \tag{2.3.11}$$

$$RT^k := \{v_h \in \Pi_{T \in \mathcal{T}} RT^k(T) \,|\, [\![v_h \cdot n]\!]_F = 0 \text{ for all } F \in \mathcal{F}^{\mathrm{int}}\} \subset H(\mathrm{div}, \Omega). \tag{2.3.12}$$

Here, we defined $\mathcal{F}^{\mathrm{int}} := \mathcal{F} \backslash \partial\Omega$ as the set of all interior facets and used the notation of the normal jump across element facets $[\![v_h \cdot n]\!]_F = (v_h \cdot n)|_{T_1} + (v_h \cdot n)|_{T_2} = (v_h|_{T_1} - v_h|_{T_2}) \cdot n|_{T_1}$. In the lowest-order case $k = 0$ in 2D the three dofs correspond to the 3 edges of the triangle, whereas in 3D there are four dofs for the 4 faces of the tetrahedron.

Using the full polynomial spaces lead to Brezzi–Douglas–Marini (BDM) elements

$$\begin{aligned} BDM^k &:= \{v_h \in \mathcal{P}^k(\mathcal{T}, \mathbb{R}^d) \,|\, [\![v_h \cdot n]\!]_F = 0 \text{ for all } F \in \mathcal{F}^{\mathrm{int}}\} \subset H(\mathrm{div}, \Omega), \\ BDM_0^k &:= \{u_h \in BDM^k \,|\, \mathrm{tr}_n u_h = 0 \text{ on } \partial\Omega\}. \end{aligned} \tag{2.3.13}$$

If we do not distinguish between RT and BDM we use the notation V_h.

The functionals are the moments of the normal component on edges/faces and inner moments. The canonical interpolant $\mathcal{I}_h^{V_h,k} : C^0(\Omega, \mathbb{R}^d) \to V_h^k$ is defined for

- RT elements by

$$\Psi_F(v) = \int_F v \cdot n \, q \, ds \qquad \text{for all } q \in \mathcal{P}^k(F), F \in \mathcal{F}, \tag{2.3.14a}$$

$$\Psi_T(v) = \int_T v \cdot q \, dx \qquad \text{for all } q \in \mathcal{P}^{k-1}(T, \mathbb{R}^d), T \in \mathcal{T}. \tag{2.3.14b}$$

- BDM elements by

$$\Psi_F(v) = \int_F v \cdot n\, q\, ds \qquad \text{for all } q \in \mathcal{P}^k(F),\ F \in \mathcal{F}, \tag{2.3.15a}$$

$$\Psi_T(v) = \int_T v \cdot q\, dx \qquad \text{for all } q \in \mathcal{N}_I^{k-2}(T),\ T \in \mathcal{T}. \tag{2.3.15b}$$

By using the Piola transformation, $u \circ \Phi = \frac{1}{J}\boldsymbol{F}\hat{u}$ the normal continuity is preserved during transformation $T = \Phi(\hat{T})$ and there holds with $F = \Phi(\hat{F})$

$$\int_F u \cdot n\, ds = \int_{\hat{F}} \hat{u} \cdot \hat{n}\, d\hat{s}, \quad \text{and} \quad (\mathrm{div} u) \circ \Phi = \frac{1}{J}\mathrm{div}_{\hat{x}}\hat{u}. \tag{2.3.16}$$

2.3.4 L^2 elements and De'Rham complex

For completeness, we define the set of piece-wise polynomials of order k as $L^2(\Omega)$-conforming finite elements

$$Q_h^k = \mathcal{P}^k(\mathcal{T}) \subset L^2(\Omega). \tag{2.3.17}$$

There holds on the continuous level in three dimensions $\nabla H^1 \subset H(\mathrm{curl})$, $\mathrm{curl}(H(\mathrm{curl})) \subset H(\mathrm{div})$, and $\mathrm{div}(H(\mathrm{div})) \subset L^2$. Further, on simply connected domains the following sequence is exact. If the domain is not simply connected the range of one operator is still inside the kernel of the next, but in general the reverse does not hold.

$$\{1\} \xrightarrow{\mathrm{id}} H^1 \xrightarrow{\nabla} H(\mathrm{curl}) \xrightarrow{\mathrm{curl}} H(\mathrm{div}) \xrightarrow{\mathrm{div}} L^2 \xrightarrow{0} 0.$$

The following diagram, called De'Rham complex, commutes

$$\begin{array}{ccccccc} H^1 \cap C^0 & \xrightarrow{\nabla} & H(\mathrm{curl}) \cap C^0 & \xrightarrow{\mathrm{curl}} & H(\mathrm{div}) \cap C^0 & \xrightarrow{\mathrm{div}} & L^2 \\ \mathcal{I}_h \downarrow & & \mathcal{I}_h^{\mathcal{N}} \downarrow & & \mathcal{I}_h^{V_h} \downarrow & & \Pi^{L^2} \downarrow \\ U_h & \xrightarrow{\nabla} & \mathcal{N} & \xrightarrow{\mathrm{curl}} & V_h & \xrightarrow{\mathrm{div}} & Q_h \end{array}.$$

Remark 2.3.2 *To use the canonical interpolation operators we need to increase the regularity of spaces, as e.g. point evaluation is not well-defined for H^1 functions. Recently, local L^2-bounded and commuting projection operators have been constructed without the requirement of increased regularity [4].*

2.3.5 $H(\mathrm{divdiv})$, TDNNS, and Hellan–Herrmann–Johnson elements

We will consider stress fields of the form $\boldsymbol{\sigma} = \mathcal{C}\boldsymbol{\varepsilon}$ several times as additional unknown. These fields are symmetric, $\boldsymbol{\sigma}^\top = \boldsymbol{\sigma}$, and need to have a divergence operator defined due to the force balance equation

$$-\mathrm{div}(\boldsymbol{\sigma}) = f.$$

When considering linear elasticity (1.4.5) the mixed formulation reads

$$\int_\Omega \mathcal{C}^{-1}\boldsymbol{\sigma} : \boldsymbol{\tau}\, dx + \langle \mathrm{div}\boldsymbol{\tau}, u\rangle = 0 \qquad \text{for all } \boldsymbol{\tau}, \tag{2.3.18a}$$

$$\langle \mathrm{div}\boldsymbol{\sigma}, v\rangle = -\int_\Omega f\, v\, dx \quad \text{for all } v. \tag{2.3.18b}$$

The first equation forces $\boldsymbol{\sigma} = \mathcal{C}\boldsymbol{\varepsilon}(u)$, the second one the force balance equation, where $\mathcal{C}^{-1}$ is the compliance tensor (1.4.3). Note that we did not specify any spaces, regularity assumptions, or the pairings $\langle\cdot,\cdot\rangle$ so far.

If we keep $u \in H^1(\Omega, \mathbb{R}^d)$ like in the standard primal setting we can define $\langle \mathrm{div}\boldsymbol{\sigma}, u\rangle_{H^{-1}\times H^1} = -\int_\Omega \boldsymbol{\sigma} : \varepsilon(u)\, dx$ such that $\boldsymbol{\sigma} \in L^2(\Omega, \mathbb{R}^{d\times d}_{\mathrm{sym}})$ is sufficient. However, this formulation is equivalent to the primal version and thus of less interest.

Shifting the regularity from the displacement u to the stress $\boldsymbol{\sigma}$ yields the requirement $\mathrm{div}\boldsymbol{\sigma} \in L^2(\Omega,\mathbb{R}^d)$ and $u \in L^2(\Omega,\mathbb{R}^d)$. The stress has therefore to be in the space $H^{\mathrm{sym}}(\mathrm{div},\Omega) := \{\boldsymbol{\sigma} \in L^2(\Omega,\mathbb{R}^{d\times d}_{\mathrm{sym}}) \,|\, \mathrm{div}\boldsymbol{\sigma} \in L^2(\Omega,\mathbb{R}^d)\}$, which induces a continuous normal trace, $\boldsymbol{\sigma}n$, compare with $H(\mathrm{div},\Omega)$ in Section 2.3.3. Although this is a valid choice of spaces, the construction of $H^{\mathrm{sym}}(\mathrm{div})$-conforming finite element spaces is tedious and requires high polynomial degree.

Remark 2.3.3 *As a result so-called weakly symmetric methods were developed, where the symmetry of $\boldsymbol{\sigma}$ is broken and gets enforced weakly by a Lagrange multiplier leading to the construction of simpler elements.*

$\langle \mathrm{div}\boldsymbol{\sigma}, u\rangle$	$\boldsymbol{\sigma}$	u	trace $\boldsymbol{\sigma}$	trace u
$\langle \mathrm{div}\boldsymbol{\sigma}, u\rangle_{H^{-1}\times H^1}$	$L^2(\Omega,\mathbb{R}^{d\times d}_{\mathrm{sym}})$	$H^1(\Omega,\mathbb{R}^d)$	-	u
$\int_\Omega \mathrm{div}\boldsymbol{\sigma}\cdot u\,dx$	$H^{\mathrm{sym}}(\mathrm{div},\Omega)$	$L^2(\Omega,\mathbb{R}^d)$	$\boldsymbol{\sigma}n$	-
$\langle \mathrm{div}\boldsymbol{\sigma}, u\rangle_{H(\mathrm{curl})^*\times H(\mathrm{curl})}$	$H(\mathrm{divdiv},\Omega)$	$H(\mathrm{curl},\Omega)$	$n^\top\boldsymbol{\sigma}n$	u_t

Table 2.2: Depending on the interpretation of pairing $\langle \mathrm{div}\boldsymbol{\sigma}, u\rangle$ different regularity assumptions on $\boldsymbol{\sigma}$ and u are required yielding different well-defined traces.

The tangential-displacement normal normal-stress continuous element method (TDNNS) shifts the regularity half-half by requiring that $u \in H(\mathrm{curl},\Omega)$, i.e. with a tangential trace, and $\boldsymbol{\sigma} \in H(\mathrm{divdiv},\Omega) := \{\boldsymbol{\sigma} \in L^2(\Omega,\mathbb{R}^{d\times d}_{\mathrm{sym}}) \,|\, \mathrm{divdiv}\boldsymbol{\sigma} \in H^{-1}(\Omega)\}$. The norm is given by $\|\boldsymbol{\sigma}\|^2_{HDD} = \|\boldsymbol{\sigma}\|^2_{L^2} + \|\mathrm{divdiv}\boldsymbol{\sigma}\|^2_{H^{-1}}$. Then the duality pairing $\langle \mathrm{div}\boldsymbol{\sigma}, u\rangle_{H(\mathrm{curl})^*\times H(\mathrm{curl})}$ is well defined as there holds $\mathrm{div}(H(\mathrm{divdiv},\Omega)) \subset H(\mathrm{curl})^*$, the dual space of $H(\mathrm{curl})$. To see this we need the following characterization of the dual space of $H(\mathrm{curl})$.

Lemma 2.3.4 *There holds*

$$H(\mathrm{curl},\Omega)^* = H^{-1}(\mathrm{div},\Omega) := \{u \in H^{-1}(\Omega,\mathbb{R}^d) \,|\, \mathrm{div}u \in H^{-1}(\Omega)\}. \tag{2.3.19}$$

Proof: For an $u \in H_0(\mathrm{curl},\Omega)$ we use the regular decomposition $u = z + \nabla\varphi$ with $z \in H^1_0(\Omega,\mathbb{R}^d)$, $\varphi \in H^1_0(\Omega)$, and $\|z\|_{H^1} + \|\varphi\|_{H^1} \le c\|u\|_{H(\mathrm{curl})}$ to compute

$$\begin{aligned}\|f\|_{H(\mathrm{curl})^*} &= \sup_{u\in H_0(\mathrm{curl})} \frac{\langle f,u\rangle}{\|u\|_{H(\mathrm{curl})}} \simeq \sup_{z,\varphi} \frac{\langle f, z+\nabla\varphi\rangle}{\|\varphi\|_{H^1}+\|z\|_{H^1}} \simeq \sup_z \frac{\langle f,z\rangle}{\|z\|_{H^1}} + \sup_\varphi \frac{\langle \mathrm{div}f,\varphi\rangle}{\|\varphi\|_{H^1}} \\ &= \|\mathrm{div}f\|_{H^{-1}} + \|f\|_{H^{-1}} = \|f\|_{H^{-1}(\mathrm{div})}.\end{aligned}$$

□

Now there holds for $\boldsymbol{\sigma} \in H(\mathrm{divdiv},\Omega)$ that $\mathrm{div}\boldsymbol{\sigma} \in H^{-1}(\Omega,\mathbb{R}^d)$ as well as $\mathrm{divdiv}\boldsymbol{\sigma} \in H^{-1}(\Omega)$ such that $\mathrm{div}\boldsymbol{\sigma} \in H^{-1}(\mathrm{div},\Omega)$. In contrast to $H^{\mathrm{sym}}(\mathrm{div})$ the $H(\mathrm{divdiv})$ space only induces a continuous normal-normal trace, $\boldsymbol{\sigma}_{nn} := n^\top\boldsymbol{\sigma}n$, which enables to construct simpler and low-order finite elements, see [46].

If the functions are more regular at a triangulation the duality pairing can be written in terms of element and face terms

Lemma 2.3.5 *Let $\boldsymbol{\sigma}$ be a symmetric piece-wise smooth tensor with $\boldsymbol{\sigma}_{nt} \in H^{\frac12}(\partial T)$ for all $T \in \mathcal{T}$ and normal-normal continuous. Then $\mathrm{div}\boldsymbol{\sigma} \in H(\mathrm{curl},\Omega)^*$ and*

$$\begin{aligned}\langle \mathrm{div}\boldsymbol{\sigma}, u\rangle_{H(\mathrm{curl})^*\times H(\mathrm{curl})} &= \sum_{T\in\mathcal{T}} \left(\int_T \mathrm{div}\boldsymbol{\sigma}\cdot u\,dx - \int_{\partial T} \boldsymbol{\sigma}_{nt}u_t\,ds \right) \\ &= \sum_{T\in\mathcal{T}} \left(-\int_T \boldsymbol{\sigma} : \nabla u\,dx + \int_{\partial T} \boldsymbol{\sigma}_{nn}u_n\,ds \right),\end{aligned} \tag{2.3.20}$$

where for the second identity we assumed that $u \in H(\mathrm{curl},\Omega)$ is piece-wise smooth and $u_n \in H^{\frac12}(\partial T)$.

Proof: We start with a smooth test function $\Psi \in C_0^\infty(\Omega, \mathbb{R}^d)$ and use the definition of distributions, split the domain into the triangles $T \in \mathcal{T}$, and integrate by parts back on each element

$$\langle \mathrm{div}\boldsymbol{\sigma}, \Psi\rangle_{H(\mathrm{curl})^* \times H(\mathrm{curl})} = -\int_\Omega \boldsymbol{\sigma} : \nabla\Psi \, dx = -\sum_{T\in\mathcal{T}} \int_T \boldsymbol{\sigma} : \nabla\Psi \, dx = \sum_{T\in\mathcal{T}} \big(\int_T \mathrm{div}\boldsymbol{\sigma} \cdot \Psi \, dx - \int_{\partial T} \boldsymbol{\sigma}_n \cdot \Psi \, ds\big).$$

By splitting into normal and tangential components, $\boldsymbol{\sigma}_n \cdot \Psi = (\boldsymbol{\sigma}_{nn} n + \boldsymbol{P}_t\boldsymbol{\sigma}_n) \cdot (\Psi_n n + \boldsymbol{P}_t\Psi) = \boldsymbol{\sigma}_{nn}\Psi_n + \boldsymbol{P}_t\boldsymbol{\sigma}_n \cdot \boldsymbol{P}_t\Psi$, where $\boldsymbol{P}_t = \boldsymbol{I} - n \otimes n$ is the tangential projection, yields by abbreviating e.g. $\Psi_t := \boldsymbol{P}_t\Psi$ and reordering of the facet terms

$$\sum_{T\in\mathcal{T}} \int_{\partial T} \boldsymbol{\sigma}_n \cdot \Psi \, ds = \sum_{T\in\mathcal{T}} \int_{\partial T} \boldsymbol{\sigma}_{nn}\Psi_n + \boldsymbol{\sigma}_{nt} \cdot \Psi_t \, ds = \sum_{F\in\mathcal{F}\setminus\partial\Omega} \int_F [\![\boldsymbol{\sigma}_{nn}]\!]\Psi_n + [\![\boldsymbol{\sigma}_{nt}]\!] \cdot \Psi_t \, ds.$$

By using that $\boldsymbol{\sigma}_{nn}$ is continuous, $[\![\boldsymbol{\sigma}_{nn}]\!] = 0$, we obtain

$$\langle \mathrm{div}\boldsymbol{\sigma}, \Psi\rangle_{H(\mathrm{curl})^* \times H(\mathrm{curl})} = \sum_{T\in\mathcal{T}} \left(\int_T \mathrm{div}\boldsymbol{\sigma} \cdot \Psi \, dx - \int_{\partial T} \boldsymbol{\sigma}_{nt}\Psi_n \, ds \right)$$

and

$$|\langle \mathrm{div}\boldsymbol{\sigma}, \Psi\rangle_{H(\mathrm{curl})^* \times H(\mathrm{curl})}| \le \sum_{T\in\mathcal{T}} \|\mathrm{div}\boldsymbol{\sigma}\|_{L^2(T)}\|\Psi\|_{L^2(T)} + \|\boldsymbol{\sigma}_{nt}\|_{H^{\frac{1}{2}}(\partial T)}\|\Psi_t\|_{H^{-\frac{1}{2}}(\partial T)} \le C(\boldsymbol{\sigma})\|\Psi\|_{H(\mathrm{curl})}.$$

Thus, we can by density extend the formula of the duality pairing to $\Psi \in H(\mathrm{curl}, \Omega)$. The second statement follows by integration by parts element-wise and noting that $\boldsymbol{\sigma}_n \cdot \Psi - \boldsymbol{\sigma}_{nt}\Psi_t = \boldsymbol{\sigma}_{nn}\Psi_n$. □

The so-called stress or Hellan–Herrmann–Johnson finite element space is defined by

$$\begin{aligned} M_h^k &:= \{\boldsymbol{\sigma}_h \in \mathcal{P}^k(\mathcal{T}, \mathbb{R}^{d\times d}_{\mathrm{sym}}) \,|\, [\![\boldsymbol{\sigma}_{h,nn}]\!]_F = 0 \text{ for all } F \in \mathcal{F}^{\mathrm{int}}\}, \\ M_{h,0}^k &:= \{\boldsymbol{\sigma}_h \in M_h^k \,|\, \boldsymbol{\sigma}_{h,nn} = 0 \text{ on } \partial\Omega\}. \end{aligned} \tag{2.3.21}$$

Here, the normal-normal jump is given by $[\![\boldsymbol{\sigma}_{h,nn}]\!]_F = \boldsymbol{\sigma}_{h,nn}|_{T_L} - \boldsymbol{\sigma}_{h,nn}|_{T_R}$.

The functionals of M_h in the two-dimensional case are the normal-normal moments at the edges and moments over elements

$$\Psi_E(\boldsymbol{\sigma}) = \int_E J_E \, \boldsymbol{\sigma}_{nn} \, q \, ds \qquad q \in \mathcal{P}^k(E),\, E \in \mathcal{E}, \tag{2.3.22a}$$

$$\Psi_T(\boldsymbol{\sigma}) = \int_T J_T \, \boldsymbol{\sigma} : F_T^{-\top} Q F_T^{-1} \, dx \qquad Q \in \mathcal{P}^{k-1}(T, \mathbb{R}^{d\times d}_{\mathrm{sym}}),\, T \in \mathcal{T}, \tag{2.3.22b}$$

where J_E and J_T are the edge and element determinants and F_T the Jacobean of the transformation from the reference to the physical element, yielding the canonical interpolation operator $\mathcal{I}_h^{\mathrm{M_h},k} : C^0(\Omega, \mathbb{R}^{d\times d}) \to M_h^k$.

The edge based shape functions can be constructed based on barycentric coordinates

$$e_{ij} = \nabla\lambda_i^\perp \odot \nabla\lambda_j^\perp, \tag{2.3.23}$$

where $\odot$ is the symmetric dyadic product of the vectors $a \odot b = \frac{1}{2}(ab^\top + ba^\top)$ and $a^\perp$ denotes the rotation by $\frac{\pi}{2}$. High-order versions can be constructed by setting $e_{ij}q(\lambda_i - \lambda_j)$ where $q \in \mathcal{P}^l(E)$. Interior bubble shape functions are given by $e_{ij}\lambda_k p^l(x, y)$, $p(x, y) \in \mathcal{P}^l(T)$. The construction of shape functions in 3D is similar but more involved [40].

Example 2.3.6 *On the reference triangle the barycentric coordinates are* $\lambda_1 = x$, $\lambda_2 = y$, $\lambda_3 = 1 - x - y$ *and* $\nabla\lambda_1^\perp = \begin{pmatrix}0\\1\end{pmatrix}$, $\nabla\lambda_2^\perp = \begin{pmatrix}-1\\0\end{pmatrix}$, $\nabla\lambda_3^\perp = \begin{pmatrix}1\\-1\end{pmatrix}$. *The shape functions read* $e_{12} = \nabla\lambda_1^\perp \odot \nabla\lambda_2^\perp = -\frac{1}{2}\begin{pmatrix}0 & 1\\1 & 0\end{pmatrix}$, $e_{13} = \begin{pmatrix}0\\1\end{pmatrix} \odot \begin{pmatrix}1\\-1\end{pmatrix} = \begin{pmatrix}0 & 0.5\\0.5 & -1\end{pmatrix}$, $e_{23} = \begin{pmatrix}-1 & 0.5\\0.5 & 0\end{pmatrix}$. *With* $n_1 = \begin{pmatrix}-1\\0\end{pmatrix}$, $n_2 = \begin{pmatrix}0\\-1\end{pmatrix}$, $n_3 = \frac{1}{\sqrt{2}}\begin{pmatrix}1\\1\end{pmatrix}$ *there holds* $n_1^\top e_{12} n_1 = n_2^\top e_{12} n_2 = 0$ *and* $n_3 \top e_{12} n_3 = -\frac{1}{2}$. *Analogously,* $n_1^\top e_{13} n_1 = n_3^\top e_{13} n_3 = 0$, $n_2^\top e_{13} n_2 = -1$ *and* $n_2^\top e_{23} n_2 = n_3^\top e_{23} n_3 = 0$, $n_1^\top e_{23} n_1 = -1$.

To preserve the normal-normal degree of freedom during transformation from the reference to the physical element a double Piola transformation is considered $\boldsymbol{\sigma} \circ \Phi = \frac{1}{J^2} \boldsymbol{F} \hat{\boldsymbol{\sigma}} \boldsymbol{F}^\top$. Then

$$\int_F J_F \boldsymbol{\sigma}_{nn} \, ds = \int_{\hat{F}} \underbrace{J_{\hat{F}}}_{=1} \hat{\boldsymbol{\sigma}}_{\hat{n}\hat{n}} \, d\hat{s}.$$

Remark 2.3.7 *There does not hold $M_h^k \subset H(\mathrm{divdiv}, \Omega)$ as point evaluation is not a functional in $H^{-1}(\Omega)$ for dimensions higher than 1. The discrepancy is by an $\varepsilon > 0$ as $\mathrm{divdiv} M_h \subset H^{-1-\varepsilon}(\Omega)$ (Exercise!).*

2.4 Hellinger–Reissner formulation of plates

The concept of including the stresses additionally to displacements goes back to Hellinger, Reissner, and Prange [26, 44, 43]. Using more variables enables to shift regularity assumptions between the used spaces. The resulting saddle-point problems are more involved to analyze but also more robust methods can be constructed.

2.4.1 Hellan–Herrmann–Johnson (HHJ) method for Kirchhoff–Love plates

For ease of presentation we assume clamped boundary conditions in this section, such that the plate equation reads

$$\begin{cases} \mathrm{div}(\mathrm{div}(\mathcal{C}\nabla^2 w)) = f, & \text{in } \Omega, \\ w = \frac{\partial w}{\partial n} = 0 & \text{on } \partial\Omega. \end{cases} \tag{2.4.1}$$

The construction of general H^2-conforming finite elements is a difficult task as they have to be globally C^1 instead of being "just" continuous over interfaces. Examples of such elements are the Argyris and Bell triangles or the Bogner–Fox–Schmit quadrilateral. The Hsieh–Clough–Tocher element falls in the category of so-called macro-elements, where one triangle is divided into three smaller ones. The famous Morley triangle [36] is a nonconforming H^2 finite element, where the normal derivative is used as degree of freedom at the edges.

The HHJ method for fourth order Kirchhoff plates has been developed and first analyzed in the late 60s by [25, 27, 29]. Superconvergence results and postprocessing procedures were developed and analyzed until the early 90's. After a break of 20 years the method regained interest.

The HHJ method overcomes the issue of C^1-conformity by introducing the linearized moment tensor

$$\boldsymbol{\sigma} := \mathcal{C}\nabla^2 w \tag{2.4.2}$$

as an additional tensor field leading to a mixed saddle point problem: Find $(w, \boldsymbol{\sigma}) \in H_0^1(\Omega) \times H(\mathrm{divdiv}, \Omega)$ such that for all $(v, \boldsymbol{\tau}) \in H_0^1(\Omega) \times H(\mathrm{divdiv}, \Omega)$

$$\int_\Omega \mathcal{C}^{-1}\boldsymbol{\sigma} : \boldsymbol{\tau} \, dx + \langle \mathrm{div}(\boldsymbol{\tau}), \nabla w \rangle_{H(\mathrm{curl})^* \times H(\mathrm{curl})} = 0, \tag{2.4.3a}$$

$$\langle \mathrm{div}(\boldsymbol{\sigma}), \nabla v \rangle_{H(\mathrm{curl})^* \times H(\mathrm{curl})} = -\int_\Omega f v, \tag{2.4.3b}$$

where $\mathcal{C}^{-1}\boldsymbol{\sigma} = \frac{1+\nu}{E}(\boldsymbol{\sigma} - \frac{\nu}{1+\nu}\,\mathrm{tr}(\boldsymbol{\sigma})\boldsymbol{I}) = \frac{1}{E}((1+\nu)\boldsymbol{\sigma} - \nu\,\mathrm{tr}(\boldsymbol{\sigma})\boldsymbol{I})$ is the inverted plate material (2.2.6).

Due to the relation $\nabla H^1 \subset H(\mathrm{curl})$ the above involved duality pairing is well defined. With the Hellan–Herrmann–Johnson stress finite elements (2.3.21) for $\boldsymbol{\sigma}$ and Lagrange finite elements for the vertical deflection the discrete problem reads: Find $(w_h, \boldsymbol{\sigma}_h) \in U_{h,0}^{k+1} \times M_h^k$ such that for all $(v_h, \boldsymbol{\tau}_h) \in U_{h,0}^{k+1} \times M_h^k$

$$\int_\Omega \mathcal{C}^{-1}\boldsymbol{\sigma}_h : \boldsymbol{\tau}_h \, dx + \langle \mathrm{div}(\boldsymbol{\tau}_h), \nabla w_h \rangle_{H(\mathrm{curl})^* \times H(\mathrm{curl})} = 0, \tag{2.4.4a}$$

$$\langle \mathrm{div}(\boldsymbol{\sigma}_h), \nabla v_h \rangle_{H(\mathrm{curl})^* \times H(\mathrm{curl})} = -\int_\Omega f v_h, \tag{2.4.4b}$$

with the duality pairing defined as in (2.3.20).

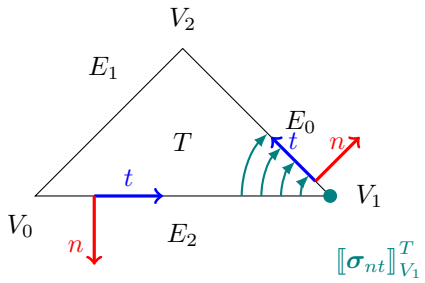

Figure 2.3: Illustration of the vertex jump.

Lemma 2.4.1 *There holds for* $\boldsymbol{\sigma}_h \in M_h^k$ *and* $w_h \in U_{h,0}^{k+1}$

$$\begin{aligned}\langle \mathrm{divdiv}(\boldsymbol{\sigma}_h), w_h\rangle_{H^{-1}\times H^1} &= -\langle \mathrm{div}(\boldsymbol{\sigma}_h), \nabla w_h\rangle_{H(\mathrm{curl})^*\times H(\mathrm{curl})}\\ &= \sum_{T\in\mathcal{T}} -\int_T \mathrm{div}\boldsymbol{\sigma}\cdot\nabla w\,dx + \int_{\partial T}\boldsymbol{\sigma}_{nt}\cdot\frac{\partial w}{\partial t}\,ds\\ &= \sum_{T\in\mathcal{T}}\int_T \mathrm{divdiv}\boldsymbol{\sigma} w\,dx - \int_{\partial T}\mathrm{div}\boldsymbol{\sigma}_n w + \frac{\partial \boldsymbol{\sigma}_{nt}}{\partial t} w\,ds + \sum_{V\in\mathcal{V}_T}[\![\boldsymbol{\sigma}_{nt}]\!]_V^T w(V),\end{aligned} \tag{2.4.5}$$

where $\mathcal{V}_T := \{V \in \mathcal{V} \,|\, V \in \overline{T}\}$ *and* $[\![\boldsymbol{\sigma}_{nt}]\!]_{V_i}^T := (\boldsymbol{\sigma}_{nt}|_{E_{i-1}} - \boldsymbol{\sigma}_{nt}|_{E_{i+1}})(V_i)$ *where the indices are understood modulus 3, cf. Figure 2.3.*

Proof: Integration by parts. □

Theorem 2.4.2 *Problems* (2.4.3) *and* (2.4.4) *are uniquely solvable.*

Proof: We prove the discrete version (2.4.4). Therefore we define the L^2 norm for the bending moment and the broken H^2-norm for the vertical deflection

$$\|\boldsymbol{\sigma}_h\|_V^2 := \|\boldsymbol{\sigma}_h\|_{L^2}^2 \simeq \|\boldsymbol{\sigma}_h\|_{L^2(\Omega)}^2 + \sum_{E\in\mathcal{E}} h\|\boldsymbol{\sigma}_{h,nn}\|_{L^2(E)}^2, \quad \|w_h\|_Q^2 := \sum_{T\in\mathcal{T}}\|\nabla^2 w_h\|_{L^2(T)}^2 + \sum_{E\in\mathcal{E}}\frac{1}{h}\|[\![\frac{\partial w_h}{\partial n}]\!]_E\|_{L^2(E)}^2.$$

With these choices the bilinear forms are continuous, e.g., with Cauchy-Schwartz

$$\begin{aligned}|b(\boldsymbol{\sigma}_h, w_h)| &\le \sum_{T\in\mathcal{T}}\|\boldsymbol{\sigma}_h\|_{L^2(T)}\|\nabla w_h\|_{-L^2(T)} + \sum_{E\in\mathcal{E}} h^{\frac12}\|\boldsymbol{\sigma}_{h,nn}\|_{L^2(E)} h^{-\frac12}\|[\![\frac{\partial w_h}{\partial n}]\!]\|_{L^2(E)}\\ &\le \Big(\sum_{T\in\mathcal{T}}\|\boldsymbol{\sigma}_h\|_{L^2(T)}^2\Big)^{\frac12}\Big(\sum_{T\in\mathcal{T}}\|\nabla^2 w_h\|_{L^2(T)}^2\Big)^{\frac12} + \Big(\sum_{E\in\mathcal{E}} h\|\boldsymbol{\sigma}_{h,nn}\|_{L^2(E)}^2\Big)^{\frac12}\Big(\sum_{E\in\mathcal{E}} h^{-1}\|[\![\frac{\partial w_h}{\partial n}]\!]\|_{L^2(E)}^2\Big)^{\frac12}\\ &\lesssim \|\sigma_h\|_V\|w_h\|_Q.\end{aligned}$$

The kernel coercivity is trivially fulfilled. We are left with the LBB condition

$$\sup_{\boldsymbol{\sigma}_h\in M_h^k}\frac{b(\boldsymbol{\sigma}_h, w_h)}{\|\boldsymbol{\sigma}_h\|_{L^2}} \ge \beta\|w_h\|_Q, \quad \beta > 0, \qquad \text{for all } w_h \in U_{h,0}^{k+1}.$$

For given $w_h \in U_{h,0}^{k+1}$ we define $\boldsymbol{\sigma}_h \in M_h^k$ such that

$$\begin{aligned}\boldsymbol{\sigma}_{h,nn} &= \frac{1}{h}[\![\frac{\partial w_h}{\partial n}]\!]_E \text{ for all } E\in\mathcal{E}\\ \int_T \boldsymbol{\sigma}_h : Q\,dx &= \int_T \nabla^2 w_h : Q\,dx \text{ for all } T\in\mathcal{T}, Q\in\mathcal{P}^{k-1}(T,\mathbb{R}^{2\times2}_{\mathrm{sym}}).\end{aligned}$$

Then there holds by construction $b(\boldsymbol{\sigma}_h, w_h) = \|w_h\|_Q^2$ and by scaling arguments the stability $\|\boldsymbol{\sigma}_h\|_{L^2} \le c\|w_h\|_Q$ such that the LBB condition is fulfilled. □

Theorem 2.4.3 (Comodi [16]) *Let $(\boldsymbol{\sigma}, w)$ be the solution of (2.4.3), $(\boldsymbol{\sigma}_h, w_h) \in M_h^k \times U_{h,\Gamma_D}^{k+1}$, with k a non-negative integer, the solution of (2.4.4) and $\tilde{w} \in H^{k+3}(\Omega) \cap H_0^2(\Omega)$ the solution of (2.4.1). Then*

$$\|\boldsymbol{\sigma} - \boldsymbol{\sigma}_h\|_{L^2} + \|w - w_h\|_{H^1} \leq ch^{k+1} \left(|\tilde{w}|_{H^{k+2}} + |\tilde{w}|_{H^{k+3}}\right) \tag{2.4.6}$$

and

$$\|w - w_h\|_{L^2} \leq ch^{k+2} \left(|\tilde{w}|_{H^{k+2}} + |\tilde{w}|_{H^{k+3}}\right). \tag{2.4.7}$$

Proof: For simplicity we assume that $w = \tilde{w}$ (and $\boldsymbol{\sigma} = \mathcal{C}\nabla^2\tilde{w}$).

For arbitrary $v_h \in U_h^{k+1}$ and $\boldsymbol{\tau}_h \in M_h^k$ there holds together with the canonical interpolation operators due to the polynomial degree the following orthogonality properties

$$\begin{aligned}
b(\mathcal{I}_h^{\mathrm{M_h},k}\boldsymbol{\sigma} - \boldsymbol{\sigma}, v_h) &= \sum_{T\in\mathcal{T}} \int_T (\mathcal{I}_h^{\mathrm{M_h},k}\boldsymbol{\sigma} - \boldsymbol{\sigma}) : \nabla^2 v_h \, dx - \int_{\partial T} (\mathcal{I}_h^{\mathrm{M_h},k}\boldsymbol{\sigma} - \boldsymbol{\sigma})_{nn} \frac{\partial v_h}{\partial n} \, ds = 0, \\
b(\boldsymbol{\tau}_h, \mathcal{I}_h^{k+1}w - w) &= \sum_{T\in\mathcal{T}} \int_T \mathrm{divdiv}\boldsymbol{\tau}_h(\mathcal{I}_h^{k+1}w - w) \, dx - \int_{\partial T} (\mathrm{div}\boldsymbol{\tau}_{h,n} + \frac{\partial \boldsymbol{\tau}_{h,nt}}{\partial t})(\mathcal{I}_h^{k+1}w - w) \, ds \\
&\quad + \sum_{V\in\mathcal{V}_T} [\![\boldsymbol{\tau}_{h,nt}]\!]_V^T (\mathcal{I}_h^{k+1}w - w)(V) = 0.
\end{aligned}$$

By triangle inequality

$$\|\boldsymbol{\sigma} - \boldsymbol{\sigma}_h\|_{L^2} + \|w - w_h\|_{H^1} \leq \|\boldsymbol{\sigma} - \mathcal{I}_h^{\mathrm{M_h},k}\boldsymbol{\sigma}\|_{L^2} + \|\mathcal{I}_h^{\mathrm{M_h},k}\boldsymbol{\sigma} - \boldsymbol{\sigma}_h\|_{L^2} + \|w - \mathcal{I}_h^{k+1}w\|_{H^1} + \|\mathcal{I}_h^{k+1}w - w_h\|_{H^1}.$$

Going to the stronger broken H^2 norm from the proof of Theorem 2.4.2 and using stability of the discrete problem, Galerkin-orthogonality, and the orthogonality properties proven above we obtain

$$\begin{aligned}
\|\mathcal{I}_h^{\mathrm{M_h},k}\boldsymbol{\sigma} - \boldsymbol{\sigma}_h\|_{L^2} + \|\mathcal{I}_h^{k+1}w - w_h\|_{H^1} &\lesssim \|\mathcal{I}_h^{\mathrm{M_h},k}\boldsymbol{\sigma} - \boldsymbol{\sigma}_h\|_{L^2} + \|\mathcal{I}_h^{k+1}w - w_h\|_{H_h^2} \\
&\lesssim \sup_{(\tau_h,v_h)\in M_h^k \times U_{h,\Gamma_D}^{k+1}} \frac{B((\mathcal{I}_h^{\mathrm{M_h},k}\boldsymbol{\sigma} - \boldsymbol{\sigma}_h, \mathcal{I}_h^{k+1}w - w_h), (\tau_h, v_h))}{\|\tau_h\|_{L^2} + \|v_h\|_{H_h^2}} \\
&= \sup_{(\tau_h,v_h)\in M_h^k \times U_{h,\Gamma_D}^{k+1}} \frac{B((\mathcal{I}_h^{\mathrm{M_h},k}\boldsymbol{\sigma} - \boldsymbol{\sigma}, \mathcal{I}_h^{k+1}w - w), (\tau_h, v_h))}{\|\tau_h\|_{L^2} + \|v_h\|_{H_h^2}} \\
&\lesssim \sup_{(\tau_h,v_h)\in M_h^k \times U_{h,\Gamma_D}^{k+1}} \frac{\|\mathcal{I}_h^{\mathrm{M_h},k}\boldsymbol{\sigma} - \boldsymbol{\sigma}_h\|_{L^2}\|\tau_h\|_{L^2}}{\|\tau_h\|_{L^2} + \|v_h\|_{H_h^2}} \leq \|\mathcal{I}_h^{\mathrm{M_h},k}\boldsymbol{\sigma} - \boldsymbol{\sigma}_h\|_{L^2},
\end{aligned}$$

where we defined $B((\sigma, w), (\tau, v)) := a(\sigma, \tau) + b(\sigma, v) + b(\tau, w)$ ($a(\cdot,\cdot), b(\cdot,\cdot)$ as in proof of Theorem 2.4.2). Thus

$$\begin{aligned}
\|\boldsymbol{\sigma} - \boldsymbol{\sigma}_h\|_{L^2} + \|w - w_h\|_{H^1} \lesssim \|\mathcal{I}_h^{\mathrm{M_h},k}\boldsymbol{\sigma} - \boldsymbol{\sigma}_h\|_{L^2} + \|w - \mathcal{I}_h^{k+1}w\|_{H^1} &\lesssim h^{k+1}(|w|_{H^{k+2}} + |\sigma|_{H^{k+1}}) \\
&\lesssim h^{k+1}(|w|_{H^{k+2}} + |w|_{H^{k+3}}).
\end{aligned}$$

□

Remark 2.4.4 *It was shown [6] that, if a domain with smooth boundary gets approximated by a polygonal domain, the solutions do not necessarily converge towards the solution of the smooth domain. This so-called Babuška paradox shows that one cannot expect convergence if a lowest-order, i.e., an affine, discretization of the geometry is considered for fourth order problems. It was shown in [5], however, that the HHJ method does not suffer from this behavior.*

Exercise 2.4.5 *The Ciarlet–Raviart method for Kirchhoff–Love plates uses that* $\mathrm{divdiv}\nabla^2 w = \Delta^2 w$ *is the bi-Laplace and defines $\sigma = \Delta u$ as additional scalar field. Derive the weak formulation for clamped plates and solve the biharmonic plate equation.*

Exercise 2.4.6 *How can the other boundary conditions be incorporated for the HHJ method?*

What changes to incorporate different boundary conditions for the Ciarlet–Raviart method?

2.4.2 TDNNS Tangential-displacement normal-normal stress elements for Reissner–Mindlin plates

As we have observed in Section 2.1.2 and Section 2.2.1 the appearance of the rotation field β yields possible shear locking. Discretizing w and β both with Lagrange finite elements does not mimic the continuous property that the gradient of H^1-functions is in $H(\mathrm{curl})$ (or in L^2 in 1D), $\nabla H^1 \subset H(\mathrm{curl})$, but $\nabla w_h \nsubseteq U_h^k$. If we discretize the rotations β with $H(\mathrm{curl})$-conforming Nédélec elements we obtain the relation $\nabla w_h \subset \mathcal{N}$ such that the constraint $\nabla w_h = \beta_h$ can be fulfilled in the discrete case. The gradient of an $H(\mathrm{curl})$ function needed for the bending energy, however, is not square-integrable and thus the linearized moment stress tensor $\boldsymbol{\sigma}$ is introduced leading to the clamped Reissner–Mindlin problem: Find $(w, \boldsymbol{\sigma}, \beta) \in H_0^1(\Omega) \times H(\mathrm{divdiv}, \Omega) \times H_0(\mathrm{curl}, \Omega)$ such that for all $(v, \boldsymbol{\tau}, \delta) \in H_0^1(\Omega) \times H(\mathrm{divdiv}, \Omega) \times H_0(\mathrm{curl}, \Omega)$

$$\int_\Omega \mathcal{C}^{-1}\boldsymbol{\sigma} : \boldsymbol{\tau}\, dx + \langle \mathrm{div}(\boldsymbol{\tau}), \beta\rangle_{H(\mathrm{curl})^* \times H(\mathrm{curl})} = 0, \tag{2.4.8a}$$

$$\langle \mathrm{div}(\boldsymbol{\sigma}), \delta\rangle_{H(\mathrm{curl})^* \times H(\mathrm{curl})} - \frac{\kappa G}{t^2} \int_\Omega (\nabla w - \beta) \cdot (\nabla v - \delta)\, dx = -\int_\Omega f v. \tag{2.4.8b}$$

The first equation states that $\boldsymbol{\sigma} = \mathcal{C}\boldsymbol{\varepsilon}(\beta)$ and the second one is the Reissner–Mindlin plate equation.

With (2.3.1), (2.3.21), and (2.3.6) the discretized problem reads: Find $(w_h, \boldsymbol{\sigma}_h, \beta_h) \in U_{h,0}^{k+1} \times M_h^k \times \mathcal{N}_{II,0}^k$ such that for all $(v_h, \boldsymbol{\tau}_h, \delta_h) \in U_{h,0}^{k+1} \times M_h^k \times \mathcal{N}_{II,0}^k$

$$\int_\Omega \mathcal{C}^{-1}\boldsymbol{\sigma}_h : \boldsymbol{\tau}_h\, dx + \langle \mathrm{div}(\boldsymbol{\tau}_h), \beta_h\rangle_{H(\mathrm{curl})^* \times H(\mathrm{curl})} = 0, \tag{2.4.9a}$$

$$\langle \mathrm{div}(\boldsymbol{\sigma}_h), \delta_h\rangle_{H(\mathrm{curl})^* \times H(\mathrm{curl})} - \frac{\kappa G}{t^2} \int_\Omega (\nabla w_h - \beta_h) \cdot (\nabla v_h - \delta_h)\, dx = -\int_\Omega f v_h. \tag{2.4.9b}$$

Formulation (2.4.9) is called the TDNNS method for Reissner–Mindlin plates [41].

Note that the same duality pairings in (2.4.3) and (2.4.8) (respectively (2.4.4) and (2.4.9)) are used as $\nabla H^1 \subset H(\mathrm{curl})$. Due to the De'Rham complex this relation is inherited to the discrete counterparts.

Using by a change of variables the shear $\gamma = \nabla w - \beta \in H(\mathrm{curl})$ instead of the rotation β as unknown, (2.4.8) changes to the equivalent form: Find $(w, \boldsymbol{\sigma}, \gamma) \in H_0^1(\Omega) \times H(\mathrm{divdiv}, \Omega) \times H_0(\mathrm{curl}, \Omega)$ such that for all $(v, \boldsymbol{\tau}, \xi) \in H_0^1(\Omega) \times H(\mathrm{divdiv}, \Omega) \times H_0(\mathrm{curl}, \Omega)$

$$\int_\Omega \mathcal{C}^{-1}\boldsymbol{\sigma} : \boldsymbol{\tau}\, dx + \langle \mathrm{div}(\boldsymbol{\tau}), \nabla w - \gamma\rangle_{H(\mathrm{curl})^* \times H(\mathrm{curl})} = 0, \tag{2.4.10a}$$

$$\langle \mathrm{div}(\boldsymbol{\sigma}), \nabla v - \xi\rangle_{H(\mathrm{curl})^* \times H(\mathrm{curl})} - \frac{\kappa G}{t^2} \int_\Omega \gamma \cdot \xi\, dx = -\int_\Omega f v. \tag{2.4.10b}$$

Here we can see the close relation to the HHJ formulation for the Kirchhoff–Love plate: We obtain that in the limit $t \to 0$ there holds $|\gamma| \to 0$ (or equivalently $|\nabla w - \beta| \to 0$) and thus, (2.4.3) is (formally) recovered. In [41] the auxiliary variable $\tilde{\gamma} := \frac{\kappa G}{t^2}(\nabla w - \beta)$, which can be seen as a kind of normalized shear stress, is introduced as additional unknown and equation to prove convergence independently of the thickness parameter t, i.e., shear locking is circumvented (similar to the analysis of the mixed Euler–Bernoulli beam).

Theorem 2.4.7 *Let $(w, \boldsymbol{\sigma}, \beta) \in H_0^1(\Omega) \times H(\mathrm{divdiv}, \Omega) \times H_0(\mathrm{curl}, \Omega)$ the exact solution of (2.4.8), $(w_h, \boldsymbol{\sigma}_h, \beta_h) \in U_{h,0}^{k+1} \times M_h^k \times \mathcal{N}_{II,0}^k$ the corresponding finite element solution, and $\tilde{\gamma} := \frac{\kappa G}{t^2}(\nabla w - \beta)$, $\tilde{\gamma}_h := \frac{\kappa G}{t^2}(\nabla w_h - \beta_h)$. Then there holds the a priori estimate for $1 \le m \le k$*

$$\|w - w_h\|_{H^1} + \|\beta - \beta_h\|_{H(\mathrm{curl})} + \|\boldsymbol{\sigma} - \boldsymbol{\sigma}_h\|_{M_h} + t\|\tilde{\gamma} - \tilde{\gamma}_h\|_{L^2} \le c h^m \left(\|\beta\|_{H^{m+1}} + \|\boldsymbol{\sigma}\|_{H^m} + t\|\tilde{\gamma}\|_{H^m}\right), \tag{2.4.11}$$

with $c \neq c(t)$.

Proof: See [41, Theorem 4]. The error is independent of w and a different norm for σ is used, namely $\|\sigma\|_{M_h}^2 = \|\sigma\|_{L^2}^2 + \sum_{E \in \mathcal{E}} h\|\sigma_{nn}\|_{L^2(E)}^2 + \sup_{w_h \in U_h} \frac{\langle \mathrm{div}\sigma, \nabla w_h\rangle^2}{\|w_h\|_{H^1}^2}$. □

2.4.3 Hybridization of HHJ and TDNNS method

One possible disadvantage of the HHJ and TDNNS method presented above is their saddle-point structure leading to an indefinite matrix after assembling. For the HHJ method for Kirchhoff–Love plates (2.4.4) the system matrix is of the form

$$\begin{pmatrix} A & B^\top \\ B & 0 \end{pmatrix} \begin{pmatrix} \underline{\boldsymbol{\sigma}} \\ \underline{w} \end{pmatrix} = \underline{f}, \tag{2.4.12}$$

where $\underline{\boldsymbol{\sigma}}$, $\underline{w}$, and $\underline{f}$ represent the coefficient vectors of the finite elements $\boldsymbol{\sigma}_h$ and w_h and the right-hand side f, respectively. The displacement w can be interpreted as Lagrange multiplier enforcing the force balance equation $-\operatorname{div}(\boldsymbol{\sigma}) = f$. With the usage of hybridization techniques, however, a positive definite matrix can be recovered.

For hybridization the continuity condition of finite elements is broken and reinforced in weak sense. Therefore, so-called hybridization or facet spaces have to be used. When breaking the normal continuity of $H(\operatorname{div})$-conforming elements V_h^k the corresponding facet space for hybridization is given by

$$\begin{aligned} \Gamma_h^k &:= \mathcal{P}^k(\mathcal{F}), \\ \Gamma_{h,0}^k &:= \{\alpha \in \Gamma_h^k \,|\, \alpha = 0 \text{ on } \partial\Omega\}, \end{aligned} \tag{2.4.13}$$

i.e., piece-wise polynomials on the skeleton $\mathcal{F}$. Reordering the facet terms of the equation

$$\sum_{T\in\mathcal{T}} \int_{\partial T} u_h \cdot n\, \xi_h \, ds = 0 \text{ for all } \xi_h \in \Gamma_h^k \tag{2.4.14}$$

for a discontinuous (dc) function in the RT or BDM space $u_h \in V_h^{k,dc} := \{u \in L^2(\Omega, \mathbb{R}^2) \,|\, u|_T = u_h|_T,\, u_h \in V_h^k(T), T \in \mathcal{T}\}$ yields

$$0 = \sum_{F\in\mathcal{F}^{\text{int}}} \int_F (u_h|_{T_1} - u_h|_{T_2}) \cdot n_F\, \xi_h \, ds + \sum_{F\in\mathcal{F}^{\text{bnd}}} \int_F u_h \cdot n\, \xi_h \, ds = \sum_{F\in\mathcal{F}} \int_F [\![u_{h,n}]\!]\, \xi_h \, ds, \tag{2.4.15}$$

where $\mathcal{F}^{\text{int}}$ and $\mathcal{F}^{\text{bnd}}$ denote all interior and boundary facets, respectively. Thus, the normal continuity $[\![u_{h,n}]\!] = 0$ and homogeneous Dirichlet boundary $u_{h,n} = 0$ on $\partial\Omega$ are forced.

Example 2.4.8 (Mixed Poisson problem with $H(\operatorname{div})$-conforming elements) *We rewrite the Poisson problem: Find $u \in H_0^1(\Omega)$ such that $-\Delta u = f$ as mixed saddle point problem using BDM elements: Find $(\sigma, u) \in BDM^k \times Q_h^{k-1}$ such that for all $(\tau, v) \in BDM^k \times Q_h^{k-1}$*

$$\begin{aligned} \int_\Omega \sigma \cdot \tau \, dx \quad &- \int_\Omega u \operatorname{div}\tau \, dx = 0, \\ -\int_\Omega v \operatorname{div}\sigma \, dx \quad &= -\int_\Omega f\, v \, dx, \end{aligned}$$

which has the saddle-point form

$$\begin{pmatrix} A & B^\top \\ B & 0 \end{pmatrix} \begin{pmatrix} \underline{\sigma} \\ \underline{u} \end{pmatrix} = \begin{pmatrix} 0 \\ \underline{f} \end{pmatrix}.$$

Breaking the normal-continuity of σ and reinforcing weakly by the facet space gives the hybridized problem: Find $(\sigma, u, \hat{v}) \in BDM^{k,\text{dc}} \times Q_h^{k-1} \times \Gamma_{h,0}^k$ such that for all $(\tau, v, \hat{v}) \in BDM^{k,\text{dc}} \times Q_h^{k-1} \times \Gamma_{h,0}^k$

$$\begin{aligned} \int_\Omega \sigma \cdot \tau \, dx \quad &- \sum_{T\in\mathcal{T}} \int_T u \operatorname{div}\tau \, dx + \sum_{T\in\mathcal{T}} \int_{\partial T} \hat{u}\tau_n \, ds = 0, \\ -\sum_{T\in\mathcal{T}} \int_T v \operatorname{div}\sigma \, dx \quad &= -\int_\Omega f\, v \, dx, \\ \sum_{T\in\mathcal{T}} \int_{\partial T} \hat{v}\sigma_n \, ds \quad &= 0, \end{aligned}$$

leads to the system matrix

$$\begin{pmatrix} A & C^\top \\ C & 0 \end{pmatrix} \begin{pmatrix} \underline{\sigma} \\ \begin{pmatrix} \underline{u} \\ \underline{\hat{u}} \end{pmatrix} \end{pmatrix} = \begin{pmatrix} 0 \\ \begin{pmatrix} \underline{f} \\ 0 \end{pmatrix} \end{pmatrix}.$$

The inversion of A is cheap and the Schur complement

$$-CA^{-1}C^\top \begin{pmatrix} \underline{u} \\ \underline{\hat{u}} \end{pmatrix} = \begin{pmatrix} \underline{f} \\ 0 \end{pmatrix}$$

is positive definite.

Note, that the boundary condition changed from essential Dirichlet for the primal to natural Neumann for the mixed version, and back again to essential Dirichlet for the hybrid mixed form. The Lagrange multiplier $\hat{u}$ enforcing the normal continuity of the stress has the physical meaning of the trace of u.

For the HHJ elements we equippe the facet space Γ_h^k with the normal vector n_F, such that its functions are facet-wise two-valued differing only in the sign. More precisely, by defining this space as the normal-facet space

$$\Lambda_h^k := \{\alpha_h n_F \,|\, \alpha_h \in \Gamma_h^k\} \tag{2.4.16}$$

we have for $\alpha_h \in \Lambda_h^k$ that $\alpha_{h,n_{T_1}} = -\alpha_{h,n_{T_2}}$. Thus, a normal-normal continuous function with zero normal-normal trace on $\partial\Omega$ of a function $\boldsymbol{\sigma}_h \in M_h^{dc,k}$ can be achieved by the equation

$$0 = \sum_{T\in\mathcal{T}} \int_{\partial T} \boldsymbol{\sigma}_{h,nn}\, \alpha_{h,n}\, ds = \sum_{F\in\mathcal{F}} \int_F [\![\boldsymbol{\sigma}_{h,nn}]\!]\, \alpha_h\, ds \text{ for all } \alpha_h \in \Lambda_h^k. \tag{2.4.17}$$

For the HHJ method we break the normal-normal-continuity and denote the discontinuous stress space by M_h^{dc}. More precisely, let $\alpha_h \in \Lambda_h$ from the hybridization space (2.4.16). Further, α_h has to satisfy the essential boundary conditions on Γ_D. Then the hybridized HHJ problem reads: Find stress, displacement, and hybridization fields $(\boldsymbol{\sigma}_h, w_h, \alpha_h) \in M_h^{\mathrm{dc},k} \times U_{h,0}^{k+1} \times \Lambda_{h,0}^k$ for all $(\boldsymbol{\tau}_h, v_h, \xi_h) \in M_h^{\mathrm{dc},k} \times U_{h,0}^{k+1} \times \Lambda_{h,0}^k$

$$\int_\Omega \mathcal{C}^{-1}\boldsymbol{\sigma}_h : \boldsymbol{\tau}_h\, dx + \langle \mathrm{div}(\boldsymbol{\tau}_h), \nabla w_h\rangle_{H(\mathrm{curl})^*\times H(\mathrm{curl})} - \sum_{T\in\mathcal{T}} \int_{\partial T} \alpha_{h,n}\boldsymbol{\tau}_{h,nn}\, ds = 0, \tag{2.4.18a}$$

$$\langle \mathrm{div}(\boldsymbol{\sigma}_h), \nabla v_h\rangle_{H(\mathrm{curl})^*\times H(\mathrm{curl})} = \int_\Omega f\, v_h\, dx, \tag{2.4.18b}$$

$$-\sum_{T\in\mathcal{T}} \int_{\partial T} \xi_{h,n}\boldsymbol{\sigma}_{h,nn}\, ds = 0, \tag{2.4.18c}$$

The Lagrange multiplier α_h enforces in equation (2.4.18c) the normal-normal continuity of $\boldsymbol{\sigma}_h$ and the boundary condition. Combining the surface terms in (2.4.18a) one observes that α_h has the physical meaning of the normal derivative of the displacement $\frac{\partial w_h}{\partial n} \approx \alpha_{h,n}$.

Exercise 2.4.9 *Incorporate and test the different boundary conditions for the mixed and hybrid mixed HHJ method for Kirchhoff–Love plates.*

As for $\boldsymbol{\sigma}_h$ and α_h the same polynomial order is used, the hybridized system (2.4.18) is equivalent to the original one (2.4.4).

However, the discontinuous stress $\boldsymbol{\sigma}_h \in M_h^{k,dc}$ does not have any coupling dofs and thus, one can use static condensation to eliminate it at element level, reducing the number of total dofs drastically for the final system, and making it therefore symmetric and positive definite (spd) again

$$\begin{gathered} \begin{pmatrix} A & B^\top \\ B & 0 \end{pmatrix} \begin{pmatrix} \underline{\boldsymbol{\sigma}} \\ \begin{pmatrix} \underline{w} \\ \underline{\alpha} \end{pmatrix} \end{pmatrix} = \begin{pmatrix} 0 \\ \underline{f} \end{pmatrix}, \\ \underline{\boldsymbol{\sigma}} = -A^{-1}B^\top \begin{pmatrix} \underline{w} \\ \underline{\alpha} \end{pmatrix}, \qquad -BA^{-1}B^\top \begin{pmatrix} \underline{w} \\ \underline{\alpha} \end{pmatrix} = \underline{f}. \end{gathered} \tag{2.4.19}$$

From the first equation $\underline{\boldsymbol{\sigma}}$ can be explicitly expressed in terms of $\underline{w}$ and $\underline{\alpha}$. This identity is inserted into the second equation leading to the Schur-complement matrix $-BA^{-1}B^\top$. Note that A is a block diagonal matrix and thus cheap to invert.

In terms of the TDNNS method α_h corresponds to the normal component of the rotations, $\alpha_{h,n} \approx \beta_{h,n}$.

Exercise 2.4.10 *Another possible drawback is the needed inversion of the material law $\mathcal{C}^{-1}$ in e.g. (2.4.3). Adding the strain $\boldsymbol{\varepsilon} = \boldsymbol{\varepsilon}(u)$ as additional unknown leads to the Hu–Washizu three-field approach. Then also nonlinear material laws can be used.*

Formulate the Hu–Washizu principle for the HHJ method for Kirchhoff–Love plates. What is the appropriate space? Under which conditions is the three-field formulation equivalent to the mixed method?

Exercise 2.4.11 *The Föppl–von Kármán equations reading*

$$\frac{Et^3}{12(1-\nu^2)}\Delta^2 w - t\sum_{i,j=1}^{2}\frac{\partial}{\partial x_j}\Big(\boldsymbol{\sigma}_{ij}\frac{\partial w}{\partial x_i}\Big) = P,$$
$$\operatorname{div}\boldsymbol{\sigma} = 0,$$

are used to simulate large deformations for thin plates. Here $\Delta^2 w$ denotes the bi-Laplace and P a volume force. In the derivation the initial stress-strain relation contains also the quadratic terms of the vertical deflection $\sigma = \mathcal{C}\boldsymbol{\varepsilon} = \mathcal{C}\big(\varepsilon(u) + 0.5\nabla w \otimes \nabla w\big)$, $u = (u_x, u_y)$ the horizontal displacement.

Show that by introducing the Airy stress function φ with $\boldsymbol{\sigma}_{11} = \frac{\partial^2\varphi}{\partial x_2^2}$, $\boldsymbol{\sigma}_{22} = \frac{\partial^2\varphi}{\partial x_1^2}$, and $\boldsymbol{\sigma}_{12} = -\frac{\partial^2\varphi}{\partial x_1 \partial x_2}$ the equations become

$$\frac{Et^3}{12(1-\nu^2)}\Delta^2 w - t\,[\varphi, w] = P,$$
$$\Delta^2\varphi + \frac{E}{2}\,[w, w] = 0,$$

with $[u,v] := \operatorname{cof}(\nabla^2 u) : \nabla^2 v = \frac{\partial^2 u}{\partial x_2^2}\frac{\partial^2 v}{\partial x_1^2} + \frac{\partial^2 u}{\partial x_1^2}\frac{\partial^2 v}{\partial x_2^2} - 2\frac{\partial^2 u}{\partial x_1 \partial x_2}\frac{\partial^2 v}{\partial x_1 \partial x_2}$. Derive the weak formulation for clamped boundary conditions $w = \frac{\partial w}{\partial n} = \varphi = \frac{\partial \varphi}{\partial n} = 0$.

Exercise 2.4.12 *Reformulate the Föppl–von Kármán equations in terms of the Hellan–Herrmann–Johnson method such that Lagrangian finite elements can be used for w and φ.*

Chapter 3

Extrinsic Differential Geometry

One fundamental difference between plates and general shell structures is that plates are non-curved (in the initial configuration). This entails the usage of standard (Euclidean) derivatives and components based on the Euclidean basis, which does not change spatially. E.g., the normal vector of a plate $\mathcal{S} \subset \mathbb{R}^2 \times \{0\}$ is $\nu = \begin{pmatrix} 0 & 0 & 1 \end{pmatrix}^\top$ and thus $\nabla\nu = 0$. To define tangential and normal components of curved surfaces, however, the basis vectors depend on the position on the surface. To define and treat objects like surface derivatives we need tools from differential geometry. If the surface is not smooth, e.g. if we use an affine triangulation consisting of piece-wise flat triangles to approximate a curved surface, additional questions arise lying in the field of discrete differential geometry (DDG).

Literature including classical, modern, and discrete differential geometry are e.g. [18, 28, 47, 9, 49, 33, 37].

Remark 3.0.1 *There are different approaches/dialects in differential geometry. For example, defining more or less all objects in terms of coordinates, or using more coordinate free notation. We will use a notation comparable to tangential differential calculus (TDC), where differential operators are defined in a more compactly notation. The notation of curvilinear coordinates is widely used. Another language used in the context of differential geometry is exterior calculus being more "abstract" compared to the others.*

As shells are obviously two-dimensional objects embedded in the three-dimensional Euclidean space, we will use in this section the concept of sub-manifolds embedded in $\mathbb{R}^n$ leading to extrinsic differential geometry. In Chapter 5 we will forget the surrounding space leading to Riemannian manifolds, where only intrinsic geometric quantities can be computed.

3.1 (Sub-) Manifolds

We start with the definition of a smooth submanifold.

Definition 3.1.1 *Let $0 \leq k < n$ be an integer. A differentiable function $\varphi : \omega \to \mathbb{R}^n$ with $\omega \subset \mathbb{R}^k$ open is called an* embedding *if $\nabla\varphi \in \mathbb{R}^{n\times k}$ has full rank, i.e., $\nabla\varphi$ is injective. $\mathcal{S} \subset \mathbb{R}^n$ is a k-dimensional* submanifold *of $\mathbb{R}^n$ if for every $x \in \mathcal{S}$ there exists an embedding $\varphi : V \to U$ from $V \subset \mathbb{R}^k$ open to an open neighborhood $U \subset \mathbb{R}^n$ of x such that $\mathcal{S} \cap U = \varphi(V)$. For $n = 3$ and $k = 2$ we call $\mathcal{S}$ a* surface *and for $k = 1$ a* curve.

In the following we assume w.l.o.g. that the manifold $\mathcal{S}$ can be parameterized with a single embedding and note that the results can easily be extended by using an atlas, i.e., a set of embeddings covering the whole manifold.

There exist several ways to define the tangent space of $\mathcal{S}$ at a point $p \in \mathcal{S}$. We make use of the embedding (the definition in fact independent of the chosen embedding).

Definition 3.1.2 *Let $\varphi : \mathbb{R}^k \to \mathcal{S}$ be an embedding such that $p \in \mathcal{S}$ is an interior point of the range of φ. Then the* tangent space *at $p \in \mathcal{S}$ is defined by*

$$T_p\mathcal{S} := \nabla\varphi(q)\mathbb{R}^k := \{\nabla\varphi(q)\eta \in \mathbb{R}^n \,|\, \eta \in \mathbb{R}^k\}, \qquad p = \varphi(q) \tag{3.1.1}$$

and the tangent bundle *by $T\mathcal{S} := \bigsqcup_{p\in\mathcal{S}} T_p\mathcal{S} := \bigcup_{p\in\mathcal{S}} \{p\} \times T_p\mathcal{S}$.*

We focus on $n-1$ dimensional submanifolds such that a unique normal vector (up to orientation) exists.

Definition 3.1.3 *Let $\mathcal{S}$ be an $n-1$ dimensional submanifold of $\mathbb{R}^n$. A function $\nu : \mathcal{S} \to \mathbb{S}^{n-1}$ is a* normal vector *field of $\mathcal{S}$ if for all $p \in \mathcal{S}$ there holds $\nu(p) \perp T_p\mathcal{S}$. A surface $\mathcal{S}$ is called* orientable *if there exists a globally continuous normal vector field $\nu : \mathcal{S} \to \mathbb{S}^{n-1}$. The* projection operator *onto the tangent bundle $\boldsymbol{P}_\mathcal{S} : \mathbb{R}^n \to T\mathcal{S}$ is defined by $\boldsymbol{P}_\mathcal{S} := \boldsymbol{I} - \nu \otimes \nu$.*

There are two, equivalent, ways to define derivatives of functions $f : \mathcal{S} \to \mathbb{R}$ on the surface: Using the embedding going back to $\mathbb{R}^k$, where we know how to differentiate, or to use the surrounding space $\mathbb{R}^n$ computing the classical derivative and projecting the result back onto the surface.

Definition 3.1.4 *Let $\mathcal{S} \subset \mathbb{R}^n$ be a smooth k-dimensional sub-manifold, $p \in \mathcal{S}$, $f : \mathcal{S} \to \mathbb{R}$ and $\varphi : \mathbb{R}^k \to \mathcal{S}$ an embedding. Then we call the function f* differentiable, *$f \in C^1(\mathcal{S})$, at $p \in \mathcal{S}$, w.l.o.g. $\varphi(0) = p$, if*

$$\nabla_{\mathcal{S}} f(p) := \nabla((f \circ \varphi)(0))(\nabla\varphi(0))^\dagger \tag{3.1.2}$$

is differentiable in classical sense and call $\nabla_{\mathcal{S}} f$ the tangential *or* surface gradient *of f. Here, $(\nabla\varphi)^\dagger \in \mathbb{R}^{k\times n}$ denotes the* Moore–Penrose pseudo-inverse *of $\nabla\varphi \in \mathbb{R}^{n\times k}$.*

The Moore–Penrose pseudo-inverse $\boldsymbol{A}^\dagger$ of a rank k matrix $\boldsymbol{A} \in \mathbb{R}^{n\times k}$ is given by $\boldsymbol{A}^\dagger = (\boldsymbol{A}^\top \boldsymbol{A})^{-1}\boldsymbol{A}^\top$.

The definition is independent of the particular embedding φ and can be extended easily to vector valued functions $f : \mathcal{S} \to \mathbb{R}^n$.

For smooth manifolds we can define an ε-tube around it, where we can then extend functions. We focus on surfaces in 3D.

Theorem 3.1.5 *Let $\omega \subset \mathbb{R}^2$ be a domain and let $\varphi \in C^3(\overline{\omega}, \mathbb{R}^3)$ be an embedding. Then there exists $\varepsilon > 0$ such that the mapping $\Theta : \overline{\Omega} \to \mathbb{R}^3$, $\Omega := \omega \times (-\varepsilon/2, \varepsilon/2)$ defined by*

$$\Theta(x, z) := \varphi(x) + z\nu(x) \qquad \text{for all } (x, z) \in \overline{\Omega} \tag{3.1.3}$$

is a C^2-diffeomorphism from $\overline{\Omega}$ onto $\Theta(\overline{\Omega})$ and $\det(\tau_1, \tau_2, \nu) > 0$ in $\overline{\Omega}$, where $\tau_i = \frac{\partial\Theta}{\partial x_i}$ and $\nu = \frac{\tau_1\times\tau_2}{\|\tau_1\times\tau_2\|_2}$.

Proof: See e.g., [15, Theorem 4.1-1]. □

The requirement on the thickness ε depends on the curvature of the surface.

With Theorem 3.1.5 and the projection $\boldsymbol{P}_{\mathcal{S}}$ for given $f : \mathcal{S} \to \mathbb{R}$ an extension $F : \mathbb{R}^3 \to \mathbb{R}$ can be defined such that $F|_{\mathcal{S}} = f$, e.g., by extending it constantly in ν direction. With this at hand we define the tangential derivative as

$$\nabla_{\mathcal{S}} f = \boldsymbol{P}_{\mathcal{S}} \nabla F, \tag{3.1.4}$$

which is independent of the choice of the extension F. Note that (3.1.4) is an equivalent definition to (3.1.2). For vector valued functions $f : \mathcal{S} \to \mathbb{R}^3$ the surface gradient via extension is given by $\nabla_{\mathcal{S}} f = \nabla F \boldsymbol{P}_{\mathcal{S}}$.

Definition 3.1.6 *The* surface divergence *of a vector valued function $u \in C^1(\mathcal{S}, \mathbb{R}^n)$ is defined by $\operatorname{div}_{\mathcal{S}}(u) := \operatorname{tr}(\nabla_{\mathcal{S}} u)$. For $n = 3$ the* surface curl *of a vector valued function u is given by $\operatorname{curl}_{\mathcal{S}}(u) := (\nabla_{\mathcal{S}} \times U) \cdot \nu = \operatorname{div}_{\mathcal{S}}(u \times \nu)$ and for a scalar $\phi \in C^1(\mathcal{S})$ $\operatorname{curl}_{\mathcal{S}}(\phi) := \nu \times \nabla_{\mathcal{S}}\phi$, where ν is the normal vector and U an extension of u into the neighborhood of $\mathcal{S}$. The* Laplace–Beltrami *operator is defined as $\Delta_{\mathcal{S}} f := \operatorname{div}_{\mathcal{S}}(\nabla_{\mathcal{S}} f)$.*

With the projection operator $\boldsymbol{P}_{\mathcal{S}}$ onto the tangent space at hand we can define the covariant surface derivative.

Definition 3.1.7 *Let $\mathcal{S} \subset \mathbb{R}^n$ be a smooth $n-1$-dimensional sub-manifold, $\boldsymbol{P}_{\mathcal{S}}$ the projection onto the tangent space, and $f : \mathcal{S} \to \mathbb{R}^n$ a differentiable vector field. The* covariant surface gradient *of f is defined by*

$$\nabla^{\text{cov}}_{\mathcal{S}} f := \boldsymbol{P}_{\mathcal{S}} \nabla_{\mathcal{S}} f \tag{3.1.5}$$

or via extension $F : \mathbb{R}^n \to \mathbb{R}^n$ as $\nabla^{\text{cov}}_{\mathcal{S}} f := \boldsymbol{P}_{\mathcal{S}} \nabla_{\mathcal{S}} F \boldsymbol{P}_{\mathcal{S}}$. The Riemannian Hesse *of $f \in C^2(\mathcal{S})$ is given by $\nabla^2_{\mathcal{S}} f := \nabla^{\text{cov}}_{\mathcal{S}} \nabla_{\mathcal{S}} f$.*

Note, that for a vector field f on $\mathcal{S}$ there holds $\nu^\top \nabla^{\text{cov}}_{\mathcal{S}} f = 0$ and $\nabla^{\text{cov}}_{\mathcal{S}} f\, \nu = 0$, but in general $\nu^\top \nabla_{\mathcal{S}} f \neq 0$ (only $\nabla_{\mathcal{S}} f\, \nu = 0$).

3.1.1 Shape operator and fundamental forms

To measure distances, angles, and curvatures on manifolds the following fundamental forms are introduced.

Definition 3.1.8 *Let $\mathcal{S}$ be a surface with normal vector ν and $v, w \in T\mathcal{S}$. Then the first, second, and third fundamental forms are given by*

$$I(v,w) := \langle v, w\rangle, \tag{3.1.6a}$$
$$II(v,w) := \langle \nabla_{\mathcal{S}}\nu\, v, w\rangle, \tag{3.1.6b}$$
$$III(v,w) := \langle \nabla_{\mathcal{S}}\nu\, v, \nabla_{\mathcal{S}}\nu\, w\rangle, \tag{3.1.6c}$$

where $\langle\cdot,\cdot\rangle$ denotes the Euclidean scalar product in $\mathbb{R}^3$ restricted on the tangent space.

$\nabla_{\mathcal{S}}\nu$ is the Weingarten tensor, which is symmetric and acts on tangent vectors. It induces the shape operator $\mathfrak{S} : T\mathcal{S} \to T\mathcal{S} : X \mapsto \nabla_{\mathcal{S}}\nu X$. It is further referred to as curvature tensor as the second derivatives of the underlying embedding of the shell contain all the curvature information. The sign convention is not unique, it is also possible to define $-\nabla_{\mathcal{S}}\nu$ as the Weingarten tensor.

3.2 Mapping between surfaces

Next, we consider two surfaces $\hat{\mathcal{S}}$ and $\mathcal{S}$ which are connected diffeomorphically by $\Phi : \hat{\mathcal{S}} \to \mathcal{S}$. In the context of shells $\hat{\mathcal{S}}$ and $\mathcal{S}$ correspond to the initial and deformed mid-surface of the shell, respectively, and Φ will be the deformation of the mid-surface. We are interested how the tangential and normal vectors as well as the fundamental forms can be expressed (pulled-back) in terms of vectors living on $\hat{\mathcal{S}}$ and the deformation Φ.

3.2.1 Pull back of vectors

We start with a tangent vector $v \in T_p\mathcal{S}$. By definition and the chain rule we obtain that $\exists q, \eta \in \mathbb{R}^2$: $\Phi\circ\varphi(q) = p, \varphi(q) = \hat{p}$, $v = \nabla(\Phi\circ\varphi)(q)\eta = (\nabla_{\hat{\mathcal{S}}}\Phi)(\hat{p})(\nabla\varphi)(q)\eta = (\nabla_{\hat{\mathcal{S}}}\Phi)(\hat{p})\hat{v}$, where $\hat{v} = (\nabla\varphi)(q)\eta \in T_{\hat{p}}\hat{\mathcal{S}}$. Thus $v = (\nabla_{\hat{\mathcal{S}}}\Phi)(\hat{p})\hat{v}$, or in terms of vector fields $v : \mathcal{S} \to T\mathcal{S}$, $v = (\nabla_{\hat{\mathcal{S}}}\Phi)\hat{v}$, $\hat{v} : \hat{\mathcal{S}} \to T\hat{\mathcal{S}}$.

We observe that the tangent vectors of $\hat{\mathcal{S}}$ get explicitly mapped to $\mathcal{S}$ by the push forward $\nabla_{\hat{\mathcal{S}}}\Phi =: \boldsymbol{F}_{\hat{\mathcal{S}}}$, which we will denote in the following by $\boldsymbol{F}_{\hat{\mathcal{S}}}$, having the physical meaning of the surface deformation gradient later in the context of shells.

The cofactor matrix $\operatorname{cof}(\boldsymbol{A})$ is well-defined for all matrices $\boldsymbol{A} \in \mathbb{R}^{n\times n}$. If $\boldsymbol{A}$ is regular there holds the identity $\operatorname{cof}(\boldsymbol{A}) = \det \boldsymbol{A}\, \boldsymbol{A}^{-\top}$. The tensor cross product is a nice tool when working for the cofactor matrix in three dimensions.

Definition 3.2.1 *Let $\boldsymbol{A}, \boldsymbol{B} \in \mathbb{R}^{3\times 3}$, $u \in \mathbb{R}^3$, and denote ε_{ijk} the Levi-Civita symbol being 1, -1, or 0 if (ijk) is an even, odd, or no permutation of $(1,2,3)$. The* tensor cross product $\times$ *between two matrices or between a matrix and a vector is defined as*

$$(\boldsymbol{A}\times\boldsymbol{B})_{ij} = \varepsilon_{ikl}\varepsilon_{jmn}\boldsymbol{A}_{km}\boldsymbol{B}_{ln}, \quad (u\times\boldsymbol{A})_{ij} = \varepsilon_{ikl}u_k\boldsymbol{A}_{lj}, \quad (\boldsymbol{A}\times u)_{ij} = \varepsilon_{jkl}\boldsymbol{A}_{ik}u_l. \tag{3.2.1}$$

Lemma 3.2.2 *There holds for $\boldsymbol{A}, \boldsymbol{B}, \boldsymbol{C} \in \mathbb{R}^{3\times 3}$ and $u, v \in \mathbb{R}^3$*

1. $\boldsymbol{A}\times\boldsymbol{B} = \boldsymbol{B}\times\boldsymbol{A}$, *and* $(c\boldsymbol{A}+\boldsymbol{B})\times\boldsymbol{C} = c\boldsymbol{A}\times\boldsymbol{C} + \boldsymbol{B}\times\boldsymbol{C}$,
2. $\operatorname{cof}(\boldsymbol{A}) = \frac{1}{2}\boldsymbol{A}\times\boldsymbol{A}$,
3. $D_{\boldsymbol{A}}\operatorname{cof}(\boldsymbol{A})[\boldsymbol{B}] = \boldsymbol{B}\times\boldsymbol{A}$,
4. $\boldsymbol{I}\times\boldsymbol{A} = \operatorname{tr}(\boldsymbol{A})\boldsymbol{I} - \boldsymbol{A}^{\top}$,
5. $(u\otimes v)\times\boldsymbol{A} = -u\times\boldsymbol{A}\times v$ *and* $(\boldsymbol{A}\times u)v = \boldsymbol{A}(u\times v)$.

Proof: Exercise. □

As $\boldsymbol{F}_{\hat{\mathcal{S}}}$ interpreted as 3×3 matrix has only rank 2, we will make use of the following results.

Lemma 3.2.3 *Let $\boldsymbol{A} \in \mathbb{R}^{3\times 3}$ with $\operatorname{rank}(\boldsymbol{A}) = 2$ and $v \in \mathbb{R}^3$ with $v \in \ker(\boldsymbol{A})$. Then there holds, with $\boldsymbol{P}^\perp = \nu \otimes \nu$ the complementary orthogonal projection of $\boldsymbol{P} = \boldsymbol{I} - \nu \otimes \nu$, where $\nu := \frac{v}{\|v\|_2}$,*

1. $\boldsymbol{A}^\top \operatorname{cof}(\boldsymbol{A}) = 0$.
2. $\operatorname{cof}(\boldsymbol{P}) = \boldsymbol{P}^\perp$.
3. $\|\operatorname{cof}(\boldsymbol{A})v\|_2 = \|v\|_2 \|\operatorname{cof}(\boldsymbol{A})\|_F$.

Proof:

1. As the set of regular matrices GL(3) is dense in the set of all matrices there exists for all $\boldsymbol{A} \in \mathbb{R}^{3\times 3}$ and $\varepsilon > 0$ some $\boldsymbol{A}_\varepsilon \in \mathrm{GL}(3)$ such that $\|\boldsymbol{A}_\varepsilon - \boldsymbol{A}\|_F < \varepsilon$. Therefore, with continuity of the determinant, there holds
$$\boldsymbol{A}^\top \operatorname{cof}(\boldsymbol{A}) = \lim_{\varepsilon\to 0} \boldsymbol{A}_\varepsilon^\top \operatorname{cof}(\boldsymbol{A}_\varepsilon) = \lim_{\varepsilon\to 0} \det(\boldsymbol{A}_\varepsilon) = 0.$$
2. We use the properties of the tensor cross product to obtain
$$\begin{aligned} 2\operatorname{cof}(\boldsymbol{P}) = (\boldsymbol{I} - \nu\otimes\nu) \times (\boldsymbol{I} - \nu\otimes\nu) &= \boldsymbol{I}\times\boldsymbol{I} - 2\boldsymbol{I}\times\nu\otimes\nu + \nu\otimes\nu\times\nu\otimes\nu \\ &= 2\boldsymbol{I} - 2(\|\nu\|_2^2\boldsymbol{I} - \nu\otimes\nu) + (\nu\times\nu)\otimes(\nu\times\nu) = 2\nu\otimes\nu. \end{aligned}$$
3. From 2) we deduce that the range, $\operatorname{range}(\operatorname{cof}(\boldsymbol{A})) = \{\nu\}$, is one-dimensional. Thus
$$\|\operatorname{cof}(\boldsymbol{A})\nu\|_2^2 = \nu^\top \operatorname{cof}(\boldsymbol{A}^\top\boldsymbol{A})\nu = \operatorname{tr}(\operatorname{cof}(\boldsymbol{A}^\top\boldsymbol{A})) = \|\operatorname{cof}(\boldsymbol{A})\|_F^2.$$

□

Lemma 3.2.3 states that the range of $\operatorname{cof}(\boldsymbol{A})$ is exactly the kernel of $\boldsymbol{A}$ for a rank two matrix, such that we can describe the transformation of normal vectors.

Lemma 3.2.4 *Let $\hat{\mathcal{S}}$ be a surface with normal vector field $\hat{\nu}$. For the mapped surface $\mathcal{S} := \phi(\hat{\mathcal{S}})$, $\phi : \hat{\mathcal{S}} \to \mathbb{R}^3$ a diffeomorphism, let ν be the corresponding normal vector. Then, with $\boldsymbol{F}_{\hat{\mathcal{S}}} := \nabla_{\hat{\mathcal{S}}}\phi$*

$$\nu \circ \phi = \frac{\operatorname{cof}(\boldsymbol{F}_{\hat{\mathcal{S}}})\hat{\nu}}{\|\operatorname{cof}(\boldsymbol{F}_{\hat{\mathcal{S}}})\hat{\nu}\|_2} = \frac{\operatorname{cof}(\boldsymbol{F}_{\hat{\mathcal{S}}})\hat{\nu}}{\|\operatorname{cof}(\boldsymbol{F}_{\hat{\mathcal{S}}})\|_F}. \tag{3.2.2}$$

Proof: Let $p \in \mathcal{S}$ and $\eta \in T_p\mathcal{S}$ be arbitrary. Then with $\eta \circ \phi = \boldsymbol{F}_{\hat{\mathcal{S}}}\hat{\eta}$ for some $\hat{\eta} \in T\hat{\mathcal{S}}$

$$\eta\circ\phi\cdot\nu\circ\phi = \frac{1}{\|\operatorname{cof}(\boldsymbol{F}_{\hat{\mathcal{S}}})\hat{\nu}\|_2}\hat{\eta}^\top\boldsymbol{F}_{\hat{\mathcal{S}}}^\top\operatorname{cof}(\boldsymbol{F}_{\hat{\mathcal{S}}})\hat{\nu} \overset{\text{Lemma } 3.2.3}{=} 0.$$

□

Having a triangulation of a surface the normal vector and the tangent vector at the edges are directly applicable. The co-normal (element-normal) vector $\mu = \nu \times \tau$ will be used to obtain the orthogonal frame (ν, τ, μ). By the push forward and Lemma 3.2.4 the deformed normal and (edge) tangential vectors are determined. To obtain the pull back of the full orthonormal frame $(\nu\circ\Phi, \tau\circ\Phi, \mu\circ\Phi)$ we need to pull back the deformed co-normal vector in an appropriate manner. This is done by the Moore–Penrose pseudo-inverse.

Lemma 3.2.5 *Adopt the assumptions of Lemma 3.2.4. Further, let $\tau \in T_p\mathcal{S}$ be a normalized tangent vector at $p \in \mathcal{S}$ with pull-back $\tau \circ \phi = \frac{\boldsymbol{F}_{\hat{\mathcal{S}}}\hat{\tau}}{\|\boldsymbol{F}_{\hat{\mathcal{S}}}\hat{\tau}\|_2}$. Then, with $\boldsymbol{F}_{\hat{\mathcal{S}}} := \nabla_{\hat{\mathcal{S}}}\phi$ and $\mu := \nu \times \tau$*

$$\mu \circ \phi = \frac{\boldsymbol{F}_{\hat{\mathcal{S}}}^{\dagger^\top}\hat{\mu}}{\|\boldsymbol{F}_{\hat{\mathcal{S}}}^{\dagger^\top}\hat{\mu}\|_2}, \tag{3.2.3}$$

where $\hat{\mu} = \hat{\nu} \times \hat{\tau}$.

Proof: We compute

$$\begin{aligned}
\mu \circ \phi \cdot \nu \circ \phi &= \frac{1}{\|\boldsymbol{F}_{\hat{\mathcal{S}}}^{\dagger^\top}\hat{\mu}\|_2 \|\operatorname{cof}(\boldsymbol{F}_{\hat{\mathcal{S}}})\hat{\nu}\|_2}\hat{\mu}^\top \boldsymbol{F}_{\hat{\mathcal{S}}}^\dagger \operatorname{cof}(\boldsymbol{F}_{\hat{\mathcal{S}}})\hat{\nu} = 0,\\
\mu \circ \phi \cdot \tau \circ \phi &= \frac{1}{\|\boldsymbol{F}_{\hat{\mathcal{S}}}^{\dagger^\top}\hat{\mu}\|_2 \|\boldsymbol{F}_{\hat{\mathcal{S}}}\hat{\tau}\|_2}\hat{\mu}^\top \boldsymbol{F}_{\hat{\mathcal{S}}}^\dagger \boldsymbol{F}_{\hat{\mathcal{S}}}\hat{\tau} = \frac{1}{\|\boldsymbol{F}_{\hat{\mathcal{S}}}^{\dagger^\top}\hat{\mu}\|_2 \|\boldsymbol{F}_{\hat{\mathcal{S}}}\hat{\tau}\|_2}\hat{\mu}^\top\hat{\tau} = 0,
\end{aligned}$$

where we used that $\boldsymbol{F}_{\hat{\mathcal{S}}}^\dagger \operatorname{cof}(\boldsymbol{F}_{\hat{\mathcal{S}}}) = \boldsymbol{F}_{\hat{\mathcal{S}}}^\dagger \boldsymbol{P}_{\mathcal{S}} \operatorname{cof}(\boldsymbol{F}_{\hat{\mathcal{S}}}) \overset{\text{Lemma } 3.2.3}{=} 0$ and $\boldsymbol{F}_{\hat{\mathcal{S}}}^\dagger \boldsymbol{F}_{\hat{\mathcal{S}}} = \boldsymbol{P}_{\hat{\mathcal{S}}}$. As the three vector fields are perpendicular and normalized there holds $\det(\nu \circ \phi, \tau \circ \phi, \mu \circ \phi) = \pm 1$. To show that the orientation is preserved we extend the vectors to full space, compare (3.1.4), by approximating $\boldsymbol{F}_{\hat{\mathcal{S}}}$ with a full rank matrix $\boldsymbol{F}_\varepsilon \in \mathbb{M}_+(3)$ and $\boldsymbol{A} := (\boldsymbol{I} - \frac{\boldsymbol{F}_\varepsilon^{-\top}\hat{\nu}}{\|\boldsymbol{F}_\varepsilon^{-\top}\hat{\nu}\|_2} \otimes \frac{\boldsymbol{F}_\varepsilon^{-\top}\hat{\nu}}{\|\boldsymbol{F}_\varepsilon^{-\top}\hat{\nu}\|_2})\boldsymbol{F}_\varepsilon^{-\top}$

$$\frac{\boldsymbol{F}_\varepsilon^{-\top}\hat{\nu}}{\|\boldsymbol{F}_\varepsilon^{-\top}\hat{\nu}\|_2}, \qquad \frac{\boldsymbol{F}_\varepsilon\hat{\tau}}{\|\boldsymbol{F}_\varepsilon\hat{\tau}\|_2}, \qquad \frac{\boldsymbol{A}\hat{\mu}}{\|\boldsymbol{A}\hat{\mu}\|_2}.$$

By neglecting the denominators we obtain

$$\begin{aligned}
\det(\boldsymbol{F}_\varepsilon^{-\top}\hat{\nu}, \boldsymbol{F}_\varepsilon\hat{\tau}, \boldsymbol{A}\hat{\mu}) &= \det(\boldsymbol{F}_\varepsilon^{-\top}\hat{\nu}, \boldsymbol{F}_\varepsilon\hat{\tau}, \boldsymbol{F}_\varepsilon^{-\top}\hat{\mu})\\
&= \det(\boldsymbol{F}_\varepsilon^{-\top}) \det(\hat{\nu}, \boldsymbol{F}_\varepsilon^\top \boldsymbol{F}_\varepsilon\hat{\tau}, \hat{\mu})\\
&= \det(\boldsymbol{F}_\varepsilon^{-\top})\hat{\mu} \times \hat{\nu} \cdot (\boldsymbol{F}_\varepsilon^\top \boldsymbol{F}_\varepsilon\hat{\tau}) = \det(\boldsymbol{F}_\varepsilon^{-\top})\|\boldsymbol{F}_\varepsilon\hat{\tau}\|_2^2 > 0.
\end{aligned}$$

□

3.2.2 Pull back of fundamental forms

The fundamental forms on the mapped surface $\mathcal{S} = \Phi(\hat{\mathcal{S}})$ can directly be pulled-back, with $\hat{v}, \hat{w} \in T\hat{\mathcal{S}}$ via

$$\Phi^* I(\hat{v}, \hat{w}) = \langle \nabla_{\hat{\mathcal{S}}}\Phi\, \hat{v}, \nabla_{\hat{\mathcal{S}}}\Phi\, \hat{w}\rangle, \tag{3.2.4a}$$
$$\Phi^* II(\hat{v}, \hat{w}) = \langle (\nabla_{\mathcal{S}}\nu) \circ \Phi\, \nabla_{\hat{\mathcal{S}}}\Phi\, \hat{v}, \nabla_{\hat{\mathcal{S}}}\Phi\, \hat{w}\rangle, \tag{3.2.4b}$$
$$\Phi^* III(\hat{v}, \hat{w}) = \langle (\nabla_{\mathcal{S}}\nu) \circ \Phi\, \nabla_{\hat{\mathcal{S}}}\Phi\, \hat{v}, (\nabla_{\mathcal{S}}\nu) \circ \Phi\, \nabla_{\hat{\mathcal{S}}}\Phi\, \hat{w}\rangle. \tag{3.2.4c}$$

We will neglect the Φ^* for ease of presentation.

3.3 Curvature

Let $\mathcal{S}$ be a surface in $\mathbb{R}^3$ throughout this section. We discuss the types and computation of different curvatures of the surface and of curves lying on $\mathcal{S}$. We start with the surface itself.

3.3.1 Gauss and mean curvature of surfaces

Definition 3.3.1 *Let κ_1, κ_2 be the two eigenvalues of the Weingarten tensor $\nabla_{\mathcal{S}}\nu$ not corresponding to the eigenvector ν. They are called the* principal curvatures *and the corresponding eigenvectors the* principal curvature directions*. The* mean *and* Gauss *curvature, respectively, are given by the mean and product of the eigenvalues, $H = \frac{1}{2}(\kappa_1 + \kappa_2)$ and $K = \kappa_1\kappa_2$.*

The mean curvature can directly be obtained from the trace of the Weingarten tensor, $H = \frac{1}{2}\operatorname{tr}(\nabla_{\mathcal{S}}\nu)$, for the Gauss curvature, however, we cannot take the determinant, which is zero. The cofactor matrix is used instead.

Lemma 3.3.2 *Let $\boldsymbol{A} \in \mathbb{R}^{3\times 3}_{\text{sym}}$ be a rank 2 matrix with kernel $v \in \mathbb{R}^3$, $\boldsymbol{A}v = 0$, such that $\|v\|_2 = 1$. Then the product of the two non-zero eigenvalues is given by $\operatorname{cof}(\boldsymbol{A})_{vv}$. Especially, there holds for the Gauss curvature $K = \operatorname{cof}(\nabla_{\mathcal{S}}\nu)_{\nu\nu}$.*

Proof: Entry $\operatorname{cof}(\boldsymbol{A})_{ij}$ is the determinant of the 2×2 sub-matrix where the i*th* row and j*th* column is neglected. Thus, $\operatorname{cof}(\boldsymbol{A})_{vv}$ is the determinant of the 2×2 matrix when deleting the zero row and column. □

Remark 3.3.3 *Another possibility the compute the Gauss curvature is to regularize the Weingarten tensor, $K = \det(\nabla_{\mathcal{S}}\nu + \nu \otimes \nu)$.*

Depending on the Gauss curvature four types of surfaces can (locally) be identified. We call a surface at point $p \in \mathcal{S}$

- elliptic, if $K(p) > 0$,
- hyperbolic, if $K(p) < 0$,
- parabolic, if $K(p) = 0$ and $\kappa_1 \neq 0$ or $\kappa_2 \neq 0$.
- flat (planar), if $K(p) = \kappa_1(p) = \kappa_2(p) = 0$

3.3.2 Curves on surfaces

Next, we consider curves γ lying on the surface $\mathcal{S}$ and discuss their curvature.

Definition 3.3.4 *Let $\gamma : [a, b] \to \mathcal{S}$ be a differentiable curve on $\mathcal{S}$ with tangent vector $\tau = \gamma'$, where γ' denotes the derivative with respect to the parameter. The* normal curvature *is defined by*

$$\kappa_n = \frac{II(\tau,\tau)}{I(\tau,\tau)} = \frac{\tau' \cdot \nu}{\|\tau\|^2}. \tag{3.3.1}$$

The (signed) geodesic curvature *is*

$$\kappa_g = \frac{\det\begin{pmatrix}\tau & \tau' & \nu\end{pmatrix}}{\|\tau\|^3} \tag{3.3.2}$$

and the total curvature $\kappa = \sqrt{\kappa_g^2 + \kappa_n^2}$.

Lemma 3.3.5 *Let $\gamma : [a, b] \to \mathcal{S}$ be a differentiable curve on $\mathcal{S}$ parameterized by arc-length and unit tangent vector τ. Then there holds $\kappa_g = \nabla_{\gamma'}\gamma'$ and*

$$\gamma'' = \kappa_n\nu + \kappa_g(\nu \times \gamma') = II(\gamma',\gamma')\nu + \nabla_{\gamma'}\gamma'(\nu \times \gamma'), \tag{3.3.3}$$

$$\kappa_g = \nabla_{\mathcal{S}}^{\text{cov}}\tau = \boldsymbol{P}_{\mathcal{S}}\nabla_{\mathcal{S}}\tau, \qquad \kappa_n = \boldsymbol{P}_{\mathcal{S}}^{\perp}\nabla_{\mathcal{S}}\tau, \quad \text{and} \quad \kappa = \|\nabla_{\mathcal{S}}\tau\|_2. \tag{3.3.4}$$

3.4 Approximated surfaces, surface finite elements, and discrete curvature

3.4.1 Sobolev spaces and finite elements on surfaces

Before introducing finite element spaces on surfaces we need to define function spaces on manifolds and start with the integration by parts formula. A comprehensive introduction of finite elements on surfaces can be found e.g. in [21].

Theorem 3.4.1 (Integration by parts on manifolds) *Let $\mathcal{S}$ by an $n-1$-dimensional submanifold of $\mathbb{R}^n$ with smooth boundary $\partial\mathcal{S}$. Further let ν be the normal vector, μ the co-normal, and $f \in C^1(\overline{\mathcal{S}})$ a differentiable function up to the boundary. Then there holds with the mean curvature H*

$$\int_{\mathcal{S}} \nabla_{\mathcal{S}} f \, ds = \int_{\mathcal{S}} f \, H\nu \, ds + \int_{\partial\mathcal{S}} f\mu \, dl. \tag{3.4.1}$$

Proof: See e.g., [21, Theorem 2.10.]. □

Definition 3.4.2 *The set of* square-integrable *functions on the surface $\mathcal{S}$ is defined as*

$$L^2(\mathcal{S}) := \{u : \mathcal{S} \to \mathbb{R} \,|\, \|u\|_{L^2(\mathcal{S})} < \infty\}. \tag{3.4.2}$$

A function $f \in L^2(\mathcal{S})$ is weakly differentiable*, $u = \nabla_{\mathcal{S}} f \in L^2(\mathcal{S}, \mathbb{R}^n)$, if for all $\Psi \in C_0^\infty(\mathcal{S}, \mathbb{R}^n)$ there holds*

$$\int_{\mathcal{S}} f \operatorname{div}_{\mathcal{S}}(\Psi) \, ds = -\int_{\mathcal{S}} u \cdot \Psi \, ds + \int_{\mathcal{S}} H f \, \Psi \cdot \nu \, ds \tag{3.4.3}$$

and the Sobolev space $H^1(\mathcal{S})$ is given by

$$H^1(\mathcal{S}) := \{u \in L^2(\mathcal{S}) \,|\, \nabla_{\mathcal{S}} u \in L^2(\mathcal{S}, \mathbb{R}^n)\}. \tag{3.4.4}$$

For vector valued function spaces on surfaces we first define

$$L^2(\mathcal{S}, T\mathcal{S}) := \{u \in L^2(\mathcal{S}, \mathbb{R}^n) \,|\, u \cdot \nu = 0\}, \tag{3.4.5a}$$

$$L^2(\mathcal{S}, T\mathcal{S} \times T\mathcal{S}) := \{\boldsymbol{\sigma} \in L^2(\mathcal{S}, \mathbb{R}^{n\times n}) \,|\, \boldsymbol{\sigma}\nu = \nu^\top \boldsymbol{\sigma} = 0\} \tag{3.4.5b}$$

as the set of square-integrable tangential vector and matrix fields on $\mathcal{S}$ and then

$$H(\operatorname{div}, \mathcal{S}) := \{u \in L^2(\mathcal{S}, T\mathcal{S}) \,|\, \operatorname{div}_{\mathcal{S}}(u) \in L^2(\mathcal{S})\}, \tag{3.4.6a}$$

$$H(\operatorname{curl}, \mathcal{S}) := \{u \in L^2(\mathcal{S}, T\mathcal{S}) \,|\, \operatorname{curl}_{\mathcal{S}}(u) \in L^2(\mathcal{S})\}, \tag{3.4.6b}$$

and analogously $H(\operatorname{divdiv}, \mathcal{S})$.

For a triangulation $\mathcal{T}$ approximating $\mathcal{S}$ we assume that it is densely inscribed, i.e., the vertices of $\mathcal{T}$ lie on $\mathcal{S}$. If the triangulation is not affine, but polynomial it will be curved for better approximation. We say a triangulation is curved of order k if for all $T \in \mathcal{T}$ there exists a function $\Phi_T \in \mathcal{P}^k(\hat{T}, \mathbb{R}^3)$ mapping the reference triangle to T, $T = \Phi_T(\hat{T})$. There are several ways to curve the triangulation appropriately. The projection based interpolation uses the dofs of Lagrangian elements, first determining the edge dofs and then the inner dofs to obtain an L^2- (or H^1-) best approximation of $\mathcal{S}$. Note, that $\mathcal{T}$ is globally continuous but in general not differentiable.

The finite element spaces introduced in Section 2.3 fall into two categories:

1. Spaces where the trace of a 3D element results in a 2D element of the same space.
2. Spaces where the trace of a 3D element does not lead to a valid 2D element of the same space.

The spaces H^1 and $H(\operatorname{curl})$ belong to the first class, whereas L^2, $H(\operatorname{div})$, and $H(\operatorname{divdiv})$ are contained in the second category.

Nevertheless, we generally describe how 2D flat elements can be mapped onto surfaces. Therefore, let $\hat{T} \subset \mathbb{R}^2$ be the reference element and $\Phi_T : \hat{T} \to \mathcal{T} \subset \mathbb{R}^3$ the mapping onto a surface element described above, i.e., Φ_T can be seen as an embedding ($\nabla\Phi_T \in \mathbb{R}^{3\times 2}$ has full rank).

Let $\hat{u}$ be an H^1-conforming finite element on $\hat{T}$. Then, with $u \circ \Phi_T := \hat{u}$ we map it onto the surface. The L^2-conforming elements follow the same idea, see Figure 3.1. Thus, we can define

$$Q_h^k(\mathcal{T}) := \{u \in L^2(\mathcal{T}) \,|\, \text{ for all } T \in \mathcal{T}\, \exists \hat{u} \in \mathcal{P}^k(\hat{T}) : \, u|_T \circ \Phi_T = \hat{u}\}, \tag{3.4.7}$$

$$U_h^k(\mathcal{T}) := \{u \in H^1(\mathcal{T}) \,|\, \text{ for all } T \in \mathcal{T}\, \exists \hat{u} \in \mathcal{P}^k(\hat{T}) : \, u|_T \circ \Phi_T = \hat{u}, \, u \text{ continuous}\}. \tag{3.4.8}$$

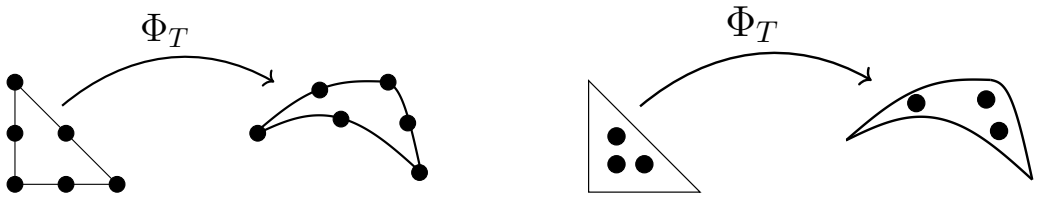

Figure 3.1: Mapping of H^1- and L^2-conforming elements from reference triangle onto a curved physical surface element.

To preserve the normal or tangential continuity of $H(\mathrm{div})$- or $H(\mathrm{curl})$-conforming finite elements the Piola and Covariant transformations are adapted (see Section 2.3.2 and Section 2.3.3)

$$u \circ \Phi_T := \frac{1}{J}\boldsymbol{F}\hat{u}, \qquad \boldsymbol{F} = \nabla\Phi_T \in \mathbb{R}^{3\times 2}, \quad J = \sqrt{\det(\boldsymbol{F}^\top \boldsymbol{F})}, \tag{3.4.9}$$

$$v \circ \Phi_T = (\boldsymbol{F}^\dagger)^\top \hat{v}, \qquad \boldsymbol{F}^\dagger = (\boldsymbol{F}^\top \boldsymbol{F})^{-1}\boldsymbol{F}^\top, \tag{3.4.10}$$

with the Moore–Penrose pseudo inverse $\boldsymbol{F}^\dagger$. Therefore

$$\mathcal{N}_{II}^k(\mathcal{T}) := \{u \in H(\mathrm{curl},\mathcal{T}) \mid \text{ for all } T \in \mathcal{T}\ \exists \hat{u} \in \mathcal{P}^k(\hat{T},\mathbb{R}^2) :\ u|_T \circ \Phi_T = (\boldsymbol{F}^\dagger)^\top \hat{u}, [\![u_t]\!]_F = 0 \text{ for all } F \in \mathcal{F}^{\mathrm{int}}\}, \tag{3.4.11}$$

$$BDM^k(\mathcal{T}) := \{u \in H(\mathrm{div},\mathcal{T}) \mid \text{ for all } T \in \mathcal{T}\ \exists \hat{u} \in \mathcal{P}^k(\hat{T},\mathbb{R}^2) :\ u|_T \circ \Phi_T = \frac{1}{J}\boldsymbol{F}\hat{u}, [\![u_\mu]\!]_F = 0 \text{ for all } F \in \mathcal{F}^{\mathrm{int}}\}. \tag{3.4.12}$$

In the same spirit the transformation rule for $H(\mathrm{divdiv})$ elements on surfaces is given by

$$\boldsymbol{\sigma} \circ \Phi_T := \frac{1}{J^2}\boldsymbol{F}\hat{\boldsymbol{\sigma}}\boldsymbol{F}^\top, \quad \hat{\boldsymbol{\sigma}} \in \mathcal{P}^k(\hat{T},\mathbb{R}^{2\times 2}_{\mathrm{sym}}). \tag{3.4.13}$$

The finite element space $M_h^k(\mathcal{T})$ is defined accordingly. To simplify notation we neglect the dependency of $\mathcal{T}$, if there is no chance of confusion.

Note that $\boldsymbol{F}$ in (3.4.9) acts as a push forward of the tangent vector field $\hat{u}$, if $\mathbb{R}^2$ is identified as a sub-manifold of $\mathbb{R}^3$. Thus, the transformed u is a tangent vector field on the surface. Further $\boldsymbol{\sigma}_h \in M_h$ acts on the tangent space of the surface, i.e., $\boldsymbol{\sigma}_h : \mathcal{T} \to T\mathcal{T} \times T\mathcal{T}$ and $\boldsymbol{\sigma}_h\nu = \nu^\top\boldsymbol{\sigma}_h = 0$.

The definitions of the facet space (2.4.13) and normal-facet space (2.4.16) on surfaces, denoted by $\Gamma_h^k(\mathcal{T})$ and $\Lambda_h^k(\mathcal{T})$, follow immediately. Note, that for the normal-facet space the Piola transformation has to be used to transform the involved co-normal vector.

3.4.2 Discrete curvatures

For an affine triangulation $\mathcal{T}$ the discrete outer normal vector ν is piece-wise constant and thus, $\nabla_{\mathcal{T}}\nu|_T = 0$ for all $T \in \mathcal{T}$, where we used the notation $\nabla_{\mathcal{T}}$ to emphasize that we are on a triangulated surface. Moreover, the normal vector may jump over the interfaces, see Figure 3.2. Hence, the discrete Weingarten tensor can at best be a distribution.

Lemma 3.4.3 *Let $\mathcal{T}$ be a triangulation of order k of a surface $\mathcal{S}$ and $\mathcal{E}$ the corresponding skeleton. Then the distributional Weingarten tensor acts on co-normal–co-normal continuous HHJ functions, $\boldsymbol{\sigma} \in M_{h,0}^k$ reading*

$$\langle \nabla_{\mathcal{T}}\nu, \boldsymbol{\sigma}\rangle = \sum_{T\in\mathcal{T}} \int_T \nabla_{\mathcal{T}}\nu|_T : \boldsymbol{\sigma}\, ds + \sum_{E\in\mathcal{E}} \int_E \sphericalangle(\nu_L,\nu_R)\boldsymbol{\sigma}_{\mu\mu}\, dl, \tag{3.4.14}$$

where $\sphericalangle(a,b) := \arccos\left(\frac{a\cdot b}{\|a\|_2\|b\|_2}\right)$ denotes the angle of two vectors and ν_L, ν_R the normal vectors on the two triangles T_L, T_R sharing the same edge E.

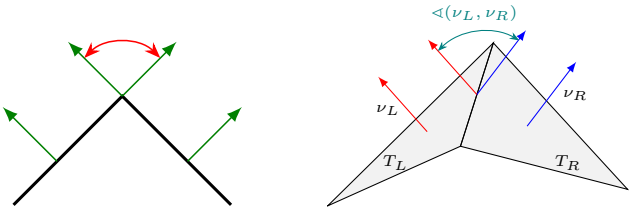

Figure 3.2: Jump of normal vector over two affine elements in 2D and 3D.

Proof: Idea: Smooth the triangulation $\mathcal{T}$ such that $\mathcal{T}_\varepsilon$ is differentiable converging to $\mathcal{T}$ for $\varepsilon \to 0$. Then compute the Weingarten tensor and perform the limit $\varepsilon \to 0$. □

Remark 3.4.4 *In the case of a polygon (affine) triangulation $\mathcal{T}$ only the edge terms in* (3.4.14) *remain, where the angle of the normal vector jump is computed. This is in common with discrete differential geometry, where the dihedral angle is also used as part of the curvature computation.*

Note, that for a high-order approximation of the surface the jump term becomes less important in terms of curvature information, however, it will be crucial for numerical stability. We are in the position to define the lifted Weingarten tensor.

Definition 3.4.5 *Let $\mathcal{T}$ be a triangulation of order k of the surface $\mathcal{S}$. Then the lifted curvature $\boldsymbol{\kappa}_h \in M^k_{h,0}$ is given as the solution of*

$$\int_{\mathcal{T}} \boldsymbol{\kappa}_h : \boldsymbol{\sigma}_h \, ds = \langle \nabla_{\mathcal{T}} \nu, \boldsymbol{\sigma}_h \rangle, \qquad \text{for all } \boldsymbol{\sigma}_h \in M^k_{h,0}. \tag{3.4.15}$$

Exercise 3.4.6 *Let $\mathcal{S}$ be a two-dimensional sub-manifold of $\mathbb{R}^3$ and I, II, and III the corresponding fundamental forms. Further, let H and K be the mean and Gaussian curvature of $\mathcal{S}$. Then there holds*

$$III - 2H\, II + K\, I = 0.$$

Chapter 4

Shells

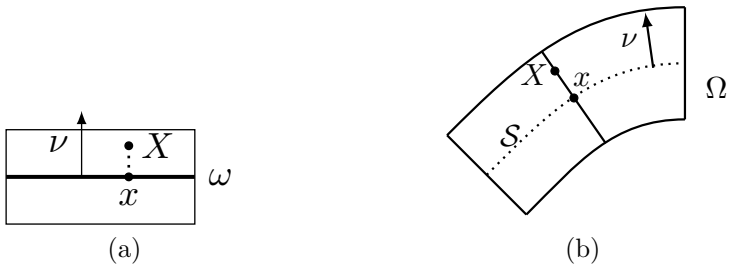

Figure 4.1: Description of shell structures by its mid-surface $\mathcal{S}$ and normal vector ν. Every point X can be represented in the form $X = x + z\nu$. (a) Flat structure. (b) Curved structure.

The appearance of shell structures, where one direction is significantly smaller than the others, are common in nature and technology. The scaling reaches from small like cell membranes to large as e.g., parts of cars and air planes. Like for beams and plates, models were developed where only the mid-surface of the structure gets discretized and assumptions are made to "neglect" the thin direction, i.e., a dimension reduction. Koiter [30] derived consistent equations for shells from continuum mechanics and Naghdi [38] proposed shell models of arbitrary order. Another idea coming from Cosserat [17] directly starts with a 2D model and postulating the balance equations. Therein the shell is described by its mid-surface and an additional independent director field on it, called geometrically exact shell models. We will follow this approach.

The behavior of shell models should coincide with the full model, especially in the limit $t \to 0$, when the thickness tends to zero. Besides asymptotic analysis in the thickness parameter t the derivation of beam, plate, and shell models from 3D elasticity has also been discussed via Γ-convergence (see e.g. [31]).

4.1 Shell description

Looking at a plate structure as depicted in Figure 4.1 (a) one can describe every point X in it by its mid-surface ω and going along the normal vector, $X = x + z\nu$. Therefore, the question arises if we can describe every thin-walled structure in this form. The answer is positive, if the structure is smooth and "thin" enough.

If the thickness t is smaller than ε of Theorem 3.1.5, it justifies to split a shell Ω into its mid-surface $\mathcal{S}$ and the corresponding normal vector ν

$$\Omega = \{X = x + z\,\nu(x) \,|\, x \in \mathcal{S},\, z \in [-t/2, t/2]\}\,, \tag{4.1.1}$$

as depicted in Figure 4.1 (b).

Definition 4.1.1 *We call a surface $\mathcal{S}$ together with its normal vector field $\nu : \mathcal{S} \to \mathbb{S}^2$ the* initial configuration *of a shell and $(\mathcal{S}, \tilde{\nu})$ with a unit vector field $\tilde{\nu} : \mathcal{S} \to \mathbb{S}^2$, also called* director*, a* configuration of a shell.

The director $\tilde{\nu}$, which does not have to be perpendicular to the shell surface, is used to model shearing. Therefore, we generalize the fundamental forms (3.1.6) and define the shear form measuring the deviation of $\tilde{\nu}$ from being perpendicular.

Definition 4.1.2 *Let $\mathcal{S}$ be a surface, $\tilde{\nu} : \mathcal{S} \to \mathbb{S}^2$ a director field, and $v, w \in T\mathcal{S}$. The generalized second and third fundamental forms are defined as*

$$II_{\tilde{\nu}}(v, w) := \frac{1}{2}\left(\langle \nabla_{\mathcal{S}}\tilde{\nu}\, v, w\rangle + \langle v, \nabla_{\mathcal{S}}\tilde{\nu}\, w\rangle\right), \tag{4.1.2a}$$

$$III_{\tilde{\nu}}(v, w) := \langle \nabla_{\mathcal{S}}\tilde{\nu}\, v, \nabla_{\mathcal{S}}\tilde{\nu}\, w\rangle, \tag{4.1.2b}$$

and the shear form $\sigma_{\tilde{\nu}} : T\mathcal{S} \to \mathbb{R}$ is given for all $p \in \mathcal{S}$ by

$$(\sigma_{\tilde{\nu}})_p : T_p\mathcal{S} \to \mathbb{R}, \quad v \mapsto \langle \tilde{\nu}(p), v\rangle. \tag{4.1.3}$$

Note, that $\langle \nabla_{\mathcal{S}} \tilde{\nu}\, v, w\rangle$ is symmetric and $\sigma_{\tilde{\nu}} \equiv 0$ only if $\tilde{\nu} = \nu$.

Definition 4.1.3 *Let $(\hat{\mathcal{S}},\ \hat{\nu})$ be the initial configuration of a shell. A deformation $\Phi = (\phi, \overline{\nu})$ of $\hat{\mathcal{S}}$ is given by*

$$\begin{aligned} \Phi : \hat{\mathcal{S}} \times [-t/2, t/2] &\to \mathbb{R}^3, \\ (x, z) &\mapsto \phi(x) + z\overline{\nu}(x), \end{aligned} \tag{4.1.4}$$

where ϕ is the deformation of the mid-surface and $\overline{\nu} : \hat{\mathcal{S}} \to \mathbb{S}^2$ a differentiable unit vector field. We call $\mathcal{S} := \phi(\hat{\mathcal{S}})$ together with $\tilde{\nu} := \overline{\nu} \circ \phi^{-1}$ a deformed configuration *of the shell.*

Analogously to (3.2.4) we can pull back the generalized fundamental and shear forms from the deformed shell configuration to the initial shell mid-surface, $\hat{v}, \hat{w} \in T\hat{\mathcal{S}}$,

$$\Phi^* II_{\tilde{\nu}}(\hat{v}, \hat{w}) := \frac{1}{2}\left(\langle (\nabla_{\mathcal{S}} \tilde{\nu}) \circ \Phi\, \nabla_{\hat{\mathcal{S}}} \Phi\, \hat{v}, \nabla_{\hat{\mathcal{S}}} \Phi\, \hat{w}\rangle + \langle \nabla_{\hat{\mathcal{S}}} \Phi\, \hat{v}, (\nabla_{\mathcal{S}} \tilde{\nu}) \circ \Phi\, \nabla_{\hat{\mathcal{S}}} \Phi\, \hat{w}\rangle\right), \tag{4.1.5a}$$

$$\Phi^* III_{\tilde{\nu}}(\hat{v}, \hat{w}) := \langle (\nabla_{\mathcal{S}} \tilde{\nu}) \circ \Phi\, \nabla_{\hat{\mathcal{S}}} \Phi\, \hat{v}, (\nabla_{\mathcal{S}} \tilde{\nu}) \circ \Phi\, \nabla_{\hat{\mathcal{S}}} \Phi\, \hat{w}\rangle, \tag{4.1.5b}$$

$$\Phi^* \sigma_{\tilde{\nu}}(\cdot) := \sigma_{\tilde{\nu}}(\nabla_{\hat{\mathcal{S}}} \Phi\, \cdot). \tag{4.1.5c}$$

We denote by $\hat{I}$, $\hat{II}$, and $\hat{III}$ the fundamental forms of the initial shell configuration. The matrix representations of the (pull-backed) forms are given, $\boldsymbol{F}_{\hat{\mathcal{S}}} := \nabla_{\hat{\mathcal{S}}} \Phi$, by

$$\begin{aligned} &\hat{I} \mathrel{\hat{=}} \boldsymbol{P}_{\hat{\mathcal{S}}}^\top \boldsymbol{P}_{\hat{\mathcal{S}}} = \boldsymbol{P}_{\hat{\mathcal{S}}}, \qquad \hat{II}_{\hat{\nu}} \mathrel{\hat{=}} \nabla_{\hat{\mathcal{S}}} \hat{\nu}, \qquad \hat{III}_{\hat{\nu}} \mathrel{\hat{=}} \nabla_{\hat{\mathcal{S}}} \hat{\nu} \nabla_{\hat{\mathcal{S}}} \hat{\nu}, \qquad \sigma_{\hat{\nu}} \equiv 0, \\ &\Phi^* I \mathrel{\hat{=}} \boldsymbol{F}_{\hat{\mathcal{S}}}^\top \boldsymbol{F}_{\hat{\mathcal{S}}}, \qquad\qquad\qquad\qquad \Phi^* II_{\tilde{\nu}} \mathrel{\hat{=}} \operatorname{sym}(\boldsymbol{F}_{\hat{\mathcal{S}}}^\top (\nabla_{\mathcal{S}} \tilde{\nu}) \circ \Phi\, \boldsymbol{F}_{\hat{\mathcal{S}}}), \\ &\Phi^* III_{\tilde{\nu}} \mathrel{\hat{=}} \boldsymbol{F}_{\hat{\mathcal{S}}}^\top (\nabla_{\mathcal{S}} \tilde{\nu}) \circ \Phi^\top (\nabla_{\mathcal{S}} \tilde{\nu}) \circ \Phi\, \boldsymbol{F}_{\hat{\mathcal{S}}}, \qquad \Phi^* \sigma_{\tilde{\nu}} \mathrel{\hat{=}} \boldsymbol{F}_{\hat{\mathcal{S}}}^\top \tilde{\nu} \circ \Phi. \end{aligned} \tag{4.1.6}$$

4.2 A geometrically nonlinear derivation

In this section we derive the nonlinear shell equations based on the geometrical nonlinear Cosserat approach. Let $\hat{\mathcal{S}}$ be the initial configuration of a shell and $\hat{\nu}$ the corresponding normal vector field. We assume that the deformation in Definition 4.1.3 is of the following form

$$\begin{aligned} \Phi : \hat{\mathcal{S}} \times [-t/2, t/2] &\to \mathbb{R}^3 \\ (x, z) &\mapsto \phi(x) + z\boldsymbol{R}(\hat{\nu}(x), \phi(x)), \end{aligned} \tag{4.2.1}$$

where ϕ is the deformation of the mid-surface and

$$\boldsymbol{R} : \mathbb{S}^2 \times \mathcal{S} \to \mathbb{S}^2 \tag{4.2.2}$$

can be understood as a nonlinear rotation of the normal vector (compare the Reissner–Mindlin assumptions in Section 2.2.1). To simplify notation we neglect the x and ϕ dependency of $\boldsymbol{R}$.

We split the full 3D gradient of the deformation Φ into its tangential and normal component, namely

$$\nabla \Phi = \nabla_{\hat{\mathcal{S}}} \Phi + \nabla_z \Phi \tag{4.2.3}$$

and denote the projection onto the normal direction by $\boldsymbol{P}_z := \boldsymbol{P}_{\hat{\mathcal{S}}}^\perp = \hat{\nu} \otimes \hat{\nu}$.

Lemma 4.2.1 *There holds for the Cauchy–Green strain tensor of the full 3D deformed shell, $\boldsymbol{C} = \nabla \Phi^\top \nabla \Phi$,*

$$\boldsymbol{C} = I + 2z II_{\boldsymbol{R}(\hat{\nu})} + z^2 III_{\boldsymbol{R}(\hat{\nu})} + \left(\sigma_{\boldsymbol{R}(\hat{\nu})} \otimes \hat{\nu} + \hat{\nu} \otimes \sigma_{\boldsymbol{R}(\hat{\nu})}\right) + \boldsymbol{P}_z \tag{4.2.4}$$

and for the undeformed Cauchy–Green tensor $\hat{\boldsymbol{C}}$

$$\hat{\boldsymbol{C}} = \hat{I} + 2z \hat{II}_{\hat{\nu}} + z^2 \hat{III}_{\hat{\nu}} + \boldsymbol{P}_z. \tag{4.2.5}$$

Proof: With $\nabla_z(z\boldsymbol{R}(\hat{\nu})) = \boldsymbol{R}(\hat{\nu}) \otimes \hat{\nu}$ and the notation $\boldsymbol{F}_{\hat{\mathcal{S}}} := \nabla_{\hat{\mathcal{S}}}\phi$ we obtain

$$\begin{aligned}\boldsymbol{C} &= (\boldsymbol{F}_{\hat{\mathcal{S}}} + z\nabla_{\hat{\mathcal{S}}}\boldsymbol{R}(\hat{\nu}) + \boldsymbol{R}(\hat{\nu}) \otimes \hat{\nu})^\top (\boldsymbol{F}_{\hat{\mathcal{S}}} + z\nabla_{\hat{\mathcal{S}}}\boldsymbol{R}(\hat{\nu}) + \boldsymbol{R}(\hat{\nu}) \otimes \hat{\nu}) \\ &= \boldsymbol{F}_{\hat{\mathcal{S}}}^\top \boldsymbol{F}_{\hat{\mathcal{S}}} + 2z \operatorname{sym}\left(\boldsymbol{F}_{\hat{\mathcal{S}}}^\top \nabla_{\hat{\mathcal{S}}}\boldsymbol{R}(\hat{\nu})\right) + z^2 \nabla_{\hat{\mathcal{S}}}\boldsymbol{R}(\hat{\nu})^\top \nabla_{\hat{\mathcal{S}}}\boldsymbol{R}(\hat{\nu}) \\ &\quad + \boldsymbol{F}_{\hat{\mathcal{S}}}^\top \boldsymbol{R}(\hat{\nu}) \otimes \hat{\nu} + (\boldsymbol{R}(\hat{\nu}) \otimes \hat{\nu})^\top \boldsymbol{F}_{\hat{\mathcal{S}}} + \underbrace{\boldsymbol{R}(\hat{\nu})^\top \boldsymbol{R}(\hat{\nu})}_{=1} \boldsymbol{P}_z,\end{aligned}$$

where we used that from $\|\boldsymbol{R}(\hat{\nu})\|_2 = 1$ there follows $\nabla_{\hat{\mathcal{S}}}\boldsymbol{R}(\hat{\nu})^\top \boldsymbol{R}(\hat{\nu}) = 0$. Note, that with the chain rule there holds $(\nabla_{\mathcal{S}}\tilde{\nu}) \circ \phi\, \boldsymbol{F}_{\hat{\mathcal{S}}} = \nabla_{\hat{\mathcal{S}}}(\tilde{\nu} \circ \phi) = \nabla_{\hat{\mathcal{S}}}\boldsymbol{R}(\hat{\nu})$. Thus, with Definitions 3.1.8 and 4.1.2, we can identify

$$\boldsymbol{C} = I + 2zII_{\boldsymbol{R}(\hat{\nu})} + z^2 III_{\boldsymbol{R}(\hat{\nu})} + \left(\sigma_{\boldsymbol{R}(\hat{\nu})} \otimes \hat{\nu} + \hat{\nu} \otimes \sigma_{\boldsymbol{R}(\hat{\nu})}\right) + \boldsymbol{P}_z.$$

The expression for the undeformed configuration follows the same lines. □

The Green strain tensor is given by

$$\boldsymbol{E} = \frac{1}{2}\left(\boldsymbol{C} - \hat{\boldsymbol{C}}\right) \tag{4.2.6}$$

and together with the linear material law of St. Venant–Kirchhoff the whole energy of the deformed shell reads

$$\mathcal{W} := \frac{1}{2}\int_{-\frac{t}{2}}^{\frac{t}{2}} \int_{\hat{\mathcal{S}}} \|\boldsymbol{E}\|_{\mathcal{C}}^2 \, ds_z \, dz, \tag{4.2.7}$$

where under the assumptions of Reissner–Mindlin, see Section 2.2.1, the material norm is of the form

$$\|\cdot\|_{\mathcal{C}}^2 := \frac{E}{1-\nu^2}\left(\nu \operatorname{tr}(\cdot)^2 + (1-\nu)\operatorname{tr}(\cdot^2)\right). \tag{4.2.8}$$

Using Steiner's formula [48]

$$ds_z = \left(1 - 2zH + z^2 K\right) ds \tag{4.2.9}$$

with the mean and Gauß curvature H and K, respectively, yields

$$\mathcal{W} = \frac{1}{2}\int_{\hat{\mathcal{S}}} \left(\int_{-\frac{t}{2}}^{\frac{t}{2}} \|\boldsymbol{E}\|_{\mathcal{C}}^2 \, dz - 2H \int_{-\frac{t}{2}}^{\frac{t}{2}} z\|\boldsymbol{E}\|_{\mathcal{C}}^2 \, dz + K \int_{-\frac{t}{2}}^{\frac{t}{2}} z^2 \|\boldsymbol{E}\|_{\mathcal{C}}^2 \, dz \right) ds. \tag{4.2.10}$$

Theorem 4.2.2 (Shell energy) *Assume that $t/L \ll 1$ (L denoting the characteristic length), $\|I - \hat{I}\|_{\mathcal{C}} \leq t$, and $K \leq t$, i.e., that the membrane energy and Gauß curvature are small. Then neglecting all terms of order $\mathcal{O}(t^4)$ yields the shell energy*

$$\mathcal{W} = \frac{1}{2}\int_{\hat{\mathcal{S}}} \left(\frac{t}{4}\|I - \hat{I}\|_{\mathcal{C}}^2 + \frac{t^3}{12}\|II_{\boldsymbol{R}(\hat{\nu})} - \hat{II}\|_{\mathcal{C}}^2 + t\kappa G|\sigma_{\boldsymbol{R}(\hat{\nu})}|^2 \right) ds, \tag{4.2.11}$$

where $G = \frac{E}{2(1+\nu)}$ and $\kappa = 5/6$ denote the shearing modulus and shear correction factor, respectively. With the matrix representations (4.1.6) *together with $\boldsymbol{E}_{\hat{\mathcal{S}}} := 0.5(\boldsymbol{F}_{\hat{\mathcal{S}}}^\top \boldsymbol{F}_{\hat{\mathcal{S}}} - \boldsymbol{P}_{\hat{\mathcal{S}}})$ the energy reads*

$$\mathcal{W} = \int_{\hat{\mathcal{S}}} \left(\frac{t}{2}\|\boldsymbol{E}_{\hat{\mathcal{S}}}\|_{\mathcal{C}}^2 + \frac{t^3}{24}\|\operatorname{sym}(\boldsymbol{F}_{\hat{\mathcal{S}}}^\top \nabla_{\hat{\mathcal{S}}}\boldsymbol{R}(\hat{\nu})) - \nabla_{\hat{\mathcal{S}}}\hat{\nu}\|_{\mathcal{C}}^2 + \frac{t\kappa G}{2}|\boldsymbol{F}_{\hat{\mathcal{S}}}^\top \boldsymbol{R}(\hat{\nu})|^2 \right) ds. \tag{4.2.12}$$

Proof: The full 3D Green strain tensor reads

$$\boldsymbol{E} = \frac{1}{2}\left(I - \hat{I} + 2z(II_{\boldsymbol{R}(\hat{\nu})} - \hat{II}_{\hat{\nu}}) + z^2(III_{\boldsymbol{R}(\hat{\nu})} - I\hat{I}I_{\hat{\nu}}) + \sigma_{\boldsymbol{R}(\hat{\nu})} \otimes \hat{\nu} + \hat{\nu} \otimes \sigma_{\boldsymbol{R}(\hat{\nu})} \right).$$

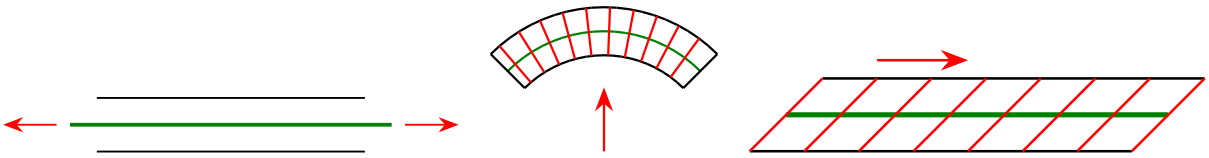

Figure 4.2: Sketched membrane, bending, and shearing energy of a shell.

Integrating the first term of (4.2.10) over the thickness using that the shear form is perpendicular to the fundamental forms leads to

$$\begin{aligned}\int_{-\frac{t}{2}}^{\frac{t}{2}} \|\boldsymbol{E}\|_{\mathcal{C}}^2 \, dz &= \frac{1}{4}\Big(t(\|I-\hat{I}\|_{\mathcal{C}}^2 + \|2\sigma_{\boldsymbol{R}(\hat{\nu})}\|_{\mathcal{C}}^2) + \frac{t^3}{3}\|II_{\boldsymbol{R}(\hat{\nu})} - \hat{I}I_{\hat{\nu}}\|_{\mathcal{C}}^2 \\ &\qquad + \frac{t^3}{6}\langle \underbrace{I-\hat{I}}_{=\mathcal{O}(t)}, III_{\boldsymbol{R}(\hat{\nu})} - I\hat{I}I_{\hat{\nu}}\rangle_{\mathcal{C}} + \frac{t^5}{80}\|III_{\boldsymbol{R}(\hat{\nu})} - I\hat{I}I_{\hat{\nu}}\|_{\mathcal{C}}^2\Big) \\ &= \frac{t}{4}\|I-\hat{I}\|_{\mathcal{C}}^2 + \frac{t^3}{12}\|II_{\boldsymbol{R}(\hat{\nu})} - \hat{I}I_{\hat{\nu}}\|_{\mathcal{C}}^2 + \|\sigma_{\boldsymbol{R}(\hat{\nu})}\|_{\mathcal{C}}^2 + \mathcal{O}(t^4),\end{aligned}$$

where we used that odd powers of z vanish due to the integration.

Integrating over the other two terms and using the assumptions they turn out to be of higher order and are thus neglected

$$2H\int_{-\frac{t}{2}}^{\frac{t}{2}} z\|\boldsymbol{E}\|_{\mathcal{C}}^2 \, dz + K\int_{-\frac{t}{2}}^{\frac{t}{2}} z^2\|\boldsymbol{E}\|_{\mathcal{C}}^2 \, dz = \mathcal{O}(t^4).$$

□

The three terms in (4.2.11) correspond to the membrane, bending, and shearing energy, cf. Figure 4.2.

Exercise 4.2.3 *Proof Steiner's formula* (4.2.9).

Remark 4.2.4 *From Steiner's formula* (4.2.9) *we observe that the shell has to be sufficiently thin such that the expression* $1-2zH+z^2K$ *stays always strictly positive, depending on the radius of curvature of the smallest modulus of the surface, compare Theorem 3.1.5.*

In the following we will derive models for (non-)linear Naghdi and (non-)linear Koiter shells.

4.2.1 Nonlinear Naghdi shell

With the Reissner–Mindlin hypothesis (H1) and (H2) from Section 2.2.1 the director $\tilde{\nu}\circ\phi = \boldsymbol{R}(\hat{\nu},\phi)$ is given by a (nonlinear) rotation matrix $\boldsymbol{R}\in \mathrm{SO}(3)$. Although rotational matrices with finite rotations can be well described by e.g., Euler parameters, Quaternions, or Rodrigues parameters, we consider a different approach better suited for the finite elements later. The rotation can be split by first rotating the normal vector such that it is orthogonal to the deformed mid-plane (compare the Kirchhoff–Love hypothesis (H5) in Section 2.2.2) and then a second rotation, the shear, is applied, i.e.,

$$\boldsymbol{R}(\hat{\nu},\phi,\gamma) = \tilde{\boldsymbol{R}}(\gamma)\nu\circ\phi = \tilde{\boldsymbol{R}}(\gamma)\frac{\operatorname{cof}(\boldsymbol{F}_{\hat{\mathcal{S}}})\hat{\nu}}{\|\operatorname{cof}(\boldsymbol{F}_{\hat{\mathcal{S}}})\hat{\nu}\|_2}, \tag{4.2.13}$$

where $\gamma=(\gamma_1,\gamma_2)$ are the two shearing parameters and $\tilde{\boldsymbol{R}}(\gamma)\in\mathrm{SO}(3)$. This hierarchical approach can be simplified under the assumption that the shearing term is small, $\gamma=\mathcal{O}(\varepsilon)$, (Exercise!)

$$\boldsymbol{R}(\hat{\nu},\phi,\gamma) = \frac{\operatorname{cof}(\boldsymbol{F}_{\hat{\mathcal{S}}})\hat{\nu}}{\|\operatorname{cof}(\boldsymbol{F}_{\hat{\mathcal{S}}})\hat{\nu}\|_2} + \gamma, \tag{4.2.14}$$

providing the advantage of an additive (instead of a multiplicative) splitting between the displacement and the shearing.

Note that $\gamma \in \{\nu \circ \phi\}^\perp$ is perpendicular to the deformed normal vector. Thus we need to pull the shear back via the classical push forward $\boldsymbol{F}_{\hat{\mathcal{S}}}$ or the covariant transformation $(\boldsymbol{F}_{\hat{\mathcal{S}}}^\dagger)^\top$

$$\gamma \circ \phi = \boldsymbol{F}_{\hat{\mathcal{S}}} \hat{\gamma}, \qquad\qquad \gamma \circ \phi = (\boldsymbol{F}_{\hat{\mathcal{S}}}^\dagger)^\top \hat{\gamma}. \tag{4.2.15}$$

Defining the director as $\boldsymbol{R}(\hat{\nu}, \phi, \hat{\gamma})$, we obtain the nonlinear Naghdi/Reissner–Mindlin shell energy (without a right-hand side)

$$\mathcal{W}_{RM} = \int_{\hat{\mathcal{S}}} \left(\frac{t}{2} \|\boldsymbol{E}_{\hat{\mathcal{S}}}\|_{\mathbb{C}}^2 + \frac{t^3}{24} \|\operatorname{sym}(\boldsymbol{F}_{\hat{\mathcal{S}}}^\top \nabla_{\hat{\mathcal{S}}} \boldsymbol{R}(\hat{\nu}, \phi, \hat{\gamma})) - \nabla_{\hat{\mathcal{S}}} \hat{\nu}\|_{\mathbb{C}}^2 + \frac{t\kappa G}{2} |\boldsymbol{F}_{\hat{\mathcal{S}}}^\top \boldsymbol{R}(\hat{\nu}, \phi, \hat{\gamma})|^2 \right) ds. \tag{4.2.16}$$

4.2.2 Linear Naghdi shell

In the following, we denote with $u : \hat{\mathcal{S}} \to \mathbb{R}^3$ the displacement of the mid-surface such that $\phi = \mathrm{id} + u$. Under the small strain assumption (e.g. $\nabla_{\hat{\mathcal{S}}} u = \mathcal{O}(\varepsilon)$) we can linearize the nonlinear shell model (4.2.16). We start with the linearization of the normal and tangential vectors. To handle the derivative of the cofactor matrix we use the tensor cross product from Section 3.2.1.

Lemma 4.2.5 *Let $\hat{\mathcal{S}}$ be a shell with normal vector field $\hat{\nu}$ and $\phi : \hat{\mathcal{S}} \to \mathbb{R}^3$ a diffeomorphism of the form $\phi = \mathrm{id} + u$. For the resulting deformed shell $\mathcal{S} := \phi(\hat{\mathcal{S}})$ let ν, τ, and μ defined as in Lemma 3.2.5. Assume that $\nabla_{\hat{\mathcal{S}}} u = \mathcal{O}(\varepsilon)$. Then the linearization of these vectors is given by*

$$\nu \circ \phi = \hat{\nu} - \nabla_{\hat{\mathcal{S}}} u^\top \hat{\nu} + \mathcal{O}(\varepsilon^2), \tag{4.2.17a}$$

$$\tau \circ \phi = \hat{\tau} + (\boldsymbol{I} - \hat{\tau} \otimes \hat{\tau}) \nabla_{\hat{\mathcal{S}}} u \, \hat{\tau} + \mathcal{O}(\varepsilon^2), \tag{4.2.17b}$$

$$\mu \circ \phi = \hat{\mu} + ((\boldsymbol{I} - \hat{\tau} \otimes \hat{\tau}) \nabla_{\hat{\mathcal{S}}} u - \nabla_{\hat{\mathcal{S}}} u^\top) \hat{\mu} + \mathcal{O}(\varepsilon^2). \tag{4.2.17c}$$

Proof: Using Taylor at $\nabla_{\hat{\mathcal{S}}} u = 0$ and the tensor cross product $\operatorname{cof}(\boldsymbol{F}_{\hat{\mathcal{S}}})\hat{\nu} = \frac{1}{2} \boldsymbol{F}_{\hat{\mathcal{S}}} \times \boldsymbol{F}_{\hat{\mathcal{S}}} \hat{\nu}$ we get

$$\begin{aligned}
\nu \circ \phi &= \hat{\nu} + D_{\nabla_{\hat{\mathcal{S}}} u} \Big(\frac{\frac{1}{2} \boldsymbol{F}_{\hat{\mathcal{S}}} \times \boldsymbol{F}_{\hat{\mathcal{S}}} \hat{\nu}}{\|\frac{1}{2} \boldsymbol{F}_{\hat{\mathcal{S}}} \times \boldsymbol{F}_{\hat{\mathcal{S}}} \hat{\nu}\|} \Big) |_{\nabla_{\hat{\mathcal{S}}} u = 0} [\nabla_{\hat{\mathcal{S}}} u] + \mathcal{O}(\|\nabla_{\hat{\mathcal{S}}} u\|^2) \\
&= \hat{\nu} + \frac{\nabla_{\hat{\mathcal{S}}} u \times \boldsymbol{P}_{\hat{\mathcal{S}}} \hat{\nu}}{\|\frac{1}{2} \boldsymbol{P}_{\hat{\mathcal{S}}} \times \boldsymbol{P}_{\hat{\mathcal{S}}} \hat{\nu}\|} - \frac{\frac{1}{2} \boldsymbol{P}_{\hat{\mathcal{S}}} \times \boldsymbol{P}_{\hat{\mathcal{S}}} \hat{\nu}}{\|\frac{1}{2} \boldsymbol{P}_{\hat{\mathcal{S}}} \times \boldsymbol{P}_{\hat{\mathcal{S}}} \hat{\nu}\|^3} (\nabla_{\hat{\mathcal{S}}} u \times \boldsymbol{P}_{\hat{\mathcal{S}}} \hat{\nu}) \cdot (\frac{1}{2} \boldsymbol{P}_{\hat{\mathcal{S}}} \times \boldsymbol{P}_{\hat{\mathcal{S}}} \hat{\nu}).
\end{aligned}$$

By noting that $\frac{1}{2} \boldsymbol{P}_{\hat{\mathcal{S}}} \times \boldsymbol{P}_{\hat{\mathcal{S}}} \hat{\nu} = \operatorname{cof}(\boldsymbol{P}_{\hat{\mathcal{S}}}) \hat{\nu} = \boldsymbol{P}_{\hat{\mathcal{S}}}^\perp \hat{\nu} \overset{\text{Lemma } 3.2.3}{=} \hat{\nu}$ and by Lemma 3.2.2 $\boldsymbol{A} \times (\hat{\nu} \otimes \hat{\nu}) \hat{\nu} = -(\hat{\nu} \times \boldsymbol{A} \times \hat{\nu}) \hat{\nu} = -(\hat{\nu} \times \boldsymbol{A})(\hat{\nu} \times \hat{\nu}) = 0$ there holds $\boldsymbol{A} \times \boldsymbol{P}_{\hat{\mathcal{S}}} \hat{\nu} = \boldsymbol{A} \times \boldsymbol{I} \hat{\nu}$ and the expression simplifies to

$$\nu \circ \phi = \hat{\nu} + \nabla_{\hat{\mathcal{S}}} u \times \boldsymbol{I} \hat{\nu} - \big((\nabla_{\hat{\mathcal{S}}} u \times \boldsymbol{I} \hat{\nu}) \cdot \hat{\nu} \big) \hat{\nu} + \mathcal{O}(\varepsilon^2).$$

Next, we use 4) from Lemma 3.2.2 to deduce $\nabla_{\hat{\mathcal{S}}} u \times \boldsymbol{I} \hat{\nu} = \operatorname{div}_{\hat{\mathcal{S}}} u \, \hat{\nu} - \nabla_{\hat{\mathcal{S}}} u^\top \hat{\nu}$ and obtain

$$\begin{aligned}
\nu \circ \phi &= \hat{\nu} + \operatorname{div}_{\hat{\mathcal{S}}} u \, \hat{\nu} - \nabla_{\hat{\mathcal{S}}} u^\top \hat{\nu} - \big((\operatorname{div}_{\hat{\mathcal{S}}} u \, \hat{\nu} - \nabla_{\hat{\mathcal{S}}} u^\top \hat{\nu}) \cdot \hat{\nu} \big) \hat{\nu} + \mathcal{O}(\varepsilon^2) \\
&= \hat{\nu} + \operatorname{div}_{\hat{\mathcal{S}}} u \, \hat{\nu} - \nabla_{\hat{\mathcal{S}}} u^\top \hat{\nu} - \operatorname{div}_{\hat{\mathcal{S}}} u \, \hat{\nu} + \mathcal{O}(\varepsilon^2) = \hat{\nu} - \nabla_{\hat{\mathcal{S}}} u^\top \hat{\nu} + \mathcal{O}(\varepsilon^2).
\end{aligned}$$

The other identities are left as exercise. □

Exercise 4.2.6 *Proof Lemma 4.2.5 by regularizing the deformation gradient $\boldsymbol{F}_{\hat{\mathcal{S}}}$ by $\boldsymbol{F} \in \mathbb{M}_+(3)$ like in the proof of Lemma 3.2.5. At the end only expressions which are valid for singular $\boldsymbol{F}_{\hat{\mathcal{S}}}$ have to remain.*

Lemma 4.2.7 *There holds for the director $\tilde{\nu}$ under the small strain assumption*

$$\tilde{\nu} \circ \phi = \hat{\nu} + \beta + \mathcal{O}(\varepsilon^2) = \hat{\nu} - \nabla_{\hat{\mathcal{S}}} u^\top \hat{\nu} + \hat{\gamma} + \mathcal{O}(\varepsilon^2), \tag{4.2.18}$$

where $\beta \in T\hat{\mathcal{S}}$ denotes the rotation and $\hat{\gamma}$ the shear.

Proof: For infinitesimal rotations there holds $\tilde{\nu}\circ\phi = \boldsymbol{R}(\hat{\nu},u) \approx (\boldsymbol{I} + \operatorname{skew}(\beta_1,\beta_2))\hat{\nu}$ as the tangent space at the identity for the special orthogonal group SO(3) is the set of skew-symmetric matrices. There holds $\operatorname{skew}(\beta_1,\beta_2)\hat{\nu} \perp \hat{\nu}$ and thus, we can identify it with a rotation vector field $\beta := \operatorname{skew}(\beta_1,\beta_2)\hat{\nu}$ in the tangent bundle $T\hat{\mathcal{S}}$, i.e., $\beta \perp \hat{\nu}$ and thus, $\tilde{\nu}\circ\phi \approx \hat{\nu} + \beta$.

To obtain the shear expression we start with the linear approximation $\gamma\circ\phi \approx \hat{\gamma} \in T\hat{\mathcal{S}}$, cf. (4.2.15). Linearizing the deformed normal vector (4.2.17a) we get with (4.2.14) $\tilde{\nu}\circ\phi \approx \hat{\nu} - \nabla_{\hat{\mathcal{S}}} u^\top \hat{\nu} + \hat{\gamma}$. □

Theorem 4.2.8 (Linearized Naghdi/Reissner–Mindlin shell) *Under the small strain assumption $u = \mathcal{O}(\varepsilon)$, $\gamma = \mathcal{O}(\varepsilon)$, $\nabla_{\hat{\mathcal{S}}} u = \mathcal{O}(\varepsilon)$, $\nabla_{\hat{\mathcal{S}}}\gamma = \mathcal{O}(\varepsilon)$ and neglecting high-order terms, model* (4.2.12) *simplifies to the linearized Naghdi shell energy*

$$\mathcal{W}_{\mathrm{RM}}^{\mathrm{lin}} = \int_{\hat{\mathcal{S}}} \left(\frac{t}{2} \| \operatorname{sym}(\nabla_{\hat{\mathcal{S}}}^{\mathrm{cov}} u)\|_{\mathcal{C}}^2 + \frac{t^3}{24} \| \operatorname{sym}(\nabla_{\hat{\mathcal{S}}}^{\mathrm{cov}} \beta + \nabla_{\hat{\mathcal{S}}} u^\top \nabla_{\hat{\mathcal{S}}} \hat{\nu})\|_{\mathcal{C}}^2 + \frac{t\kappa G}{2} |\nabla_{\hat{\mathcal{S}}} u^\top \hat{\nu} + \beta|^2 \right) ds. \quad (4.2.19)$$

Proof:

With Taylor at $\nabla_{\hat{\mathcal{S}}} u = 0$ and the small strain assumptions we obtain for the shear term

$$\boldsymbol{F}_{\hat{\mathcal{S}}}^\top \boldsymbol{R}(\hat{\nu},u,\hat{\gamma}) = 0 + \nabla_{\hat{\mathcal{S}}} u^\top(\hat{\nu}+\hat{\gamma}) + \boldsymbol{P}_{\hat{\mathcal{S}}}(-\nabla_{\hat{\mathcal{S}}} u^\top \hat{\nu} + \hat{\gamma}) + \mathcal{O}(\varepsilon^2) = \nabla_{\hat{\mathcal{S}}} u^\top \hat{\nu} + \beta + \mathcal{O}(\varepsilon^2)$$

and for the bending term

$$\begin{aligned} \boldsymbol{F}_{\hat{\mathcal{S}}}^\top \nabla_{\hat{\mathcal{S}}} \boldsymbol{R}(\hat{\nu},u,\hat{\gamma}) - \nabla_{\hat{\mathcal{S}}}\hat{\nu} &= \nabla_{\hat{\mathcal{S}}} u^\top \nabla_{\hat{\mathcal{S}}}(\hat{\nu}+\hat{\gamma}) + \boldsymbol{P}_{\hat{\mathcal{S}}} \nabla_{\hat{\mathcal{S}}}(-\nabla_{\hat{\mathcal{S}}} u^\top \hat{\nu} + \hat{\gamma}) + \mathcal{O}(\varepsilon^2) \\ &= \nabla_{\hat{\mathcal{S}}} u^\top \nabla_{\hat{\mathcal{S}}}\hat{\nu} + \nabla_{\hat{\mathcal{S}}}^{\mathrm{cov}} \beta + \mathcal{O}(\varepsilon^2). \end{aligned}$$

Together with the linearized membrane energy (Exercise!)

$$\|\boldsymbol{E}_{\hat{\mathcal{S}}}\|_{\mathcal{C}}^2 = \| \operatorname{sym}(\nabla_{\hat{\mathcal{S}}}^{\mathrm{cov}} u)\|_{\mathcal{C}}^2 + \mathcal{O}(\varepsilon^2). \quad (4.2.20)$$

the claim follows. □

Remark 4.2.9 *Using the shear $\gamma := \hat{\gamma} = \nabla_{\hat{\mathcal{S}}} u^\top \hat{\nu} + \beta$ and $\nabla_{\hat{\mathcal{S}}}^{\mathrm{cov}}(\nabla_{\hat{\mathcal{S}}} u^\top \hat{\nu}) = \mathcal{H}_{\hat{\nu}} + \nabla_{\hat{\mathcal{S}}} u^\top \nabla_{\hat{\mathcal{S}}}\hat{\nu}$,* (4.2.19) *changes to*

$$\mathcal{W}_{\mathrm{RM}}^{\mathrm{lin}} = \int_{\hat{\mathcal{S}}} \left(\frac{t}{2} \| \operatorname{sym}(\nabla_{\hat{\mathcal{S}}}^{\mathrm{cov}} u)\|_{\mathcal{C}}^2 + \frac{t^3}{24} \| \operatorname{sym}(\nabla_{\hat{\mathcal{S}}}^{\mathrm{cov}} \gamma - \mathcal{H}_{\hat{\nu}})\|_{\mathcal{C}}^2 + \frac{t\kappa G}{2} |\gamma|^2 \right) ds, \quad (4.2.21)$$

where $\mathcal{H}_{\hat{\nu}} := \sum_{i=1}^3 (\nabla_{\hat{\mathcal{S}}}^2 u_i)\hat{\nu}_i$ with $\nabla_{\hat{\mathcal{S}}}^2$ denoting the surface Hessian, cf. Definition 3.1.7. As it involves a second order operator leading to a fourth order problem, (4.2.19) *is mostly used instead of* (4.2.21).

4.2.3 Nonlinear Koiter shell

With hypothesis (H1), (H2), and (H5) together with Lemma 3.2.4 the director $\tilde{\nu}\circ\phi$ is of the form

$$\tilde{\nu}\circ\phi = \frac{1}{\| \operatorname{cof}(\boldsymbol{F}_{\hat{\mathcal{S}}})\|_F} \operatorname{cof}(\boldsymbol{F}_{\hat{\mathcal{S}}})\hat{\nu}. \quad (4.2.22)$$

Thus, the shearing energy is zero and the nonlinear Koiter shell energy is given by

$$\mathcal{W}_{\mathrm{KL}} = \int_{\hat{\mathcal{S}}} \left(\frac{t}{2} \|\boldsymbol{E}_{\hat{\mathcal{S}}}\|_{\mathcal{C}}^2 + \frac{t^3}{24} \|\boldsymbol{F}_{\hat{\mathcal{S}}}^\top \nabla_{\hat{\mathcal{S}}} \left(\frac{\operatorname{cof}(\boldsymbol{F}_{\hat{\mathcal{S}}})\hat{\nu}}{\| \operatorname{cof}(\boldsymbol{F}_{\hat{\mathcal{S}}})\|_F} \right) - \nabla_{\hat{\mathcal{S}}}\hat{\nu}\|_{\mathcal{C}}^2 \right) ds. \quad (4.2.23)$$

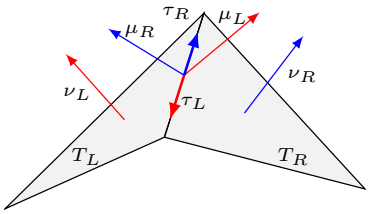

Figure 4.3: Normal, edge tangential and co-normal vectors.

4.2.4 Linear Koiter shell

Next, we linearize the Koiter shell model.

Lemma 4.2.10 *Under the small strain assumption the linearization of* (4.2.23) *is given by*

$$\mathcal{W}_{\mathrm{KL}}^{\mathrm{lin}} = \int_{\hat{\mathcal{S}}} \left(\frac{t}{2} \| \operatorname{sym}(\nabla_{\hat{\mathcal{S}}}^{\mathrm{cov}} u) \|_{\mathcal{C}}^2 + \frac{t^3}{24} \| \mathcal{H}_{\hat{\nu}} \|_{\mathcal{C}}^2 \right) ds. \tag{4.2.24}$$

Proof: By Taylor at $\nabla_{\hat{\mathcal{S}}} u = 0$ we obtain with the tensor cross product identities from Lemma 3.2.2

$$\begin{aligned} \boldsymbol{F}_{\hat{\mathcal{S}}}^{\top} \nabla_{\hat{\mathcal{S}}} (\nu \circ \phi) - \nabla_{\hat{\mathcal{S}}} \hat{\nu} &= 0 + \nabla_{\hat{\mathcal{S}}} u^{\top} \nabla_{\hat{\mathcal{S}}} \hat{\nu} + \nabla_{\hat{\mathcal{S}}}^{\mathrm{cov}} (\nabla_{\hat{\mathcal{S}}} u \times \boldsymbol{P}_{\hat{\mathcal{S}}} \hat{\nu} - \hat{\nu} \cdot (\boldsymbol{P}_{\hat{\mathcal{S}}} \times \nabla_{\hat{\mathcal{S}}} u \hat{\nu}) \hat{\nu}) + \mathcal{O}(\varepsilon^2) \\ &= \nabla_{\hat{\mathcal{S}}} u^{\top} \nabla_{\hat{\mathcal{S}}} \hat{\nu} + \nabla_{\hat{\mathcal{S}}}^{\mathrm{cov}} (-\nabla_{\hat{\mathcal{S}}} u^{\top} \hat{\nu}) + \mathcal{O}(\varepsilon^2) \\ &= -\mathcal{H}_{\hat{\nu}} + \mathcal{O}(\varepsilon^2). \end{aligned}$$

Together with the linearized membrane energy (4.2.20) the claim follows. □

Remark 4.2.11 *In the limit $t \to 0$ in* (4.2.19) *we obtain $\beta = -\nabla_{\hat{\mathcal{S}}} u^{\top} \hat{\nu}$ recovering* (4.2.24) *as then $\nabla_{\hat{\mathcal{S}}}^{\mathrm{cov}} \beta + \nabla_{\hat{\mathcal{S}}} u^{\top} \nabla_{\hat{\mathcal{S}}} \hat{\nu} = -\mathcal{H}_{\hat{\nu}}$. The same holds for the shearing formulation* (4.2.21).

4.3 Discretization of the shell equations

After the derivation of the shell equations we discuss the discretization and implementation.

First, we consider the Koiter shell model, where no shearing appears. To overcome the necessity of C^1-finite elements the mixed HHJ method is applied. Further, as the underlying shell geometry of the initial or deformed configuration is in general not C^1 (only continuous), we use the distributional Weingarten tensor from Section 3.4.2.

4.3.1 Koiter/Kirchhoff–Love shells

HHJ for nonlinear Koiter shells

We start with shell energy (4.2.23), the notation $\nu \circ \phi = \frac{\operatorname{cof}(\boldsymbol{F}_{\hat{\mathcal{S}}}) \hat{\nu}}{\| \operatorname{cof}(\boldsymbol{F}_{\hat{\mathcal{S}}}) \|_F}$, and material law (4.2.8)

$$\mathcal{W}_{\mathrm{KL}}(u_h) = \int_{\hat{\mathcal{S}}} \left(\frac{t}{2} \| \boldsymbol{E}_{\hat{\mathcal{S}}} \|_{\mathcal{C}}^2 + \frac{t^3}{24} \| \operatorname{sym}(\boldsymbol{F}_{\hat{\mathcal{S}}}^{\top} \nabla_{\hat{\mathcal{S}}} (\nu \circ \phi)) - \nabla_{\hat{\mathcal{S}}} \hat{\nu} \|_{\mathcal{C}}^2 \right) ds. \tag{4.3.1}$$

In the following we neglect for ease of presentation the subscript h for the finite element functions. Further, we use e.g. $\nabla_{\hat{\mathcal{S}}}$ instead of $\nabla_{\mathcal{T}}$. For a possibly curved but not C^1 triangulation $\mathcal{T}$ of $\hat{\mathcal{S}}$ consisting of triangles and quadrilaterals we cannot use the bending energy term in (4.3.1). Instead we use the distributional curvature (3.4.14) for the initial and deformed configuration and define a lifting to a new unknown, the curvature difference $\boldsymbol{\kappa}^{\mathrm{diff}}$, according to Definition 3.4.5. The resulting Lagrangian of the three-field formulation reads

$$\begin{aligned} \mathcal{L}(u, \boldsymbol{\kappa}^{\mathrm{diff}}, \boldsymbol{\sigma}) = \int_{\mathcal{T}} \frac{t}{2} \| \boldsymbol{E}_{\hat{\mathcal{S}}} \|_{\mathcal{C}}^2 + \frac{t^3}{24} \| \boldsymbol{\kappa}^{\mathrm{diff}} \|_{\mathcal{C}}^2 \, ds + \sum_{T \in \mathcal{T}} \int_T \left((\boldsymbol{F}_{\hat{\mathcal{S}}}^{\top} \nabla_{\hat{\mathcal{S}}} \nu \circ \phi - \nabla_{\hat{\mathcal{S}}} \hat{\nu}) - \boldsymbol{\kappa}^{\mathrm{diff}} \right) : \boldsymbol{\sigma} \, ds \\ + \sum_{E \in \mathcal{E}} \int_E (\sphericalangle(\nu_L, \nu_R) \circ \phi - \sphericalangle(\hat{\nu}_L, \hat{\nu}_R)) \boldsymbol{\sigma}_{\hat{\mu}\hat{\mu}} \, dl, \end{aligned} \tag{4.3.2}$$

compare Figure 4.3 for the normal vector ν_L and ν_R on neighbored elements.

The Lagrange parameter $\boldsymbol{\sigma}$ has the physical meaning of the moment tensor, which is the energetic conjugate of the difference of the curvatures of the deformed and initial configuration. We can eliminate $\boldsymbol{\kappa}^{\text{diff}}$ if $\mathcal{C}$ is invertible.

Lemma 4.3.1 *Three-field formulation* (4.3.2) *is equivalent to the two-field formulation*

$$\begin{aligned}\mathcal{L}(u,\boldsymbol{\sigma}) = \frac{t}{2}\int_{\mathcal{T}} \|\boldsymbol{E}_{\hat{\mathcal{S}}}\|^2_{\mathcal{C}}\,ds - \int_{\mathcal{T}} \frac{6}{t^3}\|\boldsymbol{\sigma}\|^2_{\mathcal{C}^{-1}}\,ds + \sum_{T\in\mathcal{T}}\int_T (\boldsymbol{F}_{\hat{\mathcal{S}}}^\top \nabla_{\hat{\mathcal{S}}}(\nu\circ\phi) - \nabla_{\hat{\mathcal{S}}}\hat{\nu}) : \boldsymbol{\sigma}\,ds \\ + \sum_{E\in\mathcal{E}}\int_E (\sphericalangle(\nu_L,\nu_R)\circ\phi - \sphericalangle(\hat{\nu}_L,\hat{\nu}_R))\,\boldsymbol{\sigma}_{\hat{\mu}\hat{\mu}}\,dl, \end{aligned} \tag{4.3.3}$$

where the inverse material is given by $\|\cdot\|^2_{\mathcal{C}^{-1}} := \frac{1+\nu}{E}(\operatorname{tr}(\cdot^2) - \frac{\nu}{\nu+1}\operatorname{tr}(\cdot)^2)$.

Proof: Taking the variation of (4.3.2) with respect to $\boldsymbol{\kappa}^{\text{diff}}$ yields

$$D_{\boldsymbol{\kappa}^{\text{diff}}}\mathcal{L}(u,\boldsymbol{\kappa}^{\text{diff}},\boldsymbol{\sigma})[\delta\boldsymbol{\kappa}] = \frac{t^3}{12}(\mathcal{C}\boldsymbol{\kappa}^{\text{diff}}) : \delta\boldsymbol{\kappa} - \delta\boldsymbol{\kappa} : \boldsymbol{\sigma}\,ds \overset{!}{=} 0 \text{ for all } \delta\boldsymbol{\kappa}$$

and thus $\boldsymbol{\kappa}^{\text{diff}} = \frac{12}{t^3}\mathcal{C}^{-1}\boldsymbol{\sigma}$. Eliminating $\boldsymbol{\kappa}^{\text{diff}}$ in (4.3.2) finishes the proof. □

Note that the thickness parameter t appears now also in the denominator. In the smooth case the Lagrange functional is equivalent to the original minimization problem and thus consistent.

Theorem 4.3.2 *Assume that $\mathcal{T}$ is a globally smooth manifold, $\mathcal{T}\in C^1$, and $\boldsymbol{\sigma}\in L^2(\mathcal{T}, T\mathcal{T}\times T\mathcal{T})$, $u\in H^2(\mathcal{T},\mathbb{R}^3)$. Then, solving the saddle point problem* (4.3.3) *is equivalent to minimizing the energy* (4.3.1).

Proof: We compute the variations of the Lagrange functional in (4.3.3), noting that for a smooth triangulation $\mathcal{T}$ the jump term vanishes,

$$D_{\boldsymbol{\sigma}}\mathcal{L}(u,\boldsymbol{\sigma})[\delta\boldsymbol{\sigma}] = \int_{\mathcal{T}} -\frac{12}{t^3}\mathcal{C}^{-1}\boldsymbol{\sigma} : \delta\boldsymbol{\sigma} + (\boldsymbol{F}_{\hat{\mathcal{S}}}^\top\nabla_{\hat{\mathcal{S}}}(\nu\circ\phi) - \nabla_{\hat{\mathcal{S}}}\hat{\nu}) : \delta\boldsymbol{\sigma}\,ds \overset{!}{=} 0, \qquad \text{for all } \delta\boldsymbol{\sigma}, \tag{4.3.4a}$$

$$D_u\mathcal{L}(u,\boldsymbol{\sigma})[\delta u] = D_u\Big(\frac{t}{2}\|\boldsymbol{E}_{\hat{\mathcal{S}}}\|^2_{\mathcal{C}}\Big)[\delta u] + \int_{\mathcal{T}}\boldsymbol{\sigma} : D_u(\boldsymbol{F}_{\hat{\mathcal{S}}}^\top\nabla_{\hat{\mathcal{S}}}(\nu\circ\phi) - \nabla_{\hat{\mathcal{S}}}\hat{\nu})[\delta u]\,ds \overset{!}{=} 0, \text{ for all } \delta u. \tag{4.3.4b}$$

Expressing $\boldsymbol{\sigma}$ from (4.3.4a), $\boldsymbol{\sigma} = \frac{t^3}{12}\mathcal{C}(\boldsymbol{F}_{\hat{\mathcal{S}}}^\top\nabla_{\hat{\mathcal{S}}}(\nu\circ\phi) - \nabla_{\hat{\mathcal{S}}}\hat{\nu})$, and inserting this into (4.3.4b) yields

$$\begin{aligned} 0 &= D_u\Big(\frac{t}{2}\|\boldsymbol{E}_{\hat{\mathcal{S}}}\|^2_{\mathcal{C}}\Big)[\delta u] + \int_{\mathcal{T}}\frac{t^3}{12}\mathcal{C}(\boldsymbol{F}_{\hat{\mathcal{S}}}^\top\nabla_{\hat{\mathcal{S}}}(\nu\circ\phi) - \nabla_{\hat{\mathcal{S}}}\hat{\nu}) : D_u(\boldsymbol{F}_{\hat{\mathcal{S}}}^\top\nabla_{\hat{\mathcal{S}}}(\nu\circ\phi) - \nabla_{\hat{\mathcal{S}}}\hat{\nu})[\delta u] \\ &= D_u\Big(\frac{t}{2}\|\boldsymbol{E}_{\hat{\mathcal{S}}}\|^2_{\mathcal{C}}\Big)[\delta u] + D_u\Big(\frac{t^3}{24}\|\boldsymbol{F}_{\hat{\mathcal{S}}}^\top\nabla_{\hat{\mathcal{S}}}(\nu\circ\phi) - \nabla_{\hat{\mathcal{S}}}\hat{\nu}\|^2_{\mathcal{C}}\Big)[\delta u] = D_u\mathcal{W}_{\text{KL}}(u)[\delta u]. \end{aligned}$$

Thus, we conclude that (4.3.1) and (4.3.3) are equivalent. □

We reduced the fourth order minimization problem (4.3.1) to a second order mixed saddle point problem. With some computations, we finally obtain the following Lagrange functional.

Lemma 4.3.3 *For Lagrange functional* (4.3.3) *there holds*

$$\begin{aligned}\mathcal{L}(u,\boldsymbol{\sigma}) = \frac{t}{2}\int_{\mathcal{T}}\|\boldsymbol{E}_{\hat{\mathcal{S}}}\|^2_{\mathcal{C}}\,ds - \frac{6}{t^3}\int_{\mathcal{T}}\|\boldsymbol{\sigma}\|^2_{\mathcal{C}^{-1}}\,ds - \int_{\mathcal{T}}(\mathcal{H}_{\nu\circ\phi} + (1-\hat{\nu}\cdot\nu\circ\phi)\nabla_{\hat{\mathcal{S}}}\hat{\nu}) : \boldsymbol{\sigma}\,ds \\ + \sum_{E\in\mathcal{E}}\int_E (\sphericalangle(\nu_L,\nu_R)\circ\phi - \sphericalangle(\hat{\nu}_L,\hat{\nu}_R))\boldsymbol{\sigma}_{\hat{\mu}\hat{\mu}}\,dl, \end{aligned} \tag{4.3.5}$$

where $\mathcal{H}_{\nu\circ\phi} := \sum_{i=1}^3(\nabla^2_{\hat{\mathcal{S}}}u_i)\nu_i\circ\phi$.

Proof: Equivalence of (4.3.5) and (4.3.3) follows by differentiating the identity $\boldsymbol{F}_{\hat{\mathcal{S}}}^\top \nu \circ \phi = 0$ and some computations on $T \in \mathcal{T}$

$$\int_T \boldsymbol{\sigma} : \boldsymbol{F}_{\hat{\mathcal{S}}}^\top \nabla_{\hat{\mathcal{S}}}(\nu \circ \phi)\, ds = -\int_T \begin{pmatrix} \boldsymbol{H}_1 : \boldsymbol{\sigma} \\ \boldsymbol{H}_2 : \boldsymbol{\sigma} \\ \boldsymbol{H}_3 : \boldsymbol{\sigma} \end{pmatrix} \cdot \nu \circ \phi \, ds,$$

where $\boldsymbol{H}_i := \nabla_{\hat{\mathcal{S}}}^2 u_i + \nabla_{\hat{\mathcal{S}}}((\boldsymbol{P}_{\hat{\mathcal{S}}})_i)$, $(\boldsymbol{P}_{\hat{\mathcal{S}}})_i$ denoting the i-th column of $\boldsymbol{P}_{\hat{\mathcal{S}}}$. With $\boldsymbol{P}_{\hat{\mathcal{S}}} = \boldsymbol{I} - \hat{\nu} \otimes \hat{\nu}$ we obtain

$$\begin{aligned}
\nu \circ \phi \cdot \begin{pmatrix} \boldsymbol{H}_1 : \boldsymbol{\sigma} \\ \boldsymbol{H}_2 : \boldsymbol{\sigma} \\ \boldsymbol{H}_3 : \boldsymbol{\sigma} \end{pmatrix} &= \sum_{i=1}^3 \nu_i \circ \phi \nabla_{\hat{\mathcal{S}}}((\boldsymbol{P}_{\hat{\mathcal{S}}})_i + \nabla_{\hat{\mathcal{S}}} u_i) : \boldsymbol{\sigma} = -\sum_{i=1}^3 \nu_i \circ \phi (\nabla_{\hat{\mathcal{S}}}(\hat{\nu} \otimes \hat{\nu})_i - \nabla_{\hat{\mathcal{S}}}^2 u_i) : \boldsymbol{\sigma} \\
&= -\sum_{i=1}^3 \nu_i \circ \phi ((\nabla_{\hat{\mathcal{S}}} \hat{\nu}_i) \otimes \hat{\nu} + \hat{\nu}_i \nabla_{\hat{\mathcal{S}}} \hat{\nu} - \nabla_{\hat{\mathcal{S}}}^2 u_i) : \boldsymbol{\sigma} \\
&= -((\nu \circ \phi \cdot \hat{\nu}) \nabla_{\hat{\mathcal{S}}} \hat{\nu} - \sum_{i=1}^3 \nu_i \circ \phi \nabla_{\hat{\mathcal{S}}}^2 u_i) : \boldsymbol{\sigma} = -((\nu \circ \phi \cdot \hat{\nu}) \nabla_{\hat{\mathcal{S}}} \hat{\nu} - \mathcal{H}_{\nu \circ \phi}) : \boldsymbol{\sigma},
\end{aligned}$$

where we used that $\nabla_{\hat{\mathcal{S}}} \hat{\nu}_i \otimes \hat{\nu} : \boldsymbol{\sigma} \equiv 0$ as $\boldsymbol{\sigma}$ acts on the tangent bundle. □

Remark 4.3.4 *In case of a flat plane as initial configuration* (4.3.5) *simplifies to*

$$\mathcal{L}(u, \boldsymbol{\sigma}) = \frac{t}{2} \int_{\mathcal{T}} \|\boldsymbol{E}_{\hat{\mathcal{S}}}\|_{\mathbb{C}}^2 \, ds - \frac{6}{t^3} \int_{\mathcal{T}} \|\boldsymbol{\sigma}\|_{\mathbb{C}^{-1}}^2 \, ds - \int_{\mathcal{T}} \mathcal{H}_{\nu \circ \phi} : \boldsymbol{\sigma} \, ds + \sum_{E \in \mathcal{E}} \int_E \sphericalangle(\nu_L, \nu_R) \circ \phi \, \boldsymbol{\sigma}_{\hat{\mu}\hat{\mu}} \, dl, \quad (4.3.6)$$

as $\hat{\nu} = const$ *and* $\sphericalangle(\hat{\nu}_L, \hat{\nu}_R) = 0$.

The resulting system is a saddle point problem, which would lead to an indefinite matrix after assembling. To overcome this problem, we can use completely discontinuous elements for the moment tensor $\boldsymbol{\sigma} \in M_h^{\mathrm{dc}}$ and introduce a hybridization variable $\alpha \in \Lambda_h^{k-1}$ to reinforce the normal-normal continuity of $\boldsymbol{\sigma}$, see Section 2.4.3. Find $(u, \boldsymbol{\sigma}, \alpha) \in \boldsymbol{U}_h^k \times M_h^{\mathrm{dc},k-1} \times \Lambda_h^{k-1}$ for the saddle point problem

$$\begin{aligned}
\mathcal{L}^{\mathrm{hyb}}(u, \boldsymbol{\sigma}, \alpha) = \frac{t}{2} \int_{\mathcal{T}} \|\boldsymbol{E}_{\hat{\mathcal{S}}}\|_{\mathbb{C}}^2 \, ds - \frac{6}{t^3} \int_{\mathcal{T}} \|\boldsymbol{\sigma}\|_{\mathbb{C}^{-1}}^2 \, ds - \int_{\mathcal{T}} (\mathcal{H}_{\nu \circ \phi} + (1 - \hat{\nu} \cdot \nu \circ \phi) \nabla_{\hat{\mathcal{S}}} \hat{\nu}) : \boldsymbol{\sigma} \, ds \\
+ \sum_{E \in \mathcal{E}} \int_E (\sphericalangle(\nu_L, \nu_R) \circ \phi - \sphericalangle(\hat{\nu}_L, \hat{\nu}_R)) \langle\!\langle \boldsymbol{\sigma}_{\hat{\mu}\hat{\mu}} \rangle\!\rangle + \alpha_{\hat{\mu}} [\![\boldsymbol{\sigma}_{\hat{\mu}\hat{\mu}}]\!] \, dl, \quad (4.3.7)
\end{aligned}$$

with $\langle\!\langle \boldsymbol{\sigma}_{\hat{\mu}\hat{\mu}} \rangle\!\rangle := \frac{1}{2}((\boldsymbol{\sigma}_{\hat{\mu}\hat{\mu}})|_{T_L} + (\boldsymbol{\sigma}_{\hat{\mu}\hat{\mu}})|_{T_R})$ denoting the mean value of $\boldsymbol{\sigma}_{\hat{\mu}\hat{\mu}}$.

Due to the hybridization variable α, we can use static condensation to eliminate the degrees of freedom of the moment tensor $\boldsymbol{\sigma}$ locally, which leads to a minimization problem (in u and α) again. The new unknown α has the physical meaning of the changed angle, the rotation, between elements and is zero for (4.3.7), i.e., a virtual Lagrange multiplier.

Computational aspects

The usage of the angle $\sphericalangle(\nu_L, \nu_R)$ is numerically unstable if $\nu_L \approx \nu_R$. Therefore, we rewrite it in an equivalent form

$$\begin{aligned}
\sum_{E \in \mathcal{E}} \int_E \sphericalangle(\nu_L, \nu_R) \circ \phi - \sphericalangle(\hat{\nu}_L, \hat{\nu}_R) \, dl &= \sum_{T \in \mathcal{T}} \int_{\partial T} \sphericalangle(\{\nu\}, \nu) \circ \phi - \sphericalangle(\{\hat{\nu}\}, \hat{\nu}) \, dl \quad (4.3.8) \\
&= \sum_{T \in \mathcal{T}} \int_{\partial T} \sphericalangle(\{\hat{\nu}\}, \hat{\mu}) - \sphericalangle(\{\nu\}, \mu) \circ \phi \, dl, \quad (4.3.9)
\end{aligned}$$

as $\sphericalangle(\{\nu\}, \nu) = \frac{\pi}{2} - \sphericalangle(\{\nu\}, \mu)$, see Figure 4.4. Here, $\{\nu\} := \frac{1}{\|\nu_L + \nu_R\|_2}(\nu_L + \nu_R)$ denotes the averaged normal vector. This algebraic equivalent reformulation is numerically much more stable as the derivative

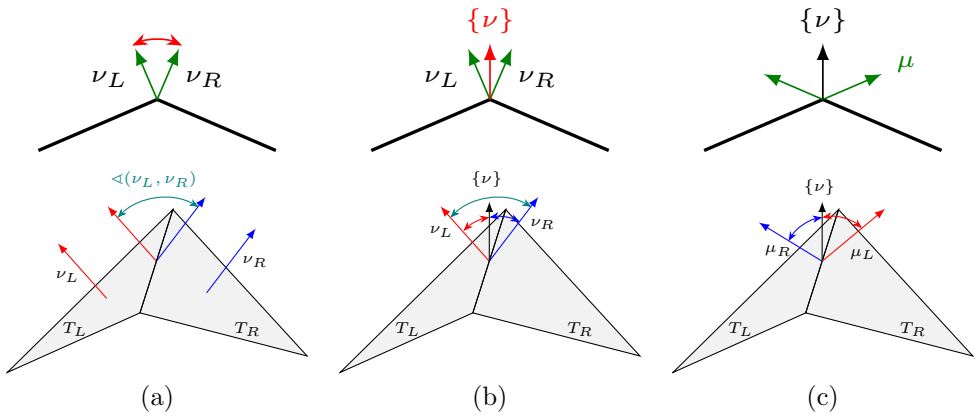

Figure 4.4: Angle computation in 2D and 3D: (a) Angle between ν_L and ν_R. (b) Averaged normal vector with normal vector ν. (c) Averaged normal vector with element normal vector μ.

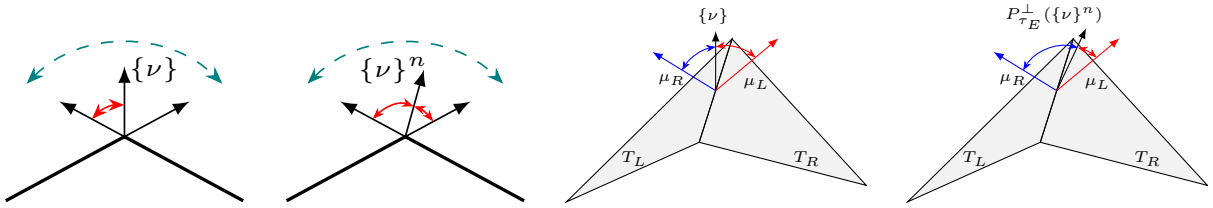

Figure 4.5: Angle computation with the current averaged normal vector $\{\nu\}$ and the averaged normal vector $\{\nu\}^n$ from the previous step in 2D and 3D.

of $\arccos(x)$, $\arccos'(x) = -\frac{1}{\sqrt{1-x^2}}$, has singularities at $x = \pm 1$ and we expect (for the triangulation of a smooth surface) $\{\nu\} \cdot \nu \approx 1$, whereas for $\{\nu\} \cdot \mu \approx 0$ the derivatives of arccos are well-defined.

To compute the deformed averaged normal vector $\{\nu\} \circ \phi$ on an edge, information of the two neighbored elements is needed at once, which would require e.g., Discontinuous Galerkin techniques leading to a denser stiffness matrix. Instead, one can use the information of the last (loadstep or Newton iteration) solution $\{\nu\}^n$, cf. Figure 4.5. This, and also (4.3.8), is based on the following simple geometric observation.

Lemma 4.3.5 *Let $a, b \in \mathbb{R}^3$ with $\|a\|_2 = \|b\|_2 = 1$. Further let $c \in \mathbb{R}^3$ with $\|c\|_2 = 1$ and c "lies between" a and b, i.e., there exists $t \in (0,1)$ such that $c \in \operatorname{span}\{t\,a + (1-t)b\}$. Then there holds*

$$\arccos(a \cdot b) = \arccos(a \cdot c) + \arccos(c \cdot b). \tag{4.3.10}$$

In three spatial dimensions, to fulfill the requirement of Lemma 4.3.5 that $\{\nu\}^n$ "lies between" μ_R and μ_L, i.e., to measure the correct angle, we have to project $\{\nu\}^n$ to the plane orthogonal to the tangent vector τ by using the orthogonal projection $\boldsymbol{P}^{\perp}_{\tau_E} = \boldsymbol{I} - \tau \circ \phi \otimes \tau \circ \phi$, and then re-normalize it leading to the (nonlinear) operator

$$P^{\perp}_{\tau_E}(\{\nu\}^n) := \frac{1}{\|\boldsymbol{P}^{\perp}_{\tau_E}\{\nu\}^n\|_2} \boldsymbol{P}^{\perp}_{\tau_E}\{\nu\}^n. \tag{4.3.11}$$

By using (4.3.11) we have to ensure that $\{\nu\}^n$ lies between the two element-normal vectors, see Figure 4.5. For smooth manifolds the angle between the element-normal vectors tends to 180 degree as $h \to 0$. Hence, this assumption is fulfilled, if the elements do not rotate more than half of their included angle during one loadstep, which is an acceptable and realistic assumption.

Therefore, for given averaged normal vector $\{\nu\}^n$ (4.3.7) changes to: Let $\{\nu\}^n$ be given. Find

$(u, \boldsymbol{\sigma}, \alpha) \in \boldsymbol{U}_h^k \times M_h^{\mathrm{dc},k-1} \times \Lambda_h^{k-1}$ for the saddle point problem

$$\mathcal{L}^{\mathrm{hyb}}_{\{\nu\}^n}(u, \boldsymbol{\sigma}, \alpha) = \frac{t}{2}\int_{\mathcal{T}} \|\boldsymbol{E}_{\hat{\mathcal{S}}}\|^2_{\mathcal{C}}\, ds - \frac{6}{t^3}\int_{\mathcal{T}} \|\boldsymbol{\sigma}\|^2_{\mathcal{C}^{-1}}\, ds + \sum_{T\in\mathcal{T}} \Big(- \int_T (\mathcal{H}_{\nu\circ\phi} + (1 - \hat{\nu}\cdot\nu\circ\phi)\nabla_{\hat{\mathcal{S}}}\hat{\nu}) : \boldsymbol{\sigma}\, ds$$
$$- \int_{\partial T} \big(\sphericalangle(P^{\perp}_{\tau_E}(\{\nu\}^n), \mu)\circ\phi - \sphericalangle(\{\hat{\nu}\}, \hat{\mu}) - \alpha_{\hat{\mu}}\big)\, \boldsymbol{\sigma}_{\hat{\mu}\hat{\mu}}\, dl\Big). \tag{4.3.12}$$

Exercise 4.3.6 *Does the value and physical interpretation of the Lagrange multiplier α change or remain?*

The averaged normal vector $\{\nu\}^n$ can easily be computed by the following (local) problem, where boundaries with clamped or symmetry boundary conditions have to be treated as Dirichlet boundary. For given (non-continuous) normal vector field ν^n find $\eta \in [\Gamma_h^k]^3$ such that $\eta = \hat{\nu}$ on Γ_D and for all $\xi \in [\Gamma^k_{h,\Gamma_D}]^3$

$$\sum_{T\in\mathcal{T}} \int_{\partial T} \eta\, \xi\, dl = \sum_{T\in\mathcal{T}} \int_{\partial T} \nu^n\, \xi\, dl. \tag{4.3.13}$$

Then define $\{\nu\}^n := \frac{\eta}{\|\eta\|_2}$.

Remark 4.3.7 *Procedure* (4.3.13) *can be performed edge patch-wise such that it has linear costs in number of edges. The direct use of the angle yields that the solutions are independent of the number of loadsteps, as long as Newton's method converges, in contrast to a classical updated Lagrangian formulation.*

Final algorithm: The final algorithm consists of the following steps:

1. For given displacement u^n and $\nu^n = \nu(u^n)$ compute the averaged normal vector $\{\nu\}^n$ (4.3.13).
2. Find $(u, \boldsymbol{\sigma}, \alpha)$ by solving (4.3.12).

4.3.2 Branched shells and kinks

Up to now we considered smooth surfaces. Structures with kinks or branched shells, where more than two elements are attached on an edge, occur frequently in e.g. industry.

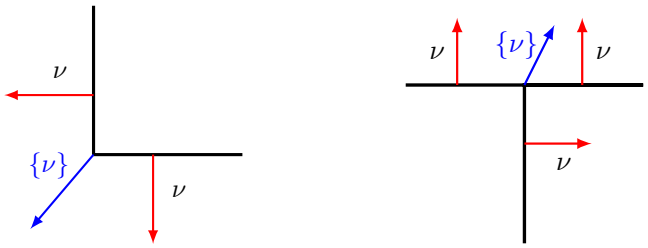

Figure 4.6: Left: Kinked shell. Right: Branched shell.

We start with kinked structures as depicted in Figure 4.6 (left), where the averaged normal vector $\{\nu\}\circ\phi$ is well defined. We recall that the co-normal co-normal component of the bending stress tensor is continuous, $[\![\boldsymbol{\sigma}_{\hat{\mu}\hat{\mu}}]\!] = 0$. Therefore, the moments enter the kink exactly go into the neighbored element. The co-normal co-normal component "does not see" the junction such that the moments are preserved, which is one of the interface conditions. Additionally, if we consider the first variation of $\boldsymbol{\sigma}$ in (4.3.5) only on one single edge, we observe from

$$\int_E (\sphericalangle(\nu_L, \nu_R)\circ\phi - \sphericalangle(\hat{\nu}_L, \hat{\nu}_R))\delta\boldsymbol{\sigma}_{\hat{\mu}\hat{\mu}}\, ds = 0, \qquad \text{for all } \delta\boldsymbol{\sigma} \in M_h \tag{4.3.14}$$

that in a weak sense the initial angle of the kink gets preserved, $\sphericalangle(\nu_L, \nu_R)\circ\phi = \sphericalangle(\hat{\nu}_L, \hat{\nu}_R)$. Thus, the method can be applied to kinked structures without the necessity of adapting terms at the kinks.

4.3.3 Branched shells

For branched shells, where edges are shared by more than two elements, the situation is more involved and the question how to define the boundary term arises. Therefore, we first define the averaged normal vector $\{\nu\} \circ \phi = \frac{\sum_{i=1}^N \nu_i \circ \phi}{\| \sum_{i=1}^N \nu_i \circ \phi \|}$, where N denotes the number of elements connected the edge and $\nu_i \circ \phi$ corresponding normal vectors of the branches, whose orientations are a priori fixed (e.g. during mesh generation), cf. Figure 4.6 (right). In this way also the possibility of cancellation, $\sum_{i=1}^N \nu_i \circ \phi = 0$, can easily be avoided by changing the orientation of one branch. Motivated by (4.3.14) a first approach would be

$$\sum_{i=1}^{N} \int_{\partial T_i \cap E} (\sphericalangle(\nu_i, \{\nu\}) \circ \phi - \sphericalangle(\hat{\nu}_i, \{\hat{\nu}\})) \boldsymbol{\sigma}_{\hat{\mu}\hat{\mu}} \, ds. \tag{4.3.15}$$

Taking again the variation of $\boldsymbol{\sigma}$ would give that the sum of the changed angles is zero, but not each angle itself. To force that each integral in the sum of (4.3.15) is zero we make $\boldsymbol{\sigma}$ discontinuous in terms of hybridization. Then we obtain that each angle is (weakly) preserved.

The Lagrange multiplier α, which reinforced the co-normal co-normal continuity of $\boldsymbol{\sigma}$ for non-branched shells, now guarantees that the sum of moment inflows is equal to the sum of moment outflows at the edge

$$\sum_{T \in \mathcal{T}: E \subset T} \int_{\partial T \cap E} \delta\alpha_{\hat{\mu}} \boldsymbol{\sigma}_{\hat{\mu}\hat{\mu}} \, ds = 0 \qquad \text{for all } \delta\alpha \in \Lambda_h. \tag{4.3.16}$$

This equilibrium of moments leads to a physically correct behavior of shells.

HHJ for linear Koiter shells

For the small deformation regime we show that (4.3.7) reduces to the (hybridized) HHJ method of the linear Koiter shell formulation (4.2.24). Find $(u, \boldsymbol{\sigma}, \alpha) \in \boldsymbol{U}_h^k \times M_h^{\mathrm{dc},k-1} \times \Lambda_h^{k-1}$ for the saddle point problem

$$\mathcal{L}_{\mathrm{lin}}^{\mathrm{hyb}}(u, \boldsymbol{\sigma}, \alpha) = \int_{\mathcal{T}} \frac{t}{2} \| \operatorname{sym}(\nabla_{\hat{\mathcal{S}}}^{\mathrm{cov}} u) \|_{\mathcal{C}}^2 - \frac{6}{t^3} \| \boldsymbol{\sigma} \|_{\mathcal{C}^{-1}}^2 \, ds + \sum_{T \in \mathcal{T}} \Big(- \int_T \mathcal{H}_{\hat{\nu}} : \boldsymbol{\sigma} \, ds + \int_{\partial T} ((\nabla_{\hat{\mathcal{S}}} u^\top \hat{\nu})_{\hat{\mu}} + \alpha_{\hat{\mu}}) \boldsymbol{\sigma}_{\hat{\mu}\hat{\mu}} \, dl \Big). \tag{4.3.17}$$

Proposition 4.3.8 (4.3.17) *is the linearization of* (4.3.7).

Proof: It is sufficient to linearize only the non-standard boundary term, the volume term has already been derived in Lemma 4.2.10.

We will proof the statement without the hybridization unknown α, which already appears linearly in the equation. Further, we will again make heavily use of the tensor cross product identities from Lemma 3.2.2 and use the trigonometric identity

$$\sqrt{1 - (\hat{\nu}_L \cdot \hat{\nu}_R)^2} = \cos(\frac{\pi}{2} - \arccos(\hat{\nu}_L \cdot \hat{\nu}_R)) = \cos(\arccos(\hat{\nu}_R \cdot \hat{\mu}_L)) = \hat{\nu}_R \cdot \hat{\mu}_L = \hat{\nu}_L \cdot \hat{\mu}_R.$$

With Taylor at $\nabla_{\hat{\mathcal{S}}} u = 0$ and using $\boldsymbol{P}_{\hat{\mathcal{S}}} \times \boldsymbol{A}\hat{\nu} = \boldsymbol{I} \times \boldsymbol{A}\hat{\nu}$ we get

$$\begin{aligned}
\sphericalangle(\nu_L, \nu_R) \circ \phi - \sphericalangle(\hat{\nu}_L, \hat{\nu}_R) = &- \frac{1}{\sqrt{1 - (\hat{\nu}_L \cdot \hat{\nu}_R)^2}} \Big((\boldsymbol{I} \times \nabla_{\hat{\mathcal{S}}} u_L \hat{\nu}_L) \cdot \hat{\nu}_R + \hat{\nu}_L \cdot (\boldsymbol{I} \times \nabla_{\hat{\mathcal{S}}} u_R \hat{\nu}_R) \\
&- \hat{\nu}_L \cdot \hat{\nu}_R ((\boldsymbol{I} \times \nabla_{\hat{\mathcal{S}}} u_L \hat{\nu}_L) \cdot \hat{\nu}_L + (\boldsymbol{I} \times \nabla_{\hat{\mathcal{S}}} u_R \hat{\nu}_R) \cdot \hat{\nu}_R) \Big) + \mathcal{O}(\varepsilon^2) \\
= &- \frac{1}{\hat{\nu}_L \cdot \hat{\mu}_R} \Big((\boldsymbol{I} \times \nabla_{\hat{\mathcal{S}}} u_L \hat{\nu}_L) \cdot \hat{\nu}_R + \hat{\nu}_L \cdot (\boldsymbol{I} \times \nabla_{\hat{\mathcal{S}}} u_R \hat{\nu}_R) \\
&- \hat{\nu}_L \cdot \hat{\nu}_R ((\boldsymbol{I} \times \nabla_{\hat{\mathcal{S}}} u_L \hat{\nu}_L) \cdot \hat{\nu}_L + (\boldsymbol{I} \times \nabla_{\hat{\mathcal{S}}} u_R \hat{\nu}_R) \cdot \hat{\nu}_R) \Big) + \mathcal{O}(\varepsilon^2).
\end{aligned}$$

Further, using $\boldsymbol{I} \times \boldsymbol{A}\hat{\nu} = \operatorname{tr}(\boldsymbol{A})\hat{\nu} - \boldsymbol{A}^\top \hat{\nu}$ yields

$$\begin{aligned}\sphericalangle(\nu_L, \nu_R) \circ \phi - \sphericalangle(\hat{\nu}_L, \hat{\nu}_R) = -\frac{1}{\hat{\nu}_L \cdot \hat{\mu}_R}\Big((\operatorname{div}_{\hat{\mathcal{S}}} u_L + \operatorname{div}_{\hat{\mathcal{S}}} u_R)\hat{\nu}_L \cdot \hat{\nu}_R - (\nabla_{\hat{\mathcal{S}}} u_L^\top \hat{\nu}_L) \cdot \hat{\nu}_R \\ - (\nabla_{\hat{\mathcal{S}}} u_R^\top \hat{\nu}_R) \cdot \hat{\nu}_L - \hat{\nu}_L \cdot \hat{\nu}_R (\operatorname{div}_{\hat{\mathcal{S}}} u_L + \operatorname{div}_{\hat{\mathcal{S}}} u_R)\Big) + \mathcal{O}(\varepsilon^2).\end{aligned}$$

By using the splitting $\hat{\nu}_R = (\hat{\nu}_R \cdot \hat{\nu}_L)\hat{\nu}_L + (\hat{\nu}_R \cdot \hat{\mu}_L)\hat{\mu}_L$ (and analogously for $\hat{\nu}_L$) yields the claim

$$\begin{aligned}\sphericalangle(\nu_L, \nu_R) \circ \phi - \sphericalangle(\hat{\nu}_L, \hat{\nu}_R) &= -\frac{1}{\hat{\nu}_L \cdot \hat{\mu}_R}\Big(\frac{\partial u_L}{\partial \hat{\mu}_L} \cdot \hat{\nu}_L(\hat{\nu}_R \cdot \hat{\mu}_L) + \frac{\partial u_R}{\partial \hat{\mu}_R} \cdot \hat{\nu}_R(\hat{\nu}_L \cdot \hat{\mu}_R)\Big) + \mathcal{O}(\varepsilon^2) \\ &= \frac{\partial u_L}{\partial \hat{\mu}_L}\hat{\nu}_L + \frac{\partial u_R}{\partial \hat{\mu}_R}\hat{\nu}_R + \mathcal{O}(\varepsilon^2).\end{aligned}$$

□

Corollary 4.3.9 *Let $\hat{\mathcal{S}}$ be a flat plate $\hat{\mathcal{S}} \subset \mathbb{R}^2 \times \{0\}$. Then the HHJ method for plates given by Problem 2.4.4 is the linearized bending term of* (4.3.7).

Proof: Follows directly from Proposition 4.3.8. □

4.3.4 Naghdi/Reissner–Mindlin shells

TDNNS for nonlinear Naghdi shells

For Reissner–Mindlin/Naghdi shells there have been proposed a vast amount of shell elements in the literature in the last decades. Most of them are tailored for low-order (linear or quadratic elements).

In this section we add an additional shearing parameter $\gamma \in H(\operatorname{curl})$ and use a hierarchical approach to extend the nonlinear HHJ method from Koiter to Naghdi shells. We will see that in the linearized case the method reduces to the TDNNS method for Reissner–Mindlin plates extended to linear shells. The shearing parameter $\tilde{\gamma} \circ \phi$ is of dimension two and perpendicular to the deformed normal vector, i.e., lives in the deformed tangent space. This motivates to use the space $H(\operatorname{curl})$ mapped onto the surface and use the corresponding covariant transformation $\tilde{\gamma} \circ \phi = (\boldsymbol{F}_{\hat{\mathcal{S}}}^\dagger)^\top \gamma$ instead of the push forward, cf. (4.2.15).

We start as in Section 4.3.1 with the shell energy (4.2.16), where $\tilde{\nu} \circ \phi = \frac{\operatorname{cof}(\boldsymbol{F}_{\hat{\mathcal{S}}})\hat{\nu} + (\boldsymbol{F}_{\hat{\mathcal{S}}}^\dagger)^\top \gamma}{\|\operatorname{cof}(\boldsymbol{F}_{\hat{\mathcal{S}}})\hat{\nu} + (\boldsymbol{F}_{\hat{\mathcal{S}}}^\dagger)^\top \gamma\|_2}$ (compare also (4.2.15)), and material law (4.2.8)

$$\mathcal{W}_{\mathrm{RM}}(u_h, \gamma_h) = \int_{\hat{\mathcal{S}}} \frac{t}{2}\|\boldsymbol{E}_{\hat{\mathcal{S}}}\|_{\mathcal{C}}^2 + \frac{t^3}{24}\|\operatorname{sym}(\boldsymbol{F}_{\hat{\mathcal{S}}}^\top \nabla_{\hat{\mathcal{S}}}(\tilde{\nu} \circ \phi)) - \nabla_{\hat{\mathcal{S}}}\hat{\nu}\|_{\mathcal{C}}^2 + \frac{t\kappa G}{2}\|\boldsymbol{F}_{\hat{\mathcal{S}}}^\top \tilde{\nu} \circ \phi\|_2^2 \, ds. \tag{4.3.18}$$

We again neglect the subscript h for the finite element functions in the following. The procedure for handling distributional forms of the difference of the shape operators can be directly extended to the curvature difference induced by the director fields, leading to the mixed saddle point problem

$$\begin{aligned}\mathcal{L}(u, \gamma, \boldsymbol{\sigma}) = \frac{t}{2}\int_{\mathcal{T}} \|\boldsymbol{E}_{\hat{\mathcal{S}}}\|_{\mathcal{C}}^2 \, ds - \frac{6}{t^3}\int_{\mathcal{T}} \|\boldsymbol{\sigma}\|_{\mathcal{C}^{-1}}^2 \, ds + \sum_{T \in \mathcal{T}} \int_T (\boldsymbol{F}_{\hat{\mathcal{S}}}^\top \nabla_{\hat{\mathcal{S}}}(\tilde{\nu} \circ \phi) - \nabla_{\hat{\mathcal{S}}}\hat{\nu}) : \boldsymbol{\sigma} \, ds \\ + \int_{\mathcal{T}} \frac{t\kappa G}{2}\|\boldsymbol{F}_{\hat{\mathcal{S}}}^\top \tilde{\nu} \circ \phi\|_2^2 \, ds + \sum_{E \in \mathcal{E}} \int_E (\sphericalangle(\tilde{\nu}_L, \tilde{\nu}_R) \circ \phi - \sphericalangle(\hat{\nu}_L, \hat{\nu}_R)) \, \boldsymbol{\sigma}_{\hat{\mu}\hat{\mu}} \, dl.\end{aligned} \tag{4.3.19}$$

One may now proceed as for Koiter shells yielding a method for nonlinear Naghdi shells. We, however, simplify the highly nonlinear expression of $\tilde{\nu} \circ \phi$ by assuming that the shearing parameter is small as discussed and applied in [39], $(\boldsymbol{F}_{\hat{\mathcal{S}}}^\dagger)^\top \gamma = \mathcal{O}(\varepsilon)$, yielding $\tilde{\nu} \approx \nu \circ \phi + (\boldsymbol{F}_{\hat{\mathcal{S}}}^\dagger)^\top \gamma$ with $\nu \circ \phi$ the deformed

surface normal vector as in the previous sections. Then, the volume term $\int_T \left(\boldsymbol{F}_{\hat{\mathcal{S}}}^\top \nabla_{\hat{\mathcal{S}}} \tilde{\nu} \circ \phi - \nabla_{\hat{\mathcal{S}}} \hat{\nu} \right) : \boldsymbol{\sigma} \, ds$ in (4.3.19) can be simplified analogously to (4.3.5)

$$\begin{aligned}\int_T \nabla_{\hat{\mathcal{S}}} \tilde{\nu} \circ \phi : (\boldsymbol{F}_{\hat{\mathcal{S}}} \boldsymbol{\sigma}) \, ds &= \int_T - \left(\mathcal{H}_{\tilde{\nu} \circ \phi} + (1 - \tilde{\nu} \circ \phi \cdot \hat{\nu}) \nabla_{\hat{\mathcal{S}}} \hat{\nu} \right) : \boldsymbol{\sigma} - (\boldsymbol{F}_{\hat{\mathcal{S}}}^\dagger)^\top \gamma \cdot (\boldsymbol{F}_{\hat{\mathcal{S}}} \operatorname{div}_{\hat{\mathcal{S}}}(\boldsymbol{\sigma})) \, ds \\ &\quad + \int_{\partial T} (\boldsymbol{F}_{\hat{\mathcal{S}}}^\dagger)^\top \gamma \cdot (\boldsymbol{F}_{\hat{\mathcal{S}}} \boldsymbol{\sigma} \hat{\mu}) \, dl \\ &= \int_T - \left(\mathcal{H}_{\tilde{\nu} \circ \phi} + (1 - \tilde{\nu} \circ \phi \cdot \hat{\nu}) \nabla_{\hat{\mathcal{S}}} \hat{\nu} - \nabla_{\hat{\mathcal{S}}} \gamma \right) : \boldsymbol{\sigma} \, ds.\end{aligned}$$

The boundary term measuring the change of angle reduces to

$$\int_{\partial T} (\sphericalangle(\nu \circ \phi, \{\nu\}) - \gamma_{\hat{\mu}} - \sphericalangle(\hat{\nu}, \{\hat{\nu}\})) \, \boldsymbol{\sigma}_{\hat{\mu}\hat{\mu}} \, dl$$

and also the shearing energy simplifies

$$\|\boldsymbol{F}_{\hat{\mathcal{S}}} \tilde{\nu} \circ \phi\|_2^2 = \|\gamma\|_2^2. \tag{4.3.20}$$

Thus, the problem of nonlinear Naghdi shells reads with $\mathcal{N}^k$ as in (3.4.11): Find $(u, \gamma, \boldsymbol{\sigma}) \in \boldsymbol{U}_h^k \times \mathcal{N}^{k-1} \times M_h^{k-1}$ which solve the saddle point problem, with $\tilde{\nu} \circ \phi := \nu \circ \phi + (\boldsymbol{F}_{\hat{\mathcal{S}}}^\dagger)^\top \gamma$,

$$\begin{aligned}\mathcal{L}(u, \gamma, \boldsymbol{\sigma}) = \frac{t}{2} \int_{\mathcal{T}} \|\boldsymbol{E}_{\hat{\mathcal{S}}}\|_{\mathbb{C}}^2 \, ds + \sum_{T \in \mathcal{T}} \int_T - \left(\mathcal{H}_{\tilde{\nu} \circ \phi} + (1 - \tilde{\nu} \circ \phi \cdot \hat{\nu}) \, \nabla_{\hat{\mathcal{S}}} \hat{\nu} - \nabla_{\hat{\mathcal{S}}} \gamma \right) : \boldsymbol{\sigma} \, ds \\ + \frac{t \kappa G}{2} \int_{\mathcal{T}} \|\gamma\|_2^2 \, ds + \int_{\partial T} (\sphericalangle(\nu, \{\nu\}) \circ \phi - \sphericalangle(\hat{\nu}, \{\hat{\nu}\}) - \gamma_{\hat{\mu}}) \, \boldsymbol{\sigma}_{\hat{\mu}\hat{\mu}} \, dl.\end{aligned} \tag{4.3.21}$$

Remark 4.3.10 *Note that we can compute the Moore–Penrose pseudo-inverse via*

$$\boldsymbol{F}_{\hat{\mathcal{S}}}^\dagger = \left(\boldsymbol{F}_{\hat{\mathcal{S}}}^\top \boldsymbol{F}_{\hat{\mathcal{S}}} + \boldsymbol{P}_{\hat{\mathcal{S}}}^\perp \right)^{-1} \boldsymbol{F}_{\hat{\mathcal{S}}}^\top \tag{4.3.22}$$

as we know that the kernel of $\boldsymbol{F}_{\hat{\mathcal{S}}}$ is spanned by $\hat{\nu}$ (Tikhonov regularization).

It is straight forward to rewrite the boundary part in terms of a projection of the averaged normal vector and hybridization, as we have in this hierarchical approach an additive splitting of the Koiter formulation and the additional shearing parameter (Exercise!).

TDNNS for linear Naghdi shells

With the small deformation assumption we directly have that $(\boldsymbol{F}_{\hat{\mathcal{S}}}^\dagger)^\top \gamma \approx \gamma = \mathcal{O}(\varepsilon)$. Therefore, the additive splitting $\tilde{\nu} \circ \phi = \nu \circ \phi + \gamma$ is automatically justified. The linear Naghdi shell problem (4.2.21) with the HHJ stress space reads: Find $(u, \gamma, \boldsymbol{\sigma}) \in \boldsymbol{U}_h^k \times \mathcal{N}^{k-1} \times M_h^{k-1}$ for the saddle point problem

$$\begin{aligned}\mathcal{L}_{\text{lin}}(u, \boldsymbol{\sigma}, \gamma) = \frac{t}{2} \int_{\mathcal{T}} \|\operatorname{sym}(\nabla_{\hat{\mathcal{S}}}^{\text{cov}} u)\|_{\mathbb{C}}^2 \, ds + \frac{t \kappa G}{2} \int_{\mathcal{T}} \|\gamma\|_2^2 \, ds - \frac{6}{t^3} \int_{\mathcal{T}} \|\boldsymbol{\sigma}\|_{\mathbb{C}^{-1}}^2 \, ds \\ + \sum_{T \in \mathcal{T}} \Big(- \int_T (\mathcal{H}_{\hat{\nu}} - \nabla_{\hat{\mathcal{S}}} \gamma) : \boldsymbol{\sigma} \, ds + \int_{\partial T} ((\nabla_{\hat{\mathcal{S}}} u^\top \hat{\nu})_{\hat{\mu}} + \gamma_{\hat{\mu}}) \boldsymbol{\sigma}_{\hat{\mu}\hat{\mu}} \, dl \Big).\end{aligned} \tag{4.3.23}$$

Due to the hierarchical ansatz we immediately obtain that the proposed method for nonlinear Naghdi shells degenerates to the linear (4.3.23).

Corollary 4.3.11 (4.3.23) *is the linearization of* (4.3.21)*. In particular, if the initial configuration $\hat{\mathcal{S}}$ is a flat plate, then the TDNNS method for Reissner–Mindlin plates* (2.4.9) *is recovered.*

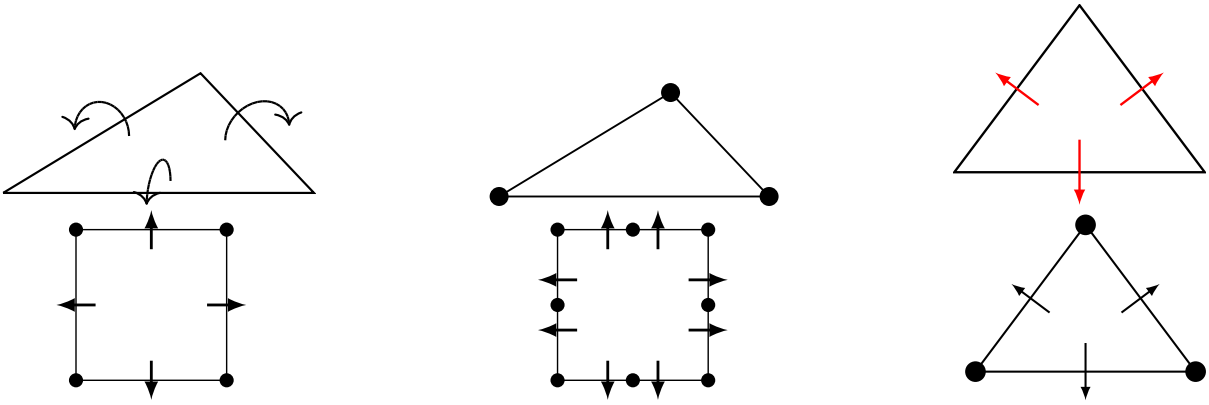

Figure 4.7: Lowest order $H(\mathrm{divdiv})$, H^1 and normal facet elements for the moment, displacement and hybridization variable (top) and lowest order, quadratic hybridized quadrilateral shell element, and Morley triangle element (bottom).

4.3.5 Boundary conditions

Koiter shell

As we use H^1-conforming elements for the displacement field u the Dirichlet boundary condition $u = u_D$ can be used to prescribe the displacement on the boundary. For $\boldsymbol{\sigma} \in H(\mathrm{divdiv})$ we can prescribe the normal-normal component $\boldsymbol{\sigma}_{\hat{\mu}\hat{\mu}}$. For free boundaries homogeneous Dirichlet data, $\boldsymbol{\sigma}_{\hat{\mu}\hat{\mu}} = 0$, are used in combination with the do-nothing Neumann condition for u. If homogeneous Dirichlet data for u and $\boldsymbol{\sigma}$ are prescribed we obtain a simply supported boundary. Do-nothing Neumann conditions for $\boldsymbol{\sigma}$ together with $u = 0$ are used for clamped boundaries. Symmetry boundary conditions can be achieved with the do-nothing Neumann condition for $\boldsymbol{\sigma}$ and the usual symmetry conditions for the displacement field u. By setting non-homogeneous Dirichlet data for $\boldsymbol{\sigma}$ one can prescribe a moment. In the case of a complete discontinuous moment tensor together with the hybridization variable α, the boundary conditions for $\boldsymbol{\sigma}$ have to be incorporated in terms of α, like in the context of plates. Again, the essential and natural boundary conditions swap, i.e., the clamped boundary condition is now set directly as homogeneous Dirichlet data, $\alpha_{\hat{\mu}} = 0$, and the prescribed moment is handled naturally as a right-hand side.

Combining the displacement $u \in \boldsymbol{U}_h^k$, the moment tensor $\boldsymbol{\sigma} \in M_h^{k-1}$ and, eventually, the hybridization space Λ_h^{k-1} leads to the Koiter HHJ shell element. In Figure 4.7 the hybridized lowest order (linear) and quadratic element for quadrilaterals is depicted. The degrees of freedom of the hybridized lowest order triangle shell element are equivalent to the (nonlinear) Morley element.

Naghdi shell

Due to the hierarchical approach additional shearing dofs γ are used. With essential Dirichlet data we can fix the tangential component of the shear in terms of e.g. clamped boundary conditions.

	u	γ	$\boldsymbol{\sigma}$	$\boldsymbol{\sigma}^{\mathrm{dc}}$	α
clamped	D	D	N	-	D
free	N	N	D	-	N
simply supported	D	N	D	-	N
symmetry	$u_{\hat{\mu}} = 0$	N	N	-	D
rigid diaphragm	$u_{\hat{\tau}_E} = u_{\hat{\nu}} = 0$	D	D	-	N

	u	γ	$\boldsymbol{\sigma}$	α
Dirichlet	u	$\gamma_{\hat{\tau}}$	$\boldsymbol{\sigma}_{\hat{\mu}\hat{\mu}}$	$\alpha_{\hat{\mu}}$

Table 4.1: Left: Requirement on spaces for different boundary conditions. D and N correspond to essential zero Dirichlet and homogeneous natural Neumann boundary conditions, respectively. For symmetry the co-normal component of u is fixed whereas for rigid diaphragm only the co-normal component of u is free. Right: Dirichlet components for the fields.

In Table 4.1 (left) the requirements on the different spaces are listed, where the first three columns

correspond to the Naghdi and (by neglecting γ) Koiter shell without hybridization and the last two columns replace the third one when hybridization is considered. The different boundary conditions for the used fields are depicted in Table 4.1 (right).

4.4 Membrane locking

As the thickness t becomes small the shell falls in one of two different categories: the membrane dominated (inhibited pure bending) or bending dominated (non-inhibited pure bending) case [13]. It relies on the specific type of geometry (elliptic, hyperbolic, parabolic), prescribed boundary conditions, and given right-hand side. For complex problems it is therefore difficult to predict the behavior a-priori.

Membrane dominated: In the membrane dominated regime the loading f has to be of magnitude $\mathcal{O}(t)$ to obtain a well-defined limit solution for $t \to 0$. Dividing the shell energy (4.2.12) by t with $f = t\tilde{f}$ ($\tilde{f} = \mathcal{O}(1)$) gives

$$\int_{\mathcal{S}} \frac{1}{2}\|\boldsymbol{E}_{\hat{\mathcal{S}}}\|_{\mathcal{C}}^2 + \frac{t^2}{24}\|\operatorname{sym}(\boldsymbol{F}_{\hat{\mathcal{S}}}^\top \nabla_{\hat{\mathcal{S}}} \boldsymbol{R}(\hat{\nu})) - \nabla_{\hat{\mathcal{S}}}\hat{\nu}\|_{\mathcal{C}}^2 + \frac{\kappa G}{2}|\boldsymbol{F}_{\hat{\mathcal{S}}}^\top \boldsymbol{R}(\hat{\nu})|^2 \, ds - \int_{\hat{\mathcal{S}}} \tilde{f} \cdot u \, ds$$

and we see that the bending energy becomes less important for $t \to 0$, the shell energy is of the form of a perturbed problem. In this setting no locking occurs.

Bending dominated: In the case of a bending dominated regime the right-hand side has to be of order $\mathcal{O}(t^3)$ and thus after dividing through t^3

$$\int_{\mathcal{S}} \frac{1}{2t^2}\|\boldsymbol{E}_{\hat{\mathcal{S}}}\|_{\mathcal{C}}^2 + \frac{1}{24}\|\operatorname{sym}(\boldsymbol{F}_{\hat{\mathcal{S}}}^\top \nabla_{\hat{\mathcal{S}}} \boldsymbol{R}(\hat{\nu})) - \nabla_{\hat{\mathcal{S}}}\hat{\nu}\|_{\mathcal{C}}^2 + \frac{\kappa G}{2t^2}|\boldsymbol{F}_{\hat{\mathcal{S}}}^\top \boldsymbol{R}(\hat{\nu})|^2 \, ds - \int_{\hat{\mathcal{S}}} \tilde{f} \cdot u \, ds$$

we observe that the membrane and shear energies are penalized to be zero in the limit $t \to 0$.

When working with finite elements these pure bending modes can in general only be approximated and thus, will induce non-zero parasitic membrane and/or shear modes. As a result of the penalty the discrete solution tends to be much smaller then expected. This is then called membrane and shear locking. Due to the absence of shearing in the Koiter shell model no shear locking can occur. Further, as discussed in Section 2.4.2 the TDNNS shell model does not suffer from shear locking, thanks to the hierarchical approach and the usage of $H(\operatorname{curl})$-conforming Nédélec elements. Nevertheless, both methods have problems with membrane locking in their current formulations. We will use Regge finite elements, especially the canonical interpolation operator into these elements to avoid membrane locking.

4.4.1 Closer look at membrane locking

We take a closer look at the membrane energy term in the linearized setting for the discrete displacement field $u_h \in \boldsymbol{U}_h^k$

$$\operatorname{sym}(\nabla_{\hat{\mathcal{S}}}^{\text{cov}} u_h) = \operatorname{sym}((\boldsymbol{I} - \hat{\nu} \otimes \hat{\nu}) \nabla_{\hat{\mathcal{S}}} u_h). \tag{4.4.1}$$

On a linear triangulation $\mathcal{T}$ with linear elements, $u_h \in \boldsymbol{U}_h^1$, $\operatorname{sym}(\nabla_{\hat{\mathcal{S}}}^{\text{cov}} u_h)$ is constant, whereas on quadratic curved geometries with quadratic elements the membrane energy is now quadratic as the discrete normal vector varies linearly on each element. Thus, $\operatorname{sym}(\nabla_{\hat{\mathcal{S}}}^{\text{cov}} u_h) \in \mathcal{P}^{2(k-1)}(\mathcal{T}, \mathbb{R}^{3\times 3}_{\text{sym}})$. Taking into account that the membrane strains live only in the tangent space $T\hat{\mathcal{S}}$, as $\hat{\nu}^\top \operatorname{sym}(\nabla_{\hat{\mathcal{S}}}^{\text{cov}} u_h) = \operatorname{sym}(\nabla_{\hat{\mathcal{S}}}^{\text{cov}} u_h)\hat{\nu} = 0$, its dimension is approximately $3(2k-1)k\,\#T$, where $\#T$ denotes the number of triangles of the triangulation.

On the other hand we only have $u_h \in \mathcal{P}^k(\mathcal{T}, \mathbb{R}^3)$ as variable, i.e. $3\#V + 3k(k-1)\#E + \frac{3}{2}(k-1)(k-2)\#T$ degrees of freedom ($\#V$ and $\#E$ denote the number of vertices and edges of $\mathcal{T}$) to fulfill the condition $\|\operatorname{sym}(\nabla_{\hat{\mathcal{S}}}^{\text{cov}} u_h)\|_{\mathcal{C}} = 0$ in the limit $t \to 0$. By the direct computation, using that asymptotically $\#E = 3/2\#T$ and $\#V = 1/2\#T$,

$$3\#V + 3k(k-1)\#E + \frac{3}{2}(k-1)(k-2)\#T \approx (6k^2 - 9k + \frac{9}{2})\#T < 3(2k-1)k\,\#T \tag{4.4.2}$$

we see that this leads to an over-determined system such that $u_h = 0$ might be the only solution. Then locking appears.

From this observation we also see that using higher polynomial degree k can lead to an improvement as it is then easier to coming closer to the zero constraint. Nevertheless, it would be beneficial to have a (low-order) method being robust. In literature different techniques relaxing the kernel constraint, i.e. decreasing the number of constraints, have been proposed. The difficulty is that too much relaxation can inducing zero energy modes, i.e. functions which have nonphysically zero energy.

4.4.2 $H(\mathrm{curlcurl})$ and Regge finite elements

We define the following function space for $d = 2, 3$

$$H(\mathrm{curlcurl}, \Omega) := \{\boldsymbol{\varepsilon} \in L^2(\Omega, \mathbb{R}^{d\times d}_{\mathrm{sym}}) \mid \operatorname{curl}((\operatorname{curl}\boldsymbol{\varepsilon})^\top) \in H^{-1}(\Omega, \mathbb{R}^{(3d-3)\times(3d-3)}_{\mathrm{sym}})\}. \tag{4.4.3}$$

with norm $\|\boldsymbol{\varepsilon}\|^2_{H(\mathrm{curlcurl})} := \|\boldsymbol{\varepsilon}\|^2_{L^2} + \|\operatorname{curl}(\operatorname{curl}\boldsymbol{\varepsilon}^\top)\|^2_{H^{-1}}$. The differential operator $\operatorname{curl}((\operatorname{curl}\boldsymbol{\varepsilon})^\top)$ is called the incompatibility of $\boldsymbol{\varepsilon}$ and denoted by $\operatorname{inc}\boldsymbol{\varepsilon}$.

The Regge finite element space is given by

$$\mathcal{R}^k := \{\boldsymbol{\varepsilon} \in L^2(\Omega, \mathbb{R}^{d\times d}_{\mathrm{sym}}) \mid \text{ for all } T \in \mathcal{T}\ \boldsymbol{\varepsilon}\circ\Phi_T = \boldsymbol{F}^{-\top}\hat{\boldsymbol{\varepsilon}}\boldsymbol{F}^{-1}, \hat{\boldsymbol{\varepsilon}} \in \mathcal{P}^k(\hat{T}, \mathbb{R}^{d\times d}_{\mathrm{sym}}), \boldsymbol{\varepsilon} \text{ is tt-continuous } \}, \tag{4.4.4}$$

which is (like for the HHJ finite element space) a slightly non-conforming subspace of (4.4.3). Here the doubled covariant transformation is used for the mapping from the reference to the physical element. Then the tangential-tangential component is preserved

$$\int_E \frac{1}{J_E}\boldsymbol{\varepsilon}_{t_E t_E}\, dl = \int_{\hat{E}} \frac{1}{J_{\hat{E}}}\hat{\boldsymbol{\varepsilon}}_{\hat{t}_{\hat{E}}\hat{t}_{\hat{E}}}\, dl.$$

The canonical Regge interpolant $\mathcal{I}_h^{\mathcal{R},k} : C^0(\Omega, \mathbb{R}^{d\times d}_{\mathrm{sym}}) \to \mathcal{R}^k$ is determined by the following functionals for a triangle

$$\Psi_E(\boldsymbol{\varepsilon}) = \int_E \frac{1}{J_E}\boldsymbol{\varepsilon} : p\, t_E \otimes t_E\, ds \qquad p \in \mathcal{P}^k(E), \tag{4.4.5a}$$

$$\Psi_T(\boldsymbol{\varepsilon}) = \int_T \frac{1}{J}\boldsymbol{\varepsilon} : FQF^\top\, dx \qquad Q \in \mathcal{P}^{k-1}(T, \mathbb{R}^{2\times 2}_{\mathrm{sym}}). \tag{4.4.5b}$$

Regge finite elements seem to be the natural space for discretizing strain and metric tensors, which have the natural continuity condition of being tangential-tangential continuous (metric lengths and strain stretches).

The relation between Regge and HHJ finite elements is similar to the relation between $H(\mathrm{curl})$-conforming and $H(\mathrm{div})$-conforming elements. Elements in the HHJ space are normal-normal continuous whereas elements in the Regge space are tangential-tangential continuous.

4.4.3 Usage of Regge elements for membrane locking

We will use the Regge finite elements to relax the kernel constraints by inserting the corresponding interpolation operator in the membrane energy part for $u_h \in \boldsymbol{U}_h^k$

$$\|\mathcal{I}_h^{\mathcal{R},k-1}\operatorname{sym}(\nabla^{\mathrm{cov}}_{\hat{\mathcal{S}}} u_h)\|^2_{\mathcal{C}} \tag{4.4.6}$$

reducing the number of constraints to the dimension of the Regge space, namely $k\#E + \frac{3}{2}k(k+1)\#T$. On an infinite triangulation $\mathcal{T}$ there holds in the lowest order case of affine displacements (and constant Regge elements) for the so-called constraint ratio (also denoted constraint count)

$$r = \frac{\#\mathrm{dofs}}{\#\mathrm{constraints}} = \frac{3\#V}{\#E} \approx \frac{\#E}{\#E} = 1. \tag{4.4.7}$$

Here, the number of dofs are given by the three Lagrangian displacement fields at each vertex, involved in the membrane energy, and the number of constraints is the amount of dofs of the Regge space. For Lagrangian elements of polynomial order k and corresponding Regge elements of order $k-1$ the constraint ratio is thus given by

$$r = \frac{3(\#V + (k-1)\#E + \frac{(k-2)(k-1)}{2}\#T)}{k\#E + \frac{3(k-1)k}{2}\#T} = \frac{k^2\#E}{k^2\#E} = 1 \tag{4.4.8}$$

and therefore, the ratio is 1 for arbitrary order. In the continuous setting the constraint ratio is also 1 (three displacement fields and three equations forcing zero membrane energy in the limit $t \to 0$). As a result, (immense) locking ($r < 1$) is not expected. Further relaxation of the constraint would lead to $r > 1$ and thus, the constraints may be underrepresented and possibly spurious energy modes appear. Note that the concept of constraint ratio is not a rigorous mathematical proof whether locking is avoided or not!

Remark 4.4.1 *The Regge interpolation operator would require to solve a global system. However, if the to interpolate function is already tangential-tangential continuous we can apply the interpolant element-wise giving the same result. This makes the method cheap. To prove that* $\operatorname{sym}(\nabla^{\mathrm{cov}}_{\hat{\mathcal{S}}} u_h)$ *is tt-continuous we first notice that* $\nabla_{\hat{\mathcal{S}}} u_h$ *is tangential continuous for* u_h *in the Lagrange finite elements, which are continuous. Also the normal vector* $\hat{\nu}$ *is tangentially continuous and thus the product* $\nabla^{\mathrm{cov}}_{\hat{\mathcal{S}}} u_h = \boldsymbol{P}_{\hat{\mathcal{S}}} \nabla_{\hat{\mathcal{S}}} u_h = (\boldsymbol{I} - \hat{\nu} \otimes \hat{\nu}) \nabla_{\hat{\mathcal{S}}} u_h$ *is at least tt-continuous. Taking the symmetric part of it does not destroy this continuity.*

Exercise 4.4.2 *Show by counting constraints that inserting the element-wise* L^2*-projection operator* $\Pi^{L^2,k-1}$ *in* (4.4.6) *instead of the Regge interpolant does not cure membrane locking. Test it in a numerical example.*

4.5 Boundary layer in shells

If shear dofs are included all plate and shell examples where transversal deflection appears, i.e., except a pure membrane problem, boundary layers of order of the thickness $\mathcal{O}(t)$ may occur. These layers are called short range or "plate layer modes", which are independent of the curvature and thus 1-dimensional.

For shells additional boundary layers of magnitude $\mathcal{O}(\sqrt{t})$ might appear called simple edge effects. In the case of hyperbolic and parabolic geometries layers of order $\mathcal{O}(\sqrt[3]{t})$ and $\mathcal{O}(\sqrt[4]{t})$, respectively, can be induced by a singularity due to the loading, reentering corners, or change of boundary conditions. These layers, sometimes named generalized edge effects, spread along the characteristic lines of the geometry and might be "reflected" at boundaries. Further, they depend also on the curvature of the shell. As a result (at most) two different boundary layers have to be resolved per edge to obtain reliable numerical results.

Chapter 5

Intrinsic Differential Geometry

In Chapter 3 we considered embedded manifolds, mostly surfaces in $\mathbb{R}^3$. Now we will forget the surrounding space and consider general manifolds, which can be equipped with a scalar product such that Riemannian manifolds are given. We investigate and repeat covariant differentiation and curvatures of Riemannian manifolds. In this chapter we stick to smooth fields as preparation for Chapter 6, where the case of an approximated, non-smooth metric is investigated. Recommended books on Riemannian manifolds are e.g. [19, 33, 49, 42]. For finite element exterior calculus (FEEC) standard references are e.g., [3, 1].

5.1 Tensors

Let V be a finite-dimensional vector space with dimension n over $\mathbb{R}$ and denote its dual space with V^*, which members are called covectors. The duality pairing is given by $V^* \times V \to \mathbb{R}$, $(\omega, X) \mapsto \omega(X)$ for $\omega \in V^*$ and $X \in V$.

Definition 5.1.1 *A* covariant k-tensor F*, a* contravariant l-tensor G*, and a mixed tensor of type* (k,l) H *is, respectively, a multilinear mapping*

$$F : \underbrace{V \times \cdots \times V}_{k \text{ copies}} \to \mathbb{R}, \qquad G : \underbrace{V^* \times \cdots \times V^*}_{l \text{ copies}} \to \mathbb{R}, \qquad H : \underbrace{V \times \cdots \times V}_{k \text{ copies}} \times \underbrace{V^* \times \cdots \times V^*}_{l \text{ copies}} \to \mathbb{R}.$$

E.g., there holds for all $X_1, \dots, X_k, Y \in V$, $f, g \in C^\infty(\mathbb{R})$

$$F(X_1, \dots, fX_i + gY, \dots, X_k) = f\, F(X_1, \dots, X_i, \dots, X_k) + g\, F(X_1, \dots, Y, \dots, X_k).$$

We denote with $\mathscr{T}^k(V)$ *the set of all covariant* k*-tensors, with* $\mathscr{T}_l(V)$ *the set of all contravariant* l*-tensors, and with* $\mathscr{T}_l^k(V)$ *the set of all mixed tensors of type* (k,l)*. There holds* $\mathscr{T}_0^k(V) = \mathscr{T}^k(V)$, $\mathscr{T}^0(V) = \mathbb{R}$, $\mathscr{T}^1(V) = V^*$, $\mathscr{T}_1(V) = V^{**} = V$, $\mathscr{T}_1^1(V) = \mathrm{Hom}(V, V)$.

Definition 5.1.2 *The* tensor product $F \otimes G$ *between* $F \in \mathscr{T}_l^k(V)$ *and* $G \in \mathscr{T}_q^p(V)$ *is the* $\mathscr{T}_{l+q}^{k+p}(V)$ *tensor*

$$\begin{aligned}(F \otimes G)(X_1, \dots, X_k, X_{k+1}, \dots, X_{k+p}, \omega_1, \dots, \omega_l, \omega_{l+1}, \dots, \omega_{l+q}) :=\\ F(X_1, \dots, X_k, \omega_1, \dots, \omega_l) G(X_{k+1}, \dots, X_{k+p}, \omega_{l+1}, \dots, \omega_{l+q}).\end{aligned}$$

Let E_i a basis of V and φ^i the corresponding dual basis, i.e., $\varphi^i(E_j) = \delta^i_j$ (δ^i_j denoting the Kronecker delta). Then a tensor $F \in \mathscr{T}_l^k(V)$ can be written in the basis by

$$F = \sum_{j_1, \dots, j_l, i_1, \dots, i_k = 1}^{n} F^{j_1, \dots, j_l}_{i_1, \dots, i_k} \varphi^{i_1} \otimes \cdots \otimes \varphi^{i_k} \otimes E_{j_1} \otimes \cdots \otimes E_{j_l}, \quad F^{j_1, \dots, j_l}_{i_1, \dots, i_k} = F(E_1, \dots, E_k, \varphi^1, \dots, \varphi^l).$$

We will use Einstein summation convention of repeated indices, where we automatically sum over indices which appear as lower and upper index. E.g.,

$$F = F^{j_1, \dots, j_l}_{i_1, \dots, i_k} \varphi^{i_1} \otimes \cdots \otimes \varphi^{i_k} \otimes E_{j_1} \otimes \cdots \otimes E_{j_l}.$$

Definition 5.1.3 *The set of covariant alternating* k*-tensors is denoted by* $\bigwedge^k(V)$ *and call its elements* k*-covectors or (exterior)* k*-forms. The wedge product* $\wedge$ *of 1-forms* $\omega^1, \dots, \omega^k$ *is defined by*

$$\omega^1 \wedge \cdots \wedge \omega^k(X_1, \dots, X_k) = \det(\omega^i(X_j)) \text{ for all } X_1, \dots, X_k \in V.$$

For $\alpha \in \bigwedge^k(V)$ *its degree is* $\deg \alpha = k$*. The* exterior derivative $d^k : \bigwedge^k(V) \to \bigwedge^{k+1}(V)$ *is the unique operator fulfilling*

1. $d^{k+l}(\omega \wedge \tau) = d^k\omega \wedge \tau + (-1)^k \omega \wedge d^l\tau$, *for all* $\omega \in \bigwedge^k(V), \tau \in \bigwedge^l(V)$,
2. $d^{k+1} \circ d^k = 0$,

3. d^0 is the differential d.

The superscript k is often neglected.

Example 5.1.4 *There holds for $\alpha, \beta \in \bigwedge^1(V)$ $(\alpha \wedge \beta)(X_1, X_2) = \alpha(X_1)\beta(X_2) - \alpha(X_2)\beta(X_1)$ and for general forms there holds the anti-commutativity $\alpha \wedge \beta = (-1)^{\deg\alpha \deg\beta}\beta \wedge \alpha$.*

For an n-dimensional differentiable (Hausdorff) manifold M (with countable basis) for a given embedding $\phi : \mathbb{R}^n \to M$ we can define local coordinates at a point $p = \phi(q)$ by $x^i := \phi(q_1, \dots, q_i + t, \dots, q_n)$. Then the partial derivatives $\frac{\partial}{\partial x_i}$ span the tangent space T_pM. We abbreviate the basis vectors by ∂_i and the dual basis co-vectors dx^j. Therefore, each tangent vector $X \in T_pM$ can be written as $X = X^i\partial_i$, where $X^i = dx^i(X)$.

Definition 5.1.5 *At each $p \in M$ we define the cotangent space $T_p^*M := (T_pM)^*$ and denote the cotangent bundle by T^*M. Further we set*

$$\mathscr{T}_l^k M := \bigsqcup_{p\in M} \mathscr{T}_l^k(T_pM), \quad \bigwedge^k M := \bigcup_{p\in M} \bigwedge^k(T_pM).$$

The set of tangent vector fields is therefore $\mathfrak{X}(M) := \mathscr{T}_1(M) = TM$ and the set of differential 1-forms (covector fields) $\mathscr{T}^1M = \bigwedge^1 M = T^*M$.

Denote $\mathcal{D}(M)$ the ring of real valued smooth functions (with point-wise addition and multiplication). The linearity of a tensor field $F \in \mathscr{T}^k(M)$ reads now: for all $X_1, \dots, X_k, Y \in \mathfrak{X}(M)$ and $f, g \in \mathcal{D}(M)$

$$F(X_1, \dots, fX_i + gY, \dots, X_k) = f\,F(X_1, \dots, X_i, \dots, X_k) + g\,F(X_1, \dots, Y, \dots, X_k).$$

Definition 5.1.6 *Let M be a smooth n-dimensional manifold. We call a set of tangent vector fields $(E_1, \dots, E_k)$ a frame if it builds at each point $p \in M$ a basis of T_pM. We call $(\partial_1, \dots, \partial_k)$ the (local) coordinate frame and $(dx^1, \dots, dx^k)$ the dual coframe.*

Remark 5.1.7 (Hairy Ball Theorem) *The Hairy ball theorem states that there exists no non-vanishing continuous vector fields on even-dimensional n-spheres. Thus, the coordinate frame $(\partial_1, \dots, \partial_k)$ can be defined only locally. An atlas of charts has to be used to cover general manifolds.*

Remark 5.1.8 *In local coordinates a vector field $X \in \mathfrak{X}(M)$ can be written in coordinates $X = X^i\partial_i$. One can interpret vector fields as directional derivatives of functions, i.e., $X : \mathcal{D}(M) \to \mathcal{D}(M)$ via $(Xf)(p) = X^i(p)(\partial_i f)(p)$.*

5.2 Riemannian manifolds

Definition 5.2.1 *A Riemannian metric on a smooth manifold M is a 2-tensor field $g \in \mathscr{T}^2(M)$, which is symmetric and positive definite*

$$g(X, Y) = g(Y, X) \text{ for all } X, Y \in \mathfrak{X}(M), \qquad g(X, X) > 0 \text{ for all } 0 \neq X \in \mathfrak{X}(M).$$

It induces a scalar product on the tangent space T_pM, $\langle X, Y\rangle := g(X, Y)$ for $X, Y \in \mathfrak{X}(M)$. We call (M, g) a Riemannian manifold.

Proposition 5.2.2 *Every differentiable manifold (Hausdorff with countable basis) can be equipped by a Riemannian metric.*

We can ask what kind of quantities we can compute using solely the metric tensor. Obviously:

Definition 5.2.3 *The length of a tangent vector $X \in T_pM$ is $\|X\| := \sqrt{g(X, X)}$ and the angle between two tangent vectors is given by $\Theta = \arccos(\frac{g(X,Y)}{\|X\|\|Y\|})$.*

In the local coordinate frame ∂_i the metric tensor reads

$$g = g_{ij} dx^i \otimes dx^j, \qquad g_{ji} = g_{ij} = g(\partial_i, \partial_j)$$

and its inverse $g^{-1} = g^{ij} \partial_i \otimes \partial_j$, where $g^{ij} = (g^{-1})_{ij}$.

With the metric tensor we can identify vector fields and 1-forms by the Riesz-isomorphism.

Definition 5.2.4 *The musical isomorphisms $\flat : \mathfrak{X}(M) \to \Lambda^1(M)$ and $\sharp : \Lambda^1(M) \to \mathfrak{X}(M)$, called* flat *and* sharp*, respectively, are defined for $X \in \mathfrak{X}(M)$ and $\omega \in \Lambda^1(M)$ by*

$$X^\flat(Y) = g(X, Y) \text{ for all } Y \in \mathfrak{X}(M), \qquad \varphi(\omega^\sharp) = g^{-1}(\varphi, \omega) \text{ for all } \varphi \in \bigwedge^1(M). \tag{5.2.1}$$

In coordinates they read

$$X^\flat = g(X^i \partial_i, \cdot) = g_{ij} X^i dx^j =: X_j dx^j, \qquad \omega^\sharp = g^{ij} \omega_j \partial_i =: \omega^i \partial_i. \tag{5.2.2}$$

Thus, the isomorphisms are also called to lower and raise indices.

The inner product of 1-forms $\omega, \varphi \in \Lambda^1(M)$ is given via $g(\omega, \varphi) := g(\omega^\sharp, \varphi^\sharp)$. For two general tensor field $A, B \in \mathscr{T}^k_l(M)$ the inner product is applied component wise by using the linearity and on the basis

$$\begin{aligned} g(\partial_{i_1} \otimes \cdots \otimes \partial_{i_k} \otimes dx^{i_1} \otimes \cdots \otimes dx^{i_k}, &\partial_{j_1} \otimes \cdots \otimes \partial_{j_k} \otimes dx^{j_1} \otimes \cdots \otimes dx^{j_k}) \\ &= g(\partial_{i_1}, \partial_{j_1}) \cdots g(\partial_{i_k}, \partial_{j_k}) g(dx^{i_1}, dx^{j_1}) \cdots g(dx^{i_l}, dx^{j_l}). \end{aligned}$$

Definition 5.2.5 *The* covariant gradient *of a differentiable function $f \in \mathcal{D}(M)$ is the unique vector field such that $(d^0 f)(Y) = g(\operatorname{grad} f, Y)$ for all $Y \in \mathfrak{X}(M)$. Thus, the gradient depends on metric whereas the differential is independent.*

5.2.1 Volume element and integration

Definition 5.2.6 *We call the unique n-form $\operatorname{vol}_{M,g}$ fulfilling $\operatorname{vol}_{M,g}(\partial_1, \ldots, \partial_n) = 1$ the volume form. In coordinates it reads $\operatorname{vol}_{M,g} = \sqrt{\det(g_{ij})}\, dx^1 \wedge \cdots \wedge dx^n$. The integral of a scalar field f on M is defined by*

$$\int_M f := \int_M f \operatorname{vol}_{M,g} := \int_{\phi^{-1}(M)} f \circ \phi \sqrt{\det(g_{ij})} dx^1 \ldots dx^n. \tag{5.2.3}$$

The volume form of the $n-1$-dimensional boundary ∂M with normal vector $\hat{\nu}$ is given by $\operatorname{vol}_{\partial M,g} = l_{\hat{\nu}}(\operatorname{vol}_{M,g}) := \sum_j (-1)^{j-1} \omega^j(\hat{\nu}) \omega^1 \wedge \cdots \wedge \widehat{\omega^j} \wedge \cdots \wedge \omega^n$.

A general k-form $\omega \in \Lambda^k(M)$ can be integrated over k-dimensional boundaries, $\int_D \omega$, where D is a k-dimensional sub-manifold of M.

Theorem 5.2.7 (Stokes) *Let ω be an $n-1$-form and ∂M the boundary of M with outer normal vector $\hat{\nu}$. Further, let $X \in \mathfrak{X}(M)$, $f \in \mathcal{D}(M)$ and $\operatorname{vol}_{M,g}$, $\operatorname{vol}_{\partial M,g}$ the volume forms of M and ∂M. Then there holds the Stokes formulas and integration by parts*

$$\int_M d\omega = \int_{\partial M} \omega, \tag{5.2.4a}$$

$$\int_M \operatorname{div} X \operatorname{vol}_{M,g} = \int_{\partial M} g(X, \hat{\nu}) \operatorname{vol}_{\partial M,g}, \tag{5.2.4b}$$

$$\int_M f \operatorname{div} X \operatorname{vol}_{M,g} = -\int_M g(\operatorname{grad} f, X) \operatorname{vol}_{M,g} + \int_{\partial M} f\, g(X, \hat{\nu}) \operatorname{vol}_{\partial M,g}, \tag{5.2.4c}$$

where the covariant divergence *can be defined as the negative $L^2(M)$-adjoint of the covariant gradient*

$$\int_M f \operatorname{div} X \operatorname{vol}_{M,g} = -\int_M g(\operatorname{grad} f, X) \operatorname{vol}_{M,g}, \qquad \text{for all } X \in \mathfrak{X}(M),\ f \in \mathcal{D}(M).$$

Definition 5.2.8 *The* Hodge star *operator* $\star : \Lambda^k(V) \to \Lambda^{n-k}(V)$ *identifying* k*-forms with* $n-k$*-forms is defined by the equation*

$$\alpha \wedge (\star\beta) = g^{-1}(\alpha, \beta)\,\mathrm{vol}_{M,g}.$$

It fulfills $\star\star\,\omega = (-1)^{k(n-k)}\omega$ for $\omega \in \Lambda^k(M)$.

Exercise 5.2.9 *Define the gradient, divergence, and curl in terms of exterior calculus in 3D via* $\operatorname{grad} f := (df)^\sharp$, $\operatorname{div} v := \star d \star (v^\flat)$, $\operatorname{curl} v := (\star d(v^\flat))^\sharp$, $f \in \mathcal{D}(M)$ *and* $v \in \mathfrak{X}(M)$. *Show that* $\operatorname{curl}\operatorname{grad} f = 0$ *and* $\operatorname{div}\operatorname{curl} v = 0$ *using this notation.*

5.2.2 (Levi-Civita) Connection

To define derivatives of general tensors we need the concept of a connection.

Definition 5.2.10 *Let* M *be a differentiable manifold. A* linear connection *on* M *is a map*

$$\nabla : \mathfrak{X}(M) \times \mathfrak{X}(M) \to \mathfrak{X}(M),\ (X, Y) \mapsto \nabla_X Y$$

such that

1. $\nabla_X Y$ *is linear over* $\mathcal{D}(M)$ *in* X*:* $\nabla_{fX_1+gX_2} Y = f\nabla_{X_1} Y + g\nabla_{X_2} Y$, $f, g \in \mathcal{D}(M)$,
2. $\nabla_X Y$ *is linear over* $\mathbb{R}$ *in* Y*:* $\nabla_X Y(aY_1 + bY_2) = a\nabla_X Y_1 + b\nabla_X Y_2$, $a, b \in \mathbb{R}$,
3. ∇ *satisfies the product rule:* $\nabla_X(fY) = f\nabla_X Y + (Xf)Y$, $f \in \mathcal{D}(M)$.

We call $\nabla_X Y$ *the* covariant derivative of Y in direction X.

Remark 5.2.11 *A linear connection is not a tensor, as it is only* $\mathbb{R}$*-linear in* Y*, not* $\mathcal{D}(M)$*-linear.*

Lemma 5.2.12 *Let* ∇ *be a linear connection and* $X, Y \in \mathfrak{X}(M)$ *expressed in the coordinate frame* $X = X^i\partial_i$, $Y = Y^j\partial_j$. *Then*

$$\nabla_X Y = (X^i \partial_i Y^k + X^i Y^j \Gamma^k_{ij})\partial_k, \tag{5.2.5}$$

where Γ^k_{ij} *are the Christoffel symbols of second kind defined by the equations* $\nabla_{\partial_i}\partial_j = \Gamma^k_{ij}\partial_k$.

Lemma 5.2.13 *Every manifold admits a linear connection, which can be extended uniquely to tensor fields such that*

1. *on* $\mathscr{T}^0(M)$ *it agrees with the ordinary differentiation,* $\nabla_X f = Xf = X^i\partial_i f$,
2. $\nabla_X(F \otimes G) = (\nabla_X F) \otimes G + F \otimes (\nabla_X G)$
3. $\nabla_X(\operatorname{tr}(Y)) = \operatorname{tr}(\nabla_X Y)$,
4. $\nabla_X(\omega(Y)) = (\nabla_X\omega)(Y) + \omega(\nabla_X Y)$ *for all* $\omega \in \Lambda^1(M)$, $X, Y \in \mathfrak{X}(M)$,
5. *let* $F \in \mathscr{T}^k_l(M)$. *Then*

$$\begin{aligned}(\nabla_X F)(Y_1, \ldots, Y_k, \omega^1, \ldots, \omega^l) = X(F(Y_1, \ldots, Y_k, \omega^1, \ldots, \omega^l)) - \sum_{i=1}^{k} F(Y_1, \ldots, \nabla_X Y_i, \ldots, Y_k, \omega^1, \ldots, \omega^l) \\ - \sum_{j=1}^{l} F(Y_1, \ldots, Y_k, \omega^1, \ldots, \nabla_X \omega^j, \ldots, \omega^l),\end{aligned}$$

6. *the function* $\nabla F : \mathfrak{X}(M) \cdots \times \mathfrak{X}(M) \times \Lambda^1(M) \times \cdots \times \Lambda^1(M) \to C^\infty(M)$ *given by*

$$\nabla F(X, Y_1, \ldots, Y_k, \omega^1, \ldots, \omega^l) = \nabla_X F(Y_1, \ldots, Y_k, \omega^1, \ldots, \omega^l)$$

maps the tensor $F \in \mathscr{T}^k_l(M)$ *to a* $(k+1, l)$*-tensor field, called the* total covariant derivative of F.

Example 5.2.14 *∇u is the 1-form du for a smooth function $u \in \mathcal{D}(M)$. The 2-tensor $\nabla^2 u := \nabla(\nabla u)$ is the* covariant Hessian *of u. It holds $\nabla^2 u(Y,X) = Y(Xu) - (\nabla_Y X)u$*

$$\nabla^2 u = u_{;ij} dx^i \otimes dx^j, \qquad u_{;ij} = \partial_j \partial_i u - \Gamma^k_{ji} \partial_k u.$$

For a vector field $Y = Y^i \partial_i$ the components of the (1,1)-tensor field ∇Y are

$$\nabla Y = Y^i_{;j} dx^j \otimes \partial_i, \qquad Y^i_{;j} = \partial_j Y^i + Y^k \Gamma^i_{jk}.$$

More generally, for $F \in \mathscr{T}^k_l(M)$ there holds $\nabla F = F^{j_1 \dots j_l}_{i_1 \dots i_k ; m} dx^m \otimes dx^{i_1} \otimes \dots \otimes dx^{i_k} \otimes \partial_{j_1} \otimes \dots \otimes \partial_{j_l}$ with

$$F^{j_1 \dots j_l}_{i_1 \dots i_k ; m} = \partial_m F^{j_1 \dots j_l}_{i_1 \dots i_k} + \sum_{s=1}^{l} F^{j_1 \dots p \dots j_l}_{i_1 \dots i_k} \Gamma^{j_s}_{mp} - \sum_{s=1}^{k} F^{j_1 \dots j_l}_{i_1 \dots p \dots i_k} \Gamma^{p}_{m i_s} \tag{5.2.6}$$

The covariant derivative of a 1-form ω reads in coordinates

$$\nabla_X \omega = (X^i \partial_i \omega_k - X^i \omega_j \Gamma^j_{ik}) dx^k.$$

Definition 5.2.15 *A linear connection ∇ is* compatible with the metric g *if for all $X, Y, Z \in \mathfrak{X}(M)$*

$$\nabla_X g(Y,Z) = g(\nabla_X Y, Z) + g(Y, \nabla_X Z),$$

i.e., $\nabla g = 0$.

Lemma 5.2.16 *For $X, Y \in \mathfrak{X}(M)$ the* Lie-bracket *defined by $[X,Y]f = X(Yf) - Y(Xf)$ for all $f \in \mathcal{D}(M)$ is a vector field, $[X,Y] \in \mathfrak{X}(M)$.*

Exercise 5.2.17 *Proof that $Z := [X,Y]$ is a vector field, but that $X(Yf)$ and $Y(Xf)$ alone are not (Hint: how does the terms look like in coordinates?). Further, show that $[X,Y] = -[Y,X]$, $[X, fY] = X(f)Y + f[X,Y]$, and the Jacobi identity $[X,[Y,Z]] + [Z,[X,Y]] + [Y,[Z,X]] = 0$.*

Definition 5.2.18 *The torsion tensor $T \in \mathscr{T}^2_1(M)$ is defined by $T(X,Y) = \nabla_X Y - \nabla_Y X - [X,Y]$, where $[X,Y] \in \mathfrak{X}(M)$ denotes the Lie-bracket. A linear connection is called* symmetric *or* torsion free *if*

$$\nabla_X Y - \nabla_Y X \equiv [X,Y].$$

Remark 5.2.19 *In a coordinate system there holds for a symmetric connection ∇*

$$\nabla_{X_i} X_j - \nabla_{X_j} X_i = [X_i, X_j] = 0, \quad X_i = \partial_i,$$

which is equivalent to the symmetry of the Christoffel symbols, $\Gamma^k_{ij} = \Gamma^k_{ji}$.

Theorem 5.2.20 (Fundamental Lemma of Riemannian Geometry) *Let (M,g) be a Riemannian manifold. There exists a unique linear connection ∇ on M which is compatible with g and symmetric. This connection is called the* Riemannian connection *or* Levi–Civita connection *of g.*

Remark 5.2.21 (Koszul's formula) *There holds the Koszul formula for the Levi–Civita connection*

$$g(\nabla_X Y, Z) = \frac{1}{2}\big(Xg(Y,Z) + Yg(Z,X) - Zg(X,Y) - g(Y,[X,Z]) - g(Z,[Y,X]) + g(X,[Z,Y])\big).$$

From it, we can deduce the identities

$$\Gamma_{ijk} := \Gamma^l_{ij} g_{lk} = \frac{1}{2}\big(\partial_i g_{jk} + \partial_j g_{ki} - \partial_k g_{ij}\big), \qquad \Gamma^k_{ij} = \frac{1}{2}\big(\partial_i g_{jp} + \partial_j g_{pi} - \partial_p g_{ij}\big) g^{pk},$$

where Γ_{ijk} are the Christoffel symbols of first kind *and Γ^k_{ij} the* Christoffel symbols of second kind.

Lemma 5.2.22 *The musical isomorphisms commute with the Levi-Civita connection, $\nabla(F^\flat) = (\nabla F)^\flat$ and $\nabla(F^\sharp) = (\nabla F)^\sharp$.*

Definition 5.2.23 *The trace of a tensor is the contraction of its first two indices. E.g., for a $(0,2)$-tensor $\mathrm{tr}(\sigma) = \mathrm{tr}_{12}\sigma = g^{ij}\sigma_{ij}$. The covariant divergence of a tensor can be defined as taking first the covariant derivative and then using the trace, $\mathrm{div} F := \mathrm{tr}_{12}(\nabla F)$. The Laplace-Beltrami operator of a function $u \in \mathcal{D}(M)$ is defined as $\Delta u := \mathrm{div}(\nabla u) = \mathrm{tr}_{12}\nabla^2 u$.*

5.2.3 Curvature

After having defined derivatives on Riemannian manifolds we can investigate curvatures of the manifold.

Definition 5.2.24 *Let (M, g) be a Riemannian manifold. The* (Riemann) curvature endomorphism *is the $(3,1)$-tensor field $R : \mathfrak{X}(M) \times \mathfrak{X}(M) \times \mathfrak{X}(M) \to \mathfrak{X}(M)$ defined by*

$$R(X,Y)Z = \nabla_X \nabla_Y Z - \nabla_Y \nabla_X Z - \nabla_{[X,Y]} Z.$$

The (Riemann) curvature tensor *is the covariant 4-tensor $\mathcal{R} = R^\flat \in \mathscr{T}_0^4(M)$ with action and coordinates*

$$\mathcal{R}(X,Y,Z,W) = g(R(X,Y)Z,W), \qquad R_{ijkl} = \partial_i \Gamma_{jkl} - \partial_j \Gamma_{ikl} - \Gamma_{ilp}\Gamma^p_{jk} + \Gamma_{jlp}\Gamma^p_{ik}.$$

Note, that in contrast to the Christoffel symbols the Riemann curvature tensor is a tensor, i.e., its values depend only at the point $p \in M$ and not on an environment of p (exercise!). A Riemannian manifold is flat if and only if its curvature tensor vanishes identically.

Lemma 5.2.25 *There holds for the Riemann curvature tensor the following (skew-)symmetry properties and identities*

1. $\mathcal{R}(X,Y,Z,W) = -\mathcal{R}(Y,X,Z,W)$, $R_{ijkl} = -R_{jikl}$,
2. $\mathcal{R}(X,Y,Z,W) = -\mathcal{R}(Y,X,W,Z)$, $R_{ijkl} = -R_{ijlk}$,
3. $\mathcal{R}(X,Y,Z,W) = \mathcal{R}(Z,W,X,Y)$, $R_{ijkl} = R_{klij}$,
4. $\mathcal{R}(X,Y,Z,W) + \mathcal{R}(Y,Z,X,W) + \mathcal{R}(Z,X,Y,W) = 0$, $R_{ijkl} + R_{ikjl} + R_{jikl} = 0$ *(Bianchi identity),*
5. $\nabla\mathcal{R}(X,Y,Z,V,W) + \nabla\mathcal{R}(X,Y,V,W,Z) + \nabla\mathcal{R}(X,Y,W,Z,V) = 0$ *(2nd Bianchi identity).*

Definition 5.2.26 *The* Ricci tensor *Rc, which is a symmetric 2-tensor, is defined by the contraction of the Riemann curvature operator with the metric tensor, in coordinates*

$$R_{ij} := R_{kij}{}^k = g^{km} R_{kijm}$$

and the scalar curvature *by taking another trace*

$$S = \operatorname{tr}(Rc) = R_i{}^i = g^{ij} R_{ij}.$$

Definition 5.2.27 *Let (X,Y) be any basis of a 2-plane $\Pi \subset T_pM$. Then the* sectional curvature *defined by*

$$K(X,Y) = \frac{\mathcal{R}(X,Y,Y,X)}{\|X\|^2\|Y\|^2 - g(X,Y)^2} \tag{5.2.7}$$

is independent of the chosen basis. For a two-dimensional manifold K is the Gauss curvature.

For two-dimensional manifolds there holds $K = \frac{1}{2}S$.

5.2.4 Geodesics

Next, we consider the intrinsic curvature of curves on Riemannian manifolds.

Definition 5.2.28 *Let $c : [a,b] \to M$ be a smooth parameterized curve in a manifold M. A vector field along the curve c is a function $V : [a,b] \to \bigsqcup_{t\in[a,b]} T_{c(t)}M$ such that $V(t) \in T_{c(t)}M$. The vector space of all vector field along $c(t)$ are denoted by $\Gamma(TM|_{c(t)})$.*

Lemma 5.2.29 *Let M be a manifold with linear connection ∇ and $c : [a,b] \to M$ a smooth curve in M. Then there is a unique map $\frac{D}{dt} : \Gamma(TM|_{c(t)}) \to \Gamma(TM|_{c(t)})$ such that for $V \in \Gamma(TM|_{c(t)})$*

1. *$\frac{DV}{dt}$ is $\mathbb{R}$-linear in V,*

2. *for any* $f \in C^\infty([a,b])$ *there holds the Leibnitz rule:* $\frac{D(fV)}{dt} = \frac{df}{dt}V + f\frac{DV}{dt}$,

3. *if* V *is induced from* $\tilde{V} \in \mathfrak{X}(M)$ *such that* $V(t) = \tilde{V}_{c(t)}$ *then* $\frac{DV}{dt}(t) = \nabla_{c'(t)}\tilde{V}$.

$\frac{DV}{dt}$ *is called the* covariant derivative *(associated to* ∇*) of the vector field* V *along the curve* $c(t)$ *in* M. *If* ∇ *is compatible with the metric there holds the Leibnitz rule* $\frac{d}{dt}g(V,W) = g(\frac{DV}{dt}, W) + g(V, \frac{DW}{dt})$.

Definition 5.2.30 *Let* M *be a manifold with a linear connection* ∇. *A parameterized curve* $c : I \to M$ *is a* geodesic *if the covariant derivative* $\frac{DT}{dt}$ *of its velocity vector field* $T(t) = c'(t)$ *is zero. If* M *is a Riemannian manifold than the speed* $\|c'(t)\| = \sqrt{g(c'(t), c'(t))}$ *of a geodesic is constant.*

In a chart (U, ϕ) the curve $c : [a,b] \to M$ has the coordinates $y(t) := (\phi \circ c)(t) = (x^1(c(t)), \ldots, x^n(c(t)))$ and $y^i(t) = (x^i \circ c)(t)$. With $\dot{y}^i := \frac{dy^i}{dt}$ the covariant derivative of the velocity field is

$$T(t) = c'(t) = \dot{y}^i \partial_{i,c(t)} \qquad \frac{DT}{dt}(t) = \ddot{y}^i\partial_i + \dot{y}^i \nabla_{c'(t)}\partial_i = \ddot{y}^i\partial_i + \dot{y}^i\nabla_{\dot{y}^j\partial_j, c(t)}\partial_i = (\ddot{y}^k + \dot{y}^i\dot{y}^j\Gamma^k_{ij})\partial_k.$$

Thus, $c(t)$ is a geodesic at $c(a) = p \in M$ with $c'(a) = X \in T_pM$ if the following system of (nonlinear) differential equations are fulfilled (which is -locally- guaranteed by the Picard–Lindelöf theorem)

$$\ddot{y}^k + \dot{y}^i\dot{y}^j\Gamma^k_{ij} = 0, \qquad k = 1, \ldots, n. \tag{5.2.8}$$

Definition 5.2.31 *A smooth vector field* $V(t)$, $t \in I$, *along a curve* c *is* parallel *if* $\frac{DV}{dt} \equiv 0$ *on* I.

If $V(t)$ *is parallel along a curve* $c : [a,b] \to M$ *then we say that* $V(b)$ *is obtained from* $V(a)$ *by* parallel translation *along* c *or that* $V(b)$ *is the* parallel translate *or* parallel transport *of* $V(a)$ *along* c.

Lemma 5.2.32 *Let* M *be a manifold with a connection* ∇ *and let* $c : [a,b] \to M$ *be a smooth curve in* M. *Parallel translation is possible from* $c(a)$ *to* $c(b)$ *along* c. *I.e., for given vector* $v_0 \in T_{c(a)}M$ *there exists a parallel vector field* $V(t)$ *along* c *such that* $V(a) = v_0$. *On a Riemannian manifold parallel translation preserves length and inner product. If* $V(t)$ *and* $W(t)$ *are parallel vector fields along* c *then* $\|V(t)\|$, $\|W(t)\|$, *and* $g(V(t), W(t))$ *are constant for all* $t \in [a,b]$.

Definition 5.2.33 *Let* M *be a manifold with linear connection. For* $p \in M$ *and* $v \in T_pM$ *denote by* $\gamma_v(t,p)$ *the unique maximal geodesic with initial point* p *and initial vector* $\gamma_v'(0,p) = v$. *If* $\gamma_v(1,p)$ *is defined, set* $\mathrm{Exp}_p(v) = \gamma_v(1,p)$. *Let* M *be a Riemannian manifold. Then the exponential map* $\mathrm{Exp}_p : T_pM \supset B(0,\varepsilon) \to M$ *is well defined for a real number* $\varepsilon > 0$.

Proposition 5.2.34 *The differential of the exponential map at the origin is the identity map* $\mathrm{id} : T_pM \to T_pM$. *There is a neighborhood* V *of* 0 *in* T_pM *and* U *of* p *in* M *such that* $\mathrm{Exp}_p : V \to U$ *is a diffeomorphism.*

Definition 5.2.35 *The coordinate system in* U *obtained by starting with an orthonormal basis for* T_pM *and transferring with the exponential map is called normal neighborhood and the coordinates are called (Riemann) normal coordinates on* U.

Theorem 5.2.36 *In a normal neighborhood* U *of* p, *all partial derivatives of* g_{ij} *and all Christoffel symbols* Γ^k_{ij} *vanish at* p *(not in a neighborhood of* p*!),* $\Gamma^k_{ij} = 0$, *and the metric is the identity,* $g_{ij} = \delta_{ij}$.

Exercise 5.2.37 *Prove with Riemann normal coordinates that* $(\Delta f)(p) = \sum_i E_i(E_i(f))(p)$ *and that the product rule* $\Delta(f\,g) = f\Delta g + g\Delta f + 2g(\mathrm{grad}\, f, \mathrm{grad}\, g)$ *holds also for the covariant differential operators.*

Definition 5.2.38 *In a Riemannian manifold* M *the length of a tangent vector* $X_p \in T_pM$ *is* $\|X_p\| = \sqrt{g(X_p, X_p)}$. *For a parameterized curve* $c : [a,b] \to M$ *its arc length is given by* $l(c) = \int_a^b \|c'(t)\|\, dt$.

Definition 5.2.39 *Consider a unit-speed curve* $\gamma(s) : [a,b] \to M$ *in a Riemannian manifold* M *and* $T(s) = \gamma'(s)$. *The magnitude* $\tilde{\kappa}_g = \|\frac{DT}{ds}\|$ *is the geodesic curvature of* $\gamma(s)$.

Let M *be two-dimensional. Choose a unit vector field* $n(s)$ *along the curve such that* (T, n) *is positively oriented and orthonormal. The signed geodesic curvature at a point* $\gamma(s)$ *of a unit-speed curve in an oriented Riemannian 2-manifold* $\kappa_g(s)$ *is such that* $\frac{DT}{ds} = \kappa_g n$, *i.e.,* $\kappa_g = g(\frac{DT}{ds}, n)$.

5.2.5 Gauss–Bonnet

Let P be a polygon on an oriented two-dimensional manifold M with a piece-wise smooth closed curve $\gamma : [a, b] \to M$. Let $\gamma(s_0), \gamma(s_1), \ldots, \gamma(s_m)$ be the vertices of the curve with $s_0 = a, s_m = b$, and $\gamma(a) = \gamma(b)$. Further assume that γ has unit-speed except at the vertices. In a neighborhood of $\gamma(s_i)$ the curve is a union of two 1-dimensional manifolds. Let $\gamma'(s_i^-)$ be the outward-pointing tangent vector at $\gamma(s_i)$ of the incoming curve and $\gamma'(s_i^+)$ be the inward-pointing tangent vector of the outgoing curve, see Figure 5.1. The angle $\epsilon_i \in (-\pi, \pi)$ from the incoming tangent vector $\gamma'(s_i^-)$ to the outgoing tangent vector $\gamma'(s_i^+)$ is the *jump angle* at $\gamma(s_i)$. The *interior angle* at $\gamma(s_i)$ is given by $\beta_i := \pi - \epsilon_i$.

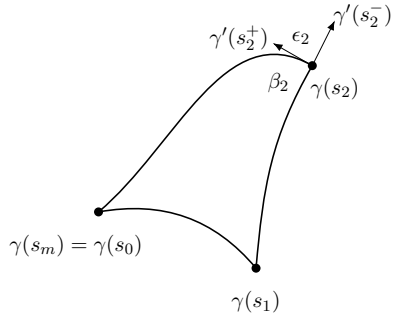

Figure 5.1: Jump angle of a polygon.

Theorem 5.2.40 (Gauss–Bonnet formula for a polygon) *Let γ be a curved polygon on an oriented Riemannian 2-manifold (M, g), and γ is positively oriented as the boundary of an open set Ω with compact closure. Then*

$$\int_\Omega K \operatorname{vol}_{\Omega,g} + \int_\gamma \kappa_g \operatorname{vol}_{\gamma,g} + \sum_i \epsilon_i = 2\pi, \tag{5.2.9}$$

where K is the Gauss curvature of g, κ_g the geodesic curvature of γ, and ϵ_i the jump angle at the vertices.

Definition 5.2.41 *The Euler-characteristic of a 2-manifold M is given by*

$$\chi(M) = V - E + F, \tag{5.2.10}$$

where V, E, F denote the number of vertices, edges, and faces of a triangulation of M and is independent of the chosen triangulation.

If M is a compact orientable surface of genus G (roughly speaking the number of holes of M) then $\chi(M) = 2 - 2G$. E.g., the surface of a sphere has genus 0, whereas that of a torus has genus 1.

Theorem 5.2.42 (Gauss–Bonnet Theorem) *If M is a compact oriented Riemannian 2-manifold, then*

$$\int_M K \operatorname{vol}_{M,g} = 2\pi\chi(M). \tag{5.2.11}$$

If M is a compact oriented Riemannian 2-manifold with boundary ∂M and the boundary positively oriented, then

$$\int_M K \operatorname{vol}_{M,g} + \int_{\partial M} \kappa_g \operatorname{vol}_{\partial M,g} = 2\pi\chi(M). \tag{5.2.12}$$

Exercise 5.2.43 *Proof that the Torsion tensor $T(X, Y)$ from Definition 5.2.18 is $\mathcal{D}(M)$-linear in X and Y and thus in fact a tensor. Check that the Riemann curvature tensor from Definition 5.2.24 is a tensor.*

Exercise 5.2.44 *Proof with the Gauss–Bonnet theorem that a compact orientable 2-dimensional Riemannian manifold, which has positive Gauss curvature K everywhere is diffeomorphic to a sphere.*

Exercise 5.2.45 *Show that for a geodesic triangle T, i.e. a triangle which edges have zero geodesic curvature, the sum of interior angles is smaller, equal, bigger than π if $K < 0$, $K > 0$, $K = 0$ everywhere on T, respectively.*

Chapter 6

Intrinsic curvature approximation with Regge elements

In the previous chapter we found that the intrinsic curvature of a Riemannian manifold is encoded in the Riemann curvature tensor $\mathcal{R}$. In 2D this information is equivalent to the Gauss-curvature K due to the (skew-) symmetry properties of the Riemann curvature tensor. Looking at its coordinate form we see that second order derivatives as well as products of first derivatives in the metric tensor g are involved. Thus, $g \in C^2(M, \mathbb{R}^{2\times 2}_{\text{sym}})$ is needed to compute the curvature in classical sense. We are interested, however, in the case where the metric tensor is not differentiable, even not completely continuous and ask how to compute the curvature in this setting and how good does it approximate the real curvature if the non-smooth g approximates a smooth Riemannian metric $\overline{g}$, i.e.,

$$\|K_h(g) - K(\overline{g})\| \leq ?$$

A second question is how we can compute geodesics on g and how good is the convergence of these approximated geodesics?

We follow in this chapter the works [34, 24, 23, 8, 22].

6.1 Discrete metric via Regge elements

We assume $(M, \overline{g})$ with $M = \Omega \subset \mathbb{R}^2$ a two-dimensional smooth Riemannian manifold. Further, let $\mathcal{T}$ be a triangulation of Ω. The simplest form to describe a two-dimensional metric on $\mathcal{T}$ is to prescribe the (quadratic) lengths of $\overline{g}$ at the edges. This means, we assign to each edge $E \in \mathcal{E}$ the value $\int_E \overline{g}_{\tau\tau}\, ds$. If $\mathcal{T}$ is fine enough (e.g. quasi uniform with mesh-size h sufficiently small) the triangle inequality is fulfilled (symmetry and positive definiteness are obvious) such that a valid metric g approximating $\overline{g}$ is given, see Figure 6.1.

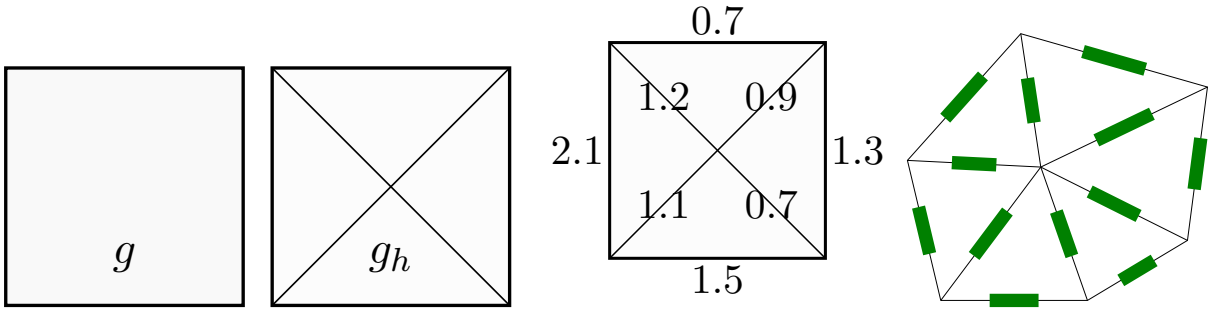

Figure 6.1: Approximating a smooth metric by prescribing the edge lengths of the underlying triangulation.

The approximated metric g can be identified with a symmetric piece-wise constant 2×2 matrix, which is tangential-tangential continuous, i.e. $g|_{T_L}(X, X) = g|_{T_R}(X, X)$ for all $X \in TE$, $E \in \mathcal{E}$. Thus, g is in the lowest order Regge finite element space (4.4.4), $g \in \mathcal{R}^0$. We can hope that for a high-order Regge metric $g \in \mathcal{R}^k$ gives a better approximation of the exact metric tensor $\overline{g}$, compare Section 4.4.2 for the definition of the Regge elements. Note, that we again have to assume that the triangulation is fine enough to guarantee that g is positive definite to induce a scalar product.

6.2 Approximation of geodesic curvature

From the previous chapter we know that in the smooth setting a curve $\gamma : [a, b] \to M$ is a geodesic if it fulfills the system of ODEs

$$\ddot{\gamma}^k + \dot{\gamma}^i \dot{\gamma}^j \Gamma^k_{ij} = 0, \qquad k = 1, \ldots, n \tag{6.2.1}$$

with appropriate initial conditions. If the underlying metric g is in $\mathcal{R}^k$, however, g is only piece-wise smooth and tangential-tangential continuous over elements. Therefore, we need to derive conditions how to handle the case when a geodesic hits an edge. If the curve hits a vertex, i.e., an $N-2$-dimensional boundary of M this is known as pathology and the algorithm would break down. However, one can

always perturb the geodesics around machine precision such that the discrete geodesics will never touch a vertex.

The length of a piece-wise smooth function $\gamma : [a, b] \to M$ is given by

$$L(\gamma) := \sum_{i=0}^{n-1} \int_{t_i}^{t_{i+1}} \sqrt{g_{ij}(\gamma(s))\dot{\gamma}^i(s)\dot{\gamma}^j(s)}\, ds. \tag{6.2.2}$$

It is known that geodesics can be (locally) characterized by its minimality property being the shortest curve. Thus, we define the energy functional

$$E(\gamma) := \frac{1}{2} \sum_{i=0}^{n-1} \int_{t_i}^{t_{i+1}} g_{ij}(\gamma(s))\dot{\gamma}^i(s)\dot{\gamma}^j(s)\, ds. \tag{6.2.3}$$

With this definition is is easy to show that geodesics are critical points of energy E. The following theorem shows under which condition a curve on a Regge metric is a geodesic. A proof can be found in [34, Theorem 3.2]. The arising normal and tangential vectors have to be understood with respect to the metric g. For example in 2D, if (τ, ν) are the Euclidean tangential and normal vectors at a facet F then the g-orthonormal tangential and normal vectors $(\hat{\tau}, \hat{\nu})$ can be expressed in coordinates (Exercise!)

$$\hat{\tau}^i = \frac{1}{\sqrt{g_{jk}\tau^j\tau^k}}\tau^i, \qquad \hat{\nu}^i = \frac{1}{\sqrt{g^{kl}\nu_k\nu_l}} g^{ij}\nu_j. \tag{6.2.4}$$

Theorem 6.2.1 *Let $\mathscr{T}$ be a triangulation of an N-dimensional Riemannian manifold $(M, \overline{g})$ and g a piece-wise smooth and tangential-tangential continuous metric approximating $\overline{g}$. A piece-wise smooth curve $\gamma : [a, b] \to \mathscr{T}$ which does not intersect any interior faces of dimension $\leq (N-2)$ is a local geodesic if and only if it satisfies the geodesic equation inside each element and at each point p where γ intersects a facet F, there holds*

$$g^+_{ij}\dot{\gamma}^i_+\hat{\tau}^j = g^-_{ij}\dot{\gamma}^i_-\hat{\tau}^j, \qquad g^+_{ij}\dot{\gamma}^i_+\hat{\nu}^j_+ = -g^-_{ij}\dot{\gamma}^i_-\hat{\nu}^j_-.$$

Especially, its kinematic energy $g_{ij}\dot{\gamma}^i\dot{\gamma}^j$ is constant along any local geodesic (even when the curve crosses a facet).

From this characterization we obtain an explicit update formula how the geodesic should change when crossing a facet.

Corollary 6.2.2 *Assume that g is piece-wise smooth and tangential-tangential continuous, and γ crosses an interior facet F. Then at point $p \in F$ the value of $\dot{\gamma}^i$ satisfies the update formula*

$$\dot{\gamma}^i_- = \dot{\gamma}^i_+ - (g^+_{ij}\dot{\gamma}^j_+\hat{\nu}^k_+)(\hat{\nu}^i_+ + \hat{\nu}^i_-). \tag{6.2.5}$$

The following result predicts convergence of the approximated geodesics for Regge metrics if the algorithm does not break-down, cf. [34, Theorem 3.6].

Theorem 6.2.3 (Convergence of geodesics) *Let M be a domain in $\mathbb{R}^n$ and $\mathscr{T}_h$ a family of triangulations of M with mesh-size h. Assume that $\overline{g}$ is a smooth Riemannian metric on M and $g_h \in \mathcal{R}^k(\mathscr{T}_h)$ a family of Regge metric fulfilling $\|\overline{g} - g_h\|_{L^\infty} \leq \frac{1}{2}\|\overline{g}^{-1}\|^{-1}_{L^\infty}$ uniformly in h. Let $\gamma : [0, T] \to M$ be a smooth geodesic with respect to $\overline{g}$ and γ_h a family of geodesics with respect to g_h with the same initial conditions as γ. Further assume that the discrete algorithm does not break down and the "no-stuck" condition: There exists a constant $C_s > 0$ such that the time γ_h needs to traverse a cell is bounded by h/C_s uniformly for all cells and h. Then, there exists a constant $C = C(\|\overline{g}\|_{W^{2,\infty}}, \|\overline{g}^{-1}\|_{L^\infty}, C_s, T, |\dot{\gamma}(0)|)$ such that*

$$|\dot{\gamma}(t) - \dot{\gamma}_h(t)| \leq C\big(\|\overline{g} - g_h\|_{W^{1,\infty}(\mathscr{T}_h)} + h^{-1}\|\overline{g} - g_h\|_{L^\infty}\big),$$
$$|\gamma(t) - \gamma_h(t)| \leq C\big(h\|\overline{g} - g_h\|_{W^{1,\infty}(\mathscr{T}_h)} + \|\overline{g} - g_h\|_{L^\infty}\big).$$

If g_h is the canonical Regge interpolant of $\overline{g}$, $g_h = \mathcal{I}_h^{\mathcal{R},k}\overline{g}$, then we obtain

$$|\dot{\gamma}(t) - \dot{\gamma}_h(t)| \leq Ch^k, \qquad |\gamma(t) - \gamma_h(t)| \leq Ch^{k+1}.$$

The Hamiltonian for geodesics is given by

$$H(p,q) := \frac{1}{2} g^{ij}(q) p_i p_j, \tag{6.2.6}$$

where $q \in M$ and $p \in T_q^* M$ such that $(p,q) \in T^*M$ are in the cotangent bundle. The corresponding equations are

$$\begin{aligned} \dot{q}^i &= \frac{\partial H}{\partial p^i} = g^{ij} p_j, \\ \dot{p}_i &= -\frac{\partial H}{\partial q^i} = -\frac{1}{2} p_j p_k \partial_i g^{jk} = \frac{1}{2} p_j p_k g^{j\alpha} \partial_i g_{\alpha\beta} g^{\beta k}. \end{aligned} \tag{6.2.7}$$

With the substitution $\gamma(t) = q(t)$ and $\dot{\gamma} = g^{ij} p_j$ the Hamiltonian equations are equivalent to the geodesic equations. Thus, local geodesics on a (smooth) Riemannian manifold is a Hamiltonian flow on the cotangent bundle, such that symplectic integrators are feasible.

Exercise 6.2.4 *The Poincare disc is given by the metric* $ds = \frac{4(dx\otimes dx + dy \otimes dy)}{(1-|z|^2)^2} = \frac{4(dx\otimes dx + dy \otimes dy)}{(1-x^2-y^2)^2}$ *on* $M = \{(x,y) \in \mathbb{R}^2 \,|\, x^2 + y^2 < 1\}$. *The Poincare half-plane* (H, g) *with* $H = \{(x,y) \in \mathbb{R}^2 \,|\, y > 0\}$ *and* $g = \frac{dx \otimes dx + dy \otimes dy}{y^2}$.

Compute geodesics with respect to the exact metric by solving the geodesic equations. Interpolate the metric into the Regge space and compute the discrete geodesics.

6.3 The angle deficit

We learned in the smooth setting that the curvature information of a Riemannian manifold is encoded by the Riemann curvature tensor. Is there a possibility to indicate curvature of the approximated Riemannian manifold (Ω, g) consisting of piece-wise flat elements, where the Riemann curvature tensor is piece-wise zero? We can embed (Ω, g) isometrically in $\mathbb{R}^3$ by using $\int_E g_{\tau\tau}\, ds$ as the real lengths of the edges, such that the triangulation is in general globally not flat anymore, illustrated in Figure 6.2.

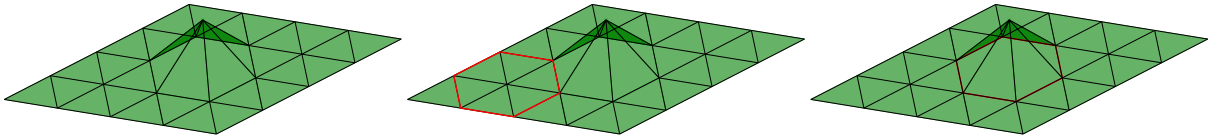

Figure 6.2: Non-flat surface consisting of piece-wise flat triangles.

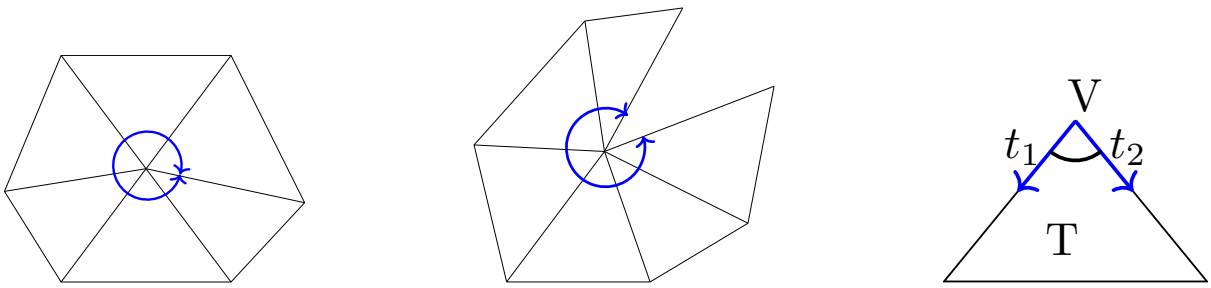

Figure 6.3: Angle deficit.

Considering a vertex patch of a flat part we observe that the sum of the inner angles is 2π, whereas on a curved (non-flat) vertex patch the angles differ from 2π. The difference is called angle deficit (or angle defect), denoted by $\sphericalangle_V(g) := 2\pi - \sum_{T \in \mathscr{T}: V \in T} \sphericalangle_V^T(g)$ for $V \in \mathcal{V}$ and is frequently used in curvature approximations of affine triangulations. We call a discrete Riemannian manifold locally

- flat if $\sphericalangle_V(g) = 0$,

- positively curved if $\sphericalangle_V(g) > 0$,
- negatively curved if $\sphericalangle_V(g) < 0$.

Thus, the curvature information sits in the vertices of the triangulation and motivates to define a measure valued (or distributional) curvature operator acting on linear Lagrangian finite elements (the hat functions):

Definition 6.3.1 *The distributional, or measure valued Gauss curvature for the lowest order Regge metric, $g \in \mathcal{R}^0(\mathscr{T})$ on the triangulation $\mathscr{T}$ is defined for $v_h \in U_h^1(\mathscr{T})$ as*

$$\langle K_h(g), v_h\rangle := \sum_{V\in\mathcal{V}} \sphericalangle_V(g) v_h(V) = \sum_{V\in\mathcal{V}} \Big(2\pi - \sum_{T\in\mathcal{T}:V\in T} \sphericalangle_V^T(g)\Big) v_h(V) \tag{6.3.1}$$

$$= \sum_{V\in\mathcal{V}} \sum_{T\in\mathcal{T}:V\in T} (\sphericalangle_V^T(\delta) - \sphericalangle_V^T(g)) v_h(V) = \sum_{T\in\mathcal{T}} \sum_{V\in\mathcal{V}:V\in T} (\sphericalangle_V^T(\delta) - \sphericalangle_V^T(g)) v_h(V), \tag{6.3.2}$$

where δ denotes the identity tensor.

To visualize this distribution we can compute an L^2-representative (a projection into the Lagrangian finite elements) by solving with the mass matrix. On the boundary of the domain we assume that the exact curvature is known and serves as Dirichlet boundary data.

Definition 6.3.2 (Curvature via angle deficit) *Let $g \in \mathcal{R}^0$ with $\det g > 0$ and $g_{\tau\tau} > 0$ and let $K(\overline{g}) = 0$ on $\partial\Omega$. The lifted distributional curvature $K_h(g) \in U_{h,0}^1$ is the solution of*

$$\int_\Omega K_h(g)\, v_h \sqrt{\det g}\, dx = \langle K_h(g), v_h\rangle, \qquad \text{for all } v_h \in U_{h,0}^1. \tag{6.3.3}$$

Exercise 6.3.3 *Consider the following metric tensor $\overline{g}$ on $\Omega = (-1,1)^2$ with Gauss curvature $K(\overline{g})$*

$$\overline{g} = \begin{pmatrix} 1 + (x - \frac{x^3}{3})^2 & (x - \frac{x^3}{3})(y - \frac{y^3}{3}) \\ (x - \frac{x^3}{3})(y - \frac{y^3}{3}) & 1 + (y - \frac{y^3}{3})^2 \end{pmatrix}, \qquad K(\overline{g}) = \frac{81(1-x^2)(1-y^2)}{(9 + x^2(x^2-3)^2 + y^2(y^2-3)^2)^2}.$$

Use lowest order Regge elements to approximate $\overline{g}$ and compute the approximated Gauss curvature $K(g)$ for a sequence of structured and unstructured meshes. How good is the L^2-convergence $\|K_h(g) - K(\overline{g})\|_{L^2}$?

Exercise 6.3.3 motivates to use either structured meshes or to use better (high-order) approximations g of $\overline{g}$ with an adapted curvature computation.

6.4 High-order curvature approximation

Motivated by $g \in \mathcal{R}^0$ we can hope that for $g \in \mathcal{R}^k$ better approximation properties are obtained. For $g \in \mathcal{R}^1$ edge and inner dofs are given, cf. (4.4.5), and if we compute $K(g)$ element-wise it does not vanish anymore. The Gauss–Bonnet theorem tells us what are the appropriate vertex, edge, and inner terms for computing the distributional curvature.

Therefore, consider a single vertex patch and a smooth metric tensor $\overline{g}$ on it. The Gauss–Bonnet theorem applied on the vertex patch ω_V reads

$$\int_{\omega_V} K(\overline{g}) \sqrt{\det \overline{g}}\, dx + \int_{\partial\omega_V} \kappa_g(\overline{g}) \sqrt{\overline{g}_{\tau\tau}}\, ds + \sum_{V\in\mathcal{V}\cap\partial\omega_V} \varepsilon_V = 2\pi$$

and on each individual triangle $T \in \omega_V$

$$\int_T K(\overline{g}) \sqrt{\det \overline{g}}\, dx + \int_{\partial T} \kappa_g(\overline{g}) \sqrt{\overline{g}_{\tau\tau}}\, ds + \sum_{i=1}^3 \varepsilon_i = 2\pi.$$

Summing over all triangles of the vertex patch yields

$$\int_{\omega_V} K(\overline{g})\,\sqrt{\det \overline{g}}\,dx + \int_{\partial\omega_V} \kappa_g(\overline{g})\sqrt{\overline{g}_{\tau\tau}}\,ds + \sum_{V\in\mathcal{V}\cap\partial\omega_V} \varepsilon_V + \sum_{E\in\mathcal{E}^{\mathrm{int}}} \int_E [\![\kappa_g(\overline{g})]\!]\sqrt{\overline{g}_{\tau\tau}}\,ds + (2\pi - \sphericalangle_V(\overline{g})) = 2\pi.$$

We recognize the angle deficit used for the lowest order computation. Further, at each interior edge the jump of the geodesic curvature appears. For a smooth metric $\overline{g}$ both are zero, but not for an approximated metric.

This motivates to define the distributional curvature and the corresponding lifting. Let $\mathcal{V}_T$ denote the set of vertices which are attached to element T.

Definition 6.4.1 (Gauss curvature lifting) *Let $g \in \mathcal{R}^k$ with $\det g > 0$ and $g_{\tau\tau} > 0$. Then the distributional curvature acting on Lagrange finite elements $v_h \in U_h^{k+1}$ is given by*

$$\langle K(g), v_h\rangle_{U_h} = \sum_{T\in\mathcal{T}} \Big(\int_T K(g)\,v_h\,\sqrt{\det g}\,dx + \int_{\partial T} \kappa_g(g)\,v_h\,\sqrt{g_{\tau\tau}}\,ds + \sum_{V\in\mathcal{V}_T} (\sphericalangle_V^T(g) - \sphericalangle_V^T(\delta))v_h(V)\Big) \tag{6.4.1}$$

and the lifted Gauss curvature $K_h(g) \in U_{h,0}^{k+1}$ fulfills (with given homogeneous Dirichlet data) the equation

$$\int_\Omega K_h(g)\,v_h\,\sqrt{\det g}\,dx = \langle K(g), v_h\rangle_{U_h} \quad \text{for all } v_h \in U_{h,0}^{k+1}. \tag{6.4.2}$$

The following theorem states the convergence rates in the H^{-1}, L^2, and stronger H^k norms under the assumption that g is the Regge interpolant of $\overline{g}$.

Theorem 6.4.2 *Let $\overline{g} \in W^{k+1,\infty}(\Omega)$, $K(\overline{g}) \in H^k(\Omega)$ with $K(\overline{g}) = 0$ on $\partial\Omega$, and $g = \mathcal{I}_h^{\mathcal{R},k}\overline{g}$ the canonical Regge interpolant of $\overline{g}$. Further, let $K_h(g) \in U_{h,0}^{k+1}$ the lifted Gauss curvature from Definition 6.4.1. Then there exists an $h_0 > 0$ such that for all $h < h_0$, $-1 \le l \le k$*

$$\|K_h(g) - K(\overline{g})\|_{H_h^l} \le C h^{-l+k}\big(\|\overline{g}\|_{W^{k+1,\infty}} + |K(\overline{g})|_{H^k}\big),$$

where $C = C(\Omega, \mathscr{T}, \|\overline{g}\|_{W^{1,\infty}}, \|\overline{g}^{-1}\|_{L^\infty}, K(\overline{g})) > 0$.

If the sequence of discrete metric tensors g is not the canonical Regge interpolant but still fulfills the optimal approximation property

$$\|g - \overline{g}\|_{H^l} \le C\,h^{k-l}\|\overline{g}\|_{H^k},$$

one order of convergence is lost compared to Theorem 6.4.2 as proved in [8, 22]. In [23] a convergence result of the scalar curvature (which is up to a factor 2 the Gauss curvature in 2D) in the H^{-2}-norm has been proved for a general sequence of metric tensors for the angle defect.

Exercise 6.4.3 *Adapt the intrinsic Gauss curvature computation for two-dimensional manifolds embedded in $\mathbb{R}^3$, e.g. a sphere, ellipsoid, or torus, to compute the Gauss curvature of them.*

Bibliography

[1] Douglas N Arnold, Richard Falk, and Ragnar Winther. Finite element exterior calculus: from Hodge theory to numerical stability. *Bulletin of the American Mathematical Society*, 47(2):281–354, 2010.

[2] Douglas N. Arnold and Richard S. Falk. Asymptotic analysis of the boundary layer for the Reissner–Mindlin plate model. *SIAM Journal on Mathematical Analysis*, 27(2):486–514, 1996.

[3] Douglas N Arnold, Richard S Falk, and Ragnar Winther. Finite element exterior calculus, homological techniques, and applications. *Acta numerica*, 15:1–155, 2006.

[4] Douglas N. Arnold and Johnny Gúzman. Local L^2-bounded commuting projections in FEEC, 2021.

[5] Douglas N. Arnold and Shawn W. Walker. The Hellan–Herrmann–Johnson method with curved elements. *SIAM Journal on Numerical Analysis*, 58(5):2829–2855, 2020.

[6] Ivo Babuška and Juhani Pitkäranta. The plate paradox for hard and soft simple support. *SIAM Journal on Mathematical Analysis*, 21(3):551–576, 1990.

[7] John M Ball. Convexity conditions and existence theorems in nonlinear elasticity. *Archive for Rational Mechanics and Analysis*, 63(4):337–403, 1976.

[8] Yakov Berchenko-Kogan and Evan S. Gawlik. Finite element approximation of the Levi-Civita connection and its curvature in two dimensions, July 2022.

[9] Marcel Berger. *A Panoramic View of Riemannian Geometry*. Springer, Heidelberg, 2003.

[10] Dietrich Braess. *Finite Elemente - Theorie, schnelle Löser und Anwendungen in der Elastizitätstheorie*. Springer-Verlag, Berlin Heidelberg, 5 edition, 2013.

[11] Dietrich Braess, Stefan Sauter, and Christoph Schwab. On the justification of plate models. *Journal of Elasticity*, 103(1):53–71, 2011.

[12] Carsten Carstensen and Georg Dolzmann. An a priori error estimate for finite element discretizations in nonlinear elasticity for polyconvex materials under small loads. *Numerische Mathematik*, 97(1):67–80, 2004.

[13] D. Chapelle and K.J. Bathe. Fundamental considerations for the finite element analysis of shell structures. *Computers & Structures*, 66(1):19–36, 1998.

[14] Philippe G Ciarlet. *Mathematical Elasticity. Vol. I: Three-Dimensional Elasticity*, volume 20. North-Holland, Amsterdam, 1988.

[15] Philippe G. Ciarlet. An introduction to differential geometry with applications to elasticity. *Journal of Elasticity*, 78-79(1):1–215, 2005.

[16] M. I. Comodi. The Hellan–Herrmann–Johnson method: Some new error estimates and postprocessing. *Mathematics of Computation*, 52(185):17–29, 1989.

[17] Eugene Cosserat and François Cosserat. Théorie des corps déformables. *Nature*, 81(67), 1909.

[18] Manfredo P. do Carmo. *Differential Geometry of Curves and Surfaces*. Prentice Hall, Inc., Englewood Cliffs, New Jersey, 1976.

[19] Manfredo Perdigão do Carmo. *Riemannian Geometry*. Mathematics. Theory & Applications. Birkhäuser, Boston, 1992.

[20] Georges Duvant and Jacques Louis Lions. *Inequalities in Mechanics and Physics*, volume 219 of *Grundlehren der mathematischen Wissenschaften*. Springer-Verlag, Berlin Heidelberg, 1 edition, 1976.

[21] Gerhard Dziuk and Charles M. Elliott. Finite element methods for surface PDEs. *Acta Numerica*, 22:289–396, 2013.

[22] Evan S. Gawlik. High-Order Approximation of Gaussian Curvature with Regge Finite Elements. *SIAM Journal on Numerical Analysis*, 58(3):1801–1821, January 2020.

[23] Evan S. Gawlik and Michael Neunteufel. Finite element approximation of scalar curvature in arbitrary dimension, January 2023.

[24] Jay Gopalakrishnan, Michael Neunteufel, Joachim Schöberl, and Max Wardetzky. Analysis of curvature approximations via covariant curl and incompatibility for Regge metrics, November 2022.

[25] Kare Hellan. Analysis of elastic plates in flexure by a simplified finite element method. *Acta Polytechnica Scandinavica, Civil Engineering Series*, 46, 1967.

[26] E. Hellinger. Die allgemeinen Ansätze der Mechanik der Kontinua. In Felix Klein and Conr. Müller, editors, *Mechanik*, pages 601–694, Wiesbaden, 1907. Vieweg+Teubner Verlag.

[27] Leonard R. Herrmann. Finite element bending analysis for plates. *Journal of the Engineering Mechanics Division*, 93(5):13–26, 1967.

[28] Noel J. Hicks. *Notes on Differential Geometry*. Van Nostrand, 1965.

[29] Claes Johnson. On the convergence of a mixed finite element method for plate bending moments. *Numerische Mathematik*, 21(1):43–62, 1973.

[30] W.T. Koiter. A consistent first approximation in the general theory of thin elastic shells. In W.T. Koiter, editor, *The theory of thin elastic shells*, pages 12–33. North-Holland, Amsterdam, 1960.

[31] Raz Kupferman and Jake P. Solomon. A Riemannian approach to reduced plate, shell, and rod theories. *Journal of Functional Analysis*, 266(5):2989–3039, 2014.

[32] Patrick Le Tallec. Numerical methods for nonlinear three-dimensional elasticity. volume 3 of *Handbook of Numerical Analysis*, pages 465–622. Elsevier, 1994.

[33] John M Lee. *Introduction to Riemannian manifolds*, volume 176. Springer, 2 edition, 2018.

[34] Lizao Li. *Regge Finite Elements with Applications in Solid Mechanics and Relativity*. PhD thesis, University of Minnesota, 2018.

[35] Jerrold E Marsden and T. J. R. Hughes. *Mathematical foundations of elasticity*. Dover Publication, Inc, New York, 1994.

[36] L. S. D. Morley. The constant-moment plate-bending element. *Journal of Strain Analysis*, 6(1):20–24, 1971.

[37] Jean-Marie Morvan. *Generalized curvatures*. Springer, 2008.

[38] PM Naghdi. The theory of shells. In S Flügge, editor, *Handbuch der Physik*, volume VI/2. Springer-Verlag, Berlin and New York, 1972.

[39] Bastian Oesterle, Renate Sachse, Ekkehard Ramm, and Manfred Bischoff. Hierarchic isogeometric large rotation shell elements including linearized transverse shear parametrization. *Computer Methods in Applied Mechanics and Engineering*, 321:383–405, 2017.

[40] A. Pechstein and J. Schöberl. Tangential-displacement and normal-normal-stress continuous mixed finite elements for elasticity. *Math. Models Methods Appl. Sci.*, 21(8):1761–1782, 2011.

[41] A. Pechstein and Joachim Schöberl. The TDNNS method for Reissner–Mindlin plates. *Numerische Mathematik*, 137(3):713–740, 2017.

[42] Peter Petersen. *Riemannian Geometry*. Springer Berlin Heidelberg, New York, NY, 2016.

[43] G. Prange. *Das Extremum der Formänderungsarbeit: Habilitationsschrift Technische Hochschule Hannover 1916*. Edited by K. Knothe , Lehrstuhl für Geschichte der Naturwissenschaften, LMU München, 1999.

[44] Eric Reissner. On a variational theorem in elasticity. *Journal of Mathematics and Physics*, 29(1-4):90–95, 1950.

[45] R. S. Rivlin and J. L. Ericksen. Stress-deformation relations for isotropic materials. *Journal of Rational Mechanics and Analysis*, 4:323–425, 1955.

[46] Astrid Sinwel. *A new family of mixed finite elements for elasticity*. PhD thesis, Johannes Kepler Universität Linz, 2009.

[47] Michael Spivak. *A comprehensive introduction to differential geometry*, volume 1. Publish or Perish, Inc., Houston, Texas, 3 edition, 1999.

[48] Jakob Steiner. Über parallele Flächen. *Monatsber. Preuss. Akad. Wiss*, 2:114–118, 1840.

[49] Loring W. Tu. *Differential Geometry: Connections, Curvature, and Characteristic Classes*. Springer Science+Business Media, New York, NY, 2017.

[50] Peter Wriggers. *Nonlinear finite element methods*. Springer Science & Business Media, Heidelberg, 1 edition, 2008.